General Disclaimer

One or more of the Following Statements may affect this Document

- This document has been reproduced from the best copy furnished by the organizational source. It is being released in the interest of making available as much information as possible.

- This document may contain data, which exceeds the sheet parameters. It was furnished in this condition by the organizational source and is the best copy available.

- This document may contain tone-on-tone or color graphs, charts and/or pictures, which have been reproduced in black and white.

- This document is paginated as submitted by the original source.

- Portions of this document are not fully legible due to the historical nature of some of the material. However, it is the best reproduction available from the original submission.

NASA CR-135025
BBN Report No. 3174

HARDWALL ACOUSTICAL CHARACTERISTICS AND MEASUREMENT CAPABILITIES OF THE NASA LEWIS 9 x 15 FOOT LOW SPEED WIND TUNNEL

by Peter E. Rentz

BOLT BERANEK AND NEWMAN INC.

prepared for

NATIONAL AERONAUTICS AND SPACE ADMINISTRATION

NASA Lewis Research Center
Contract NAS3-19410

1. Report No. NASA CR-135025	2. Government Accession No.	3. Recipient's Catalog No.
4. Title and Subtitle Hardwall Acoustical Characteristics and Measurement Capabilities of the NASA Lewis 9 x 15 Foot Low Speed Wind Tunnel		5. Report Date June 1976
		6. Performing Organization Code
7. Author(s) Peter E. Rentz		8. Performing Organization Report No. 3174
		10. Work Unit No.
9. Performing Organization Name and Address Bolt Beranek and Newman Inc. 21120 Vanowen Street Canoga Park, California 91303		
		11. Contract or Grant No. NAS3-19410
		13. Type of Report and Period Covered Contractor Report
12. Sponsoring Agency Name and Address National Aeronautics and Space Administration Washington, D. C. 20546		
		14. Sponsoring Agency Code

15. Supplementary Notes

Project Manager, James A. Diedrich
NASA Lewis Research Center, Cleveland, Ohio

16. Abstract

Experimental evaluations of the acoustical characteristics and source sound power and directionality measurement capabilities of the NASA Lewis 9 x 15 foot low speed wind tunnel in the untreated or hardwall configuration were performed.

The results indicated that source sound power estimates can be made using only settling chamber sound pressure measurements. The accuracy of these estimates, expressed as one standard deviation, can be improved from $\pm$ 4 dB to $\pm$ 1 dB if sound pressure measurements in the preparation room and diffuser are also used and source directivity information is utilized. A simple procedure is presented.

Acceptably accurate measurements of source direct field acoustic radiation were found to be limited by the test section reverberant characteristics to 3.0 feet for omni-directional and highly directional sources. The standard deviation of the measurement reproducibility ranged from 0.6 to 1.7 dB. The source measurement accuracy ranged from - 1.5 to 3.4 dB, but may be due in part to source strength variation.

Wind-on noise measurements in the test section, settling chamber and preparation room were found to depend on the sixth power of tunnel velocity. The levels were compared with various analytic models and it was concluded that:

1. Sound pressure levels measured by test section microphones are due to true acoustic levels, not turbulence induced pseudo-noise.

2. The most likely area of significant noise generation is the transition from the test section to the diffuser.

Numerous procedural recommendations are set forth.

17. Key Words (Suggested by Author(s)) Acoustic Measurement Wind Tunnel	18. Distribution Statement Unclassified – Unlimited

19. Security Classif. (of this report) Unclassified	20. Security Classif. (of this page) Unclassified	21. No. of Pages 99	22. Price*

TABLE OF CONTENTS

LIST OF TABLES

LIST OF TABLES (Cont'd)

LIST OF FIGURES

LIST OF FIGURES (Cont'd)

LIST OF FIGURES (Cont'd)

1.0 SUMMARY

Experimental evaluations of the acoustical characteristics and
source sound power and directionality measurement capabilities
of the NASA Lewis 9 x 15 foot low speed wind tunnel in the
untreated or hardwall configuration were performed.

The results indicated that source sound power estimates can be
made using only settling chamber sound pressure measurements.
The accuracy of these estimates, expressed as one standard
deviation, can be improved from ± 4 dB to ± 1 dB if sound
pressure measurements in the preparation room and diffuser are
also used and source directivity information is utilized. A
simple procedure is presented.

Acceptably accurate measurements of source direct field acoustic
radiation were found to be limited by the test section reverberant
characteristics to 3.0 feet for omni-directional and highly
directional sources. The standard deviation of the measurement
reproducibility ranged from 0.6 to 1.7 dB. The source measure-
ment accuracy ranged from - 1.5 to 3.4 dB, but may be due in
part to source strength variation.

Wind-on noise measurements in the test section, settling chamber
and preparation room were found to depend on the sixth power of
tunnel velocity. The levels were compared with various analytic
models and it was concluded that:

1. Sound pressure levels measured by test section
    microphones are due to true acoustic levels, not
    turbulence induced pseudo-noise.

2.   The most likely area of significant noise generation is
     the transition from the test section to the diffuser.

Numerous procedural recommendations are set forth.

2.0   INTRODUCTION

The 9 x 15 foot low speed wind tunnel at the NASA Lewis Research
Center (LeRC), Cleveland, Ohio (1)*, has been adapted for
measurement of the acoustic performance of model propulsion
systems. The purpose of the effort reported herein is to
evaluate the resulting acoustic measurement capabilities.

2.1   Wind Tunnel Description

The 9 x 15 foot wind tunnel at the NASA Lewis Research Center,
Cleveland, Ohio, was built in the return leg of the 8 x 6 foot
supersonic wind tunnel, Figure 1 (1). Prior to construction
of the subsonic 9 x 15 foot test section, the 8 x 6 foot
facility had received acoustic treatment downstream of the
test section for the purpose of community noise abatement. The
treatment consists of low frequency Helmholtz resonators, a
lined duct muffler, wall treatment and acoustic baffles. As
a result, noise propagating downstream from the supersonic test
section is low relative to community noise standards (2), and
subsequently does not affect acoustic measurements in the
9 x 15 foot low speed wind tunnel.

Other aspects of the construction of the facility which relate
to acoustic measurement are the presence of flow regulation
doors upstream and downstream of the 9 x 15 foot test section,
a cooler screen upstream of the settling chamber, and dryer
beds between the diffuser leg and the drive fan, Figure 1.

---

*Numbers in parentheses indicate references listed.

The test section is constructed of steel with wood lining on
the side walls. The side walls also have four inch slots
running the length of the test section, 27 ft (8.2m). Acousti-
cally, the slots provide a window of 67 ft^2 (6.2m^2) between
the test section and the surrounding preparation room.

The tunnel flow is induced by a seven stage axial flow com-
pressor. Operation of the 9 x 15 foot low speed wind tunnel
is usually conducted at a standard compressor rotational
speed which ranges from 800 to 820 rpm. The desired tunnel
flow is achieved with the flow control doors. The compressor
first stage has 52 blades, preceded by an array of 72 guide
vanes. The final stage rotor has 60 blades. This stage is
preceded by 66 stator blades and followed by 84 exit blades.

2.2   Acoustic Measurement Approaches

In the hardwall or untreated configuration the approach to
acoustic measurement has been limited to the placement of micro-
phones in appropriate locations. Four microphones in the
tunnel settling chamber have been used to evaluate relative
sound power generation. The signals from microphones placed
on rigid supports in a pattern around a model have provided
source directivity data. Finally, directional microphones
placed outside the tunnel test section have been calibrated
and utilized for source directivity evaluation (3).

2.3   Relation to Preceding Work

Increasing interest in performing aero-acoustic measurements
has resulted in a number of studies (4-15) similar to this
one. Typically, the tunnel ambient noise and reverberant

properties are described with the intended aim of making direct
field measurements in an unmodified or a treated closed test
section. Sound power measurement calibrations are also per-
formed in open test section tunnels.

Preceding work on this program resulted in a report delineating
the wind-on noise characteristics and an omnidirectional source
sound power measurement calibration (16). This report expands
on that work along with setting forth an acoustic sound power
measurement calibration for directional sources. This effort
in the LeRC hardwall 9 x 15 foot wind tunnel is unique with
respect to calibration of the adjoining tunnel chambers for
sound power measurement. In addition, the hardwall tunnel
characteristics which limit direct field measurements are
defined.

3.0   ACOUSTIC MODELS

Analytic models are appropriate for the evaluation of the
acoustic properties of a facility. The models describe the
relationships between acoustic and other physical parameters.

In the case of the hardwall 9 x 15 foot wind tunnel, one
model serves as a framework for the application of experimental
data to the reverberant calibration. Another series of models
describes the functional behavior of various candidate noise
sources, which is applicable to noise source diagnosis.

3.1   Reverberant Chamber Model

A wind tunnel may be acoustically modeled as either a duct with
propagating waves or as a collection of interconnected semi-
reverberant rooms. The approach selected depends on both the
intended purpose of the modeling exercise and on the physical
characteristics of the tunnel. The mathematical acoustic model
adopted has four interconnected semi-reverberant chambers
including the test section. These chambers, along with the
acoustically important volumes and areas, are shown in Figure 2.
The tunnel is well suited for this model for the following
reasons:

1. The facility had received acoustic treatment for community
    noise abatement. As a result, the 8 x 6 test section is
    isolated acoustically from the 9 x 15 test section,
    Figure 1.

2. The three chambers adjoining the test section are each
    somewhat isolated from the rest of the tunnel and lend

themselves to the measurement of sound power eminating
from the test section.

3. The test section has exhibited a fairly uniform reverberant
    field using an omni-directional source (16).

The interrelationships of the appropriate acoustical parameters
are given in various references on room acoustics (17-18).
For standard atmospheric conditions, the sixty dB reverberation
decay time and total absorption are related by:

$$S\alpha_t = \frac{55.2V}{c\,T_R} \qquad\qquad (1)$$

where S = area, ft.^{2} (m^2)

$\quad \alpha_t = \alpha_{SAB} + 4\,mV/S$ = total average absorption

$\quad \alpha_{SAB}$ = Sabine absorption (in the absence of atmospheric absorption)

$\quad V$ = volume, ft.^{3} (m^3)

$\quad T_R$ = reverberation time, 60 dB decay, sec.

$\quad m$ = atmospheric absorption term, 1/ft. (1/m)

$\quad c$ = speed of sound, ft/sec (m/sec)

The atmospheric absorption term is primarily a function of
relative humidity and frequency with some variation with temper-
ature. Available data for reverberant chambers (19) have been
summarized into a single curve, Figure 3. Atmospheric absorption
is also a factor in direct field sound propagation above 1000 Hz
for test section to settling chamber distances. For direct
field sound propagation, the excess atmospheric attenuation is
usually expressed in terms of dB/1000 ft (m). Standard values
for octave and one-third octave bands as a function of humidity
and temperature have been published by the Society of Automotive

Engineers (20,21). Octave band data from Reference 21 are
reproduced as Figure 4.

With an acoustic source in the room, sound power and sound
pressure level are related by

$$SPL = PWL + 10 \log \left[\frac{Q}{4\pi r^2} + \frac{4}{S\alpha_{SAB} + 4mV} \right] + 10 \qquad (2)$$

where SPL = sound pressure level, dB re 20 $\mu N/m^2$

   PWL = sound power level, dB re 10^{-12} Watt

   Q = SPL along sound source geometric centerline
       (-) SPL of an omnidirectional source having
       equivalent sound power, measured at same radius

   r = radius from source ft. (m)

Subtract 10 dB from the right hand side for SI units.

The hall radius is the point at which the direct field and
reverberant sound pressure levels are equal. From Equations 1
and 2:

$$r_H = \left[\frac{QS\alpha_t}{16 \pi} \right]^{1/2} = \left[\frac{55.2VQ}{16 \pi c T_R} \right]^{1/2} \qquad (3)$$

The sound power output of propulsion inlets has, in the past,
been evaluated by LeRC on a relative basis by measurement of
settling chamber sound pressure levels. The SPL-PWL relation-
ship, equation 2, provides a means to calculate the sound
power in the settling chamber. However, knowledge of the
fractional portion of the source sound power exiting to the
settling chamber is also required.

Recognizing these factors which contribute to settling chamber
levels, the previous sound power calibration method (16) has
been revised to place more reliance on the chamber decays

and to include physically significant acoustic source power
distribution terms.

The recommended chamber reverberant calibration is represented
in equation form:

$$PWL_{source} = SPL_i + 10 \log \left[S\bar{\alpha}_{SAB_i} + 4mV_i \right] - 10 \log P_i - 16 \quad (4)$$

where P_i = fraction of source sound power exiting to the
ith chamber

10 log P $\equiv$ Π, power index

Add 10 dB to the right hand side for SI units.

If all the source sound power is inserted into the particular
chamber, P = 1.0, and the chamber reverberant relation results.

$$PWL = SPL + 10 \log S\alpha_t - 16 \quad (5)$$

$$or \; PWL - SPL = 10 \log \frac{55.2V}{cT_R} - 16$$

$$= 10 \log \frac{V}{cT_R} + 1.5$$

Add 10 dB to the right hand side for SI units.

The ratio of source power to that exiting to the settling
chamber, the preparation room, or the diffuser depends both on
the tunnel acoustic properties and the source directivity
index. The directivity index is defined as

$$DI \equiv 10 \log Q \quad (6)$$

In words, the directivity index is the ratio of sound pressure

levels from directional and omni-directional sources having the
same sound power. This directivity index may be determined
from directionality plots or from concomitant direct field sound
pressure and sound power level measurements. For directionality
plots, the DI determination results from integrating the product
of intensity and area. Since accurate integration of this product
is tedious, a -3 dB to -5 dB point approximation can be used.
That is, the transition from high intensity to low intensity is
assumed to be instantaneous and to occur between -3 dB and -5 dB
on the directionality plot. For example, for loudspeaker data,
the -5 dB point gives a better approximation (22). In addition,
if the directionality pattern is symmetrical in the horizontal
and vertical directions, the projected area is a circular
segment and the directivity index is given by the equation

$$DI = 10 \log \frac{2}{1-\cos \gamma} \qquad (7)$$

where γ = the angle between the source centerline and the repre-
sentative transition point.

The directivity index may also be computed from sound pressure
and sound power using the following equation:

$$DI = SPL_{1.0 \text{ ft (m)}} - PWL_{source} + 1 \qquad (8)$$

where $SPL_{1.0 \text{ ft (m)}}$ = Direct field, centerline sound pressure
level dB re 20 $\mu N/m^2$, at 1.0 ft (m)

Add 10 dB to the right hand side for SI units.

The relation between source directivity index and the power
index is best determined experimentally. However, note that
this dependence on source characteristics is required because

-10-

only one chamber measurement is used. In order to minimize
inaccuracies arising from the variability of P with source
characteristics, the use of preparation room and diffuser
measurements, along with settling chamber levels, is recom-
mended. In that situation, only the acoustic energy absorbed
in the test section is not accounted for by chamber measurements.

3.2 Tunnel and Microphone Noise Models

Tunnel generated noise and turbulent wind induced microphone
noise place amplitude limits on the measurement of source
generated noise in both low velocity chambers and the higher
velocity test section. The candidate noise sources contri-
buting to test section and settling chamber measured levels
are as follows:

1. Microphone self noise in the presence of wind.
2. Test section turbulent boundary layer noise.
3. Turbulence--test object vortex noise.
4. Settling chamber cooler coil vortex noise.
5. Tunnel drive fan noise propagating through the dryer bed
    and up the diffuser.

Noise from the 8 x 6 foot supersonic wind tunnel by way of the
settling chamber, Figure 1, is not considered significant.
Levels measured at the exit prior to construction of the
9 x 15 foot wind tunnel were lower than present settling
chamber levels as indicated in Table I.

3.2.1 Microphone Wind Noise

Microphone self noise in the presence of wind is generally
attributed to fluctuating dynamic pressure –

TABLE I

COMPARISON OF UPSTREAM SOUND PRESSURE LEVELS,

dB re 20 $\mu N/m^2$

Condition	Octave Band Center Frequency, Hz						
	125	250	500	1K	2K	4K	8K
Mach 1.9 in 8 x 6, prior to 9 x 15 construction, no ram jet (2)	60	55	56	57	51	45	37
Present settling chamber levels, q = 25 psf (16)	89 to 95	87 to 93.5	83.5 to 88	81.5 to 87	72 to 81	67 to 79	65 to 70

$$q + p(t) = 1/2 \, \rho(U + u)^2 \qquad (9)$$
$$= 1/2 \, \rho[U^2 + 2Uu + u^2]$$

where q = dynamic pressure, lb/ft^2 (N/m^2)

   $p(t)$ = fluctuating dynamic pressure lb/ft^2 (N/m^2)

     ρ = density, $slugs/ft^3$ (kg/m^3)

     U = mean velocity, ft/sec (m/sec)

     u = fluctuating velocity, ft/sec (m/sec)

since U and q are not time variant and $U > u$,

$$p(t) \simeq \rho U u \qquad (10)$$

and
$$\overline{p^2(t)} = \rho^2 U^2 \overline{u^2} \qquad (11)$$

where
$$\overline{p^2(t)} = \text{time average variance of the pressure,}$$
$$\frac{lb^2}{ft^4}\left(\frac{N^2}{m^4}\right)$$

The fluctuating velocity is usually expressed in terms of a turbulence index, a fraction of the mean velocity, $\tau = u/U$.

Substituting into equation (11) yields

$$\overline{p^2(t)} = \overline{\rho^2 U^4 \tau^2} \qquad (12)$$

Taking ten times the logarithm of both sides of equation 12, using the air density for standard conditions, and converting to $20\mu N/m^2$ reference

$$SPL = 40 \log U + 20 \log \tau + 75. \qquad (13)$$

Add 20.5 dB to the right hand side for SI units.

In terms of dynamic pressure, q:

$$SPL = 20 \log q + 20 \log \tau + 133.8 \qquad (14)$$

Subtract 33.6 dB from the right hand side for SI units.

In review of aero-acoustic measurements, Fuchs (23) presents data showing that the U^4 dependence holds for circular jets and free stream measurements. However, the basic constant of proportionality differs by a factor of 1/2 from equation 12, as follows:

$$p(t) = 1/2 \, \rho U u \qquad (15)$$

In addition, for non-homogeneous turbulent boundary layers, a form proportional to $U^2 \tau^{0.5}$ gives a better fit. These results suggest that the constant of proportionality, equations 13 and 14, may have a sizable variability or may even be in error. However, since the experimental results do not consist of well documented concommitant turbulence and dynamic pressure data measurements, the analytically correct form, equation 12, will be used.

In order to model the response of typical microphones in the presence of turbulent flow, the following additional information is required:

1. Experimental assurance that microphone wind noise depends on U^4.

2. Data on the improvement afforded by microphone nose cones.

3. The intensity and spectral characteristics of the turbulence in the 9 x 15 foot test section.

Data from tests by B&K (24,25) and Noiseux (26) collapse nicely
(to different curves) if normalized by velocity to the sixth
power. However, the mid-to-high frequency spectra of both
sets of data are decreasing with increasing frequency, approx-
imately to the second power. If the higher velocity measure-
ments are shifted down in frequency, they are then related to
the lower velocity measurements by U^4.

Rasmussen (25) shows an average of 15-25 dB decrease in wind
noise with a nose cone for one-half inch microphones and 10-15 dB
for one-quarter inch microphones in the frequency range from
100 to 5000 Hz. For those tests, the reference data were
measured with a protection grid which may induce local turbu-
lence, especially in high frequency bands. This would tend to
increase the apparent nose cone improvement. Noiseux (27)
presents concomitant turbulence and wind noise data for a B&K
one-half inch microphone with nose cone. The microphone
exhibited levels which are approximately 16 dB lower than the
fluctuating dynamic pressure levels calculated from equation 13.
From these limited experiments, 15 dB is taken as the expectation
for wind noise reduction with the addition of a nose cone for
one-quarter inch microphones.

The turbulence intensity in the center of the 9 x 15 foot test
section averages 0.75% (1). The intensity averages 1.3% as
the measurement location is moved to within 10 inches of the
floor or ceiling. The electrical signals from the hot wire
probes used for those measurements were passed through low pass
filters at the time of measurement (28). The one-third octave
band spectrum of the turbulence was inferred from these measure-
ments to essentially flat, with a level of - 56.5 dB re unity.
Combining the confirmation of the U^4 dependence, the 10 dB
nose cone improvement, and measured turbulence levels, the

predicted one-third octave band wind noise sound pressure level is 90 dB re 20μN/m^2 for a tunnel dynamic pressure of 25 psf (1196 N/m^2). The microphone wind noise is also predicted to increase as U^4 (or q^2).

3.2.2 Turbulent Boundary Layer Noise

From unpublished BBN work acoustic power radiated from a turbulent boundary layer can be expressed as follows:

$$PWL\,(\omega) \simeq 10 \log \left(\frac{\rho SU^7}{c^3 \omega \delta^*}\right) + 41 \quad \text{when } \frac{\omega \delta^*}{U} > 1 \tag{16}$$

$$\simeq 10 \log \left(\frac{\rho SU^5 \delta^* \omega}{c^3}\right) + 41 \quad \text{when } \frac{\omega \delta^*}{U} < 1 \tag{17}$$

where PWL (ω) = the sound power level for one-third octave
                bandwidth, dB re 10^{-12} Watt

        ρ = air density, lb sec^2/ft^4 (N sec^2/m^4)

        S = radiative area, ft^2 (m^2)

        U = free stream velocity, ft/sec (m/sec)

        c = speed of sound, ft/sec (m/sec)

      δ^* = boundary layer displacement thickness, ft (m)

      $\omega = 2\pi f$ = radial frequency, radians/sec

Subtract 11.5 dB from the right hand side of equations 16 and 17 for SI units.

In the transitional frequency region where $\omega\delta^* \simeq U$, one-third octave band levels will increase approximately as U^6. Unfortunately, the constant of proportionality in equations 16 and 17 has a variability of $\pm$ 20 dB.

For a representative tunnel flow condition of q = 25 psf, and a boundary layer displacement thickness of 0.5 inch or 13 mm (1), the transition point frequency, $f = U/\delta^* 2\pi$ = 561 Hz. Taking the radiative area as the test section area (1643 ft^2 or 153 m^2), equations 16 and 17 both yield sound power estimates of 85 dB re 10^{-12} watt. The one-third octave band sound power levels diminish at a rate of 3 dB per octave on both sides of the transition point one-third octave band, centered at 561 Hz.

The diffuser would also be expected to generate turbulent boundary layer noise. However, the 1:3 reduction in velocity occurring in the diffuser effects almost a 30 dB reduction in the sound power production per unit of radiative area at the diffuser end, relative to the test section, from equations 16 and 17. The contribution of the diffuser turbulent boundary layer is estimated to be, at most, equal to that of the test section. This would add 3 dB to the estimate for the test section to arrive at a total turbulent boundary layers sound power estimate.

3.2.3 Vortex Noise

With respect to vortex noise, theoretical and experimental work has also been done to understand the basic process of noise generation by the interaction of flow with rigid surfaces. Current noise prediction techniques are summarized by Hayden (29) for the cases of:

a) flow past a single discontinuity-trailing edge,

b) rigid body in disturbed flow,

c) spoilers in confined environments.

Analyses show that the noise sources for (a) and (c) above are dipole, and the resulting sound power varies as U^6. Point dipole sources are also postulated for incoming turbulence although deviations apparently exist.

For flow past a single discontinuity trailing edge, the engineering form of the acoustic generation prediction is as follows:

$$PWL_{OA} = 10 \log \left(\delta W U^6 \right) - 21 \tag{18}$$

where PWL_{OA} = overall sound power, dB re 10^{-12} Watt

δ = boundary layer thickness, ft (m)

W = edge length, ft (m)

U = tunnel mean flow velocity, ft/sec (m/sec)

Add 41.3 dB to the right hand side for SI units.

The one-third octave band spectrum peaks at a frequency $f_p = 4 \times 10^{-2} U/\delta$ and at a level 10 dB lower than the overall sound power level. The spectrum decreases at 3 dB per octave above the peak frequency band.

Two trailing edges are candidate noise producers – the diffuser end, and the transition from the test section to the diffuser. The latter is postulated not so much for the clean empty test section as for when test hardware or test section wall irregularities are present, promoting local or general boundary layer separation, similar to a trailing edge situation.

For a representative test section flow condition of q = 25 psf
(1196 N/m^2), the noise related parameters and predicted sound
power generation are as follows:

End of Diffuser	End of Test Section
$\delta \simeq$ 1 ft (0.3 m)	δ = 0.4 ft (0.12 m) (1)
W = 80.5 ft (24.5 m)	W = 48 ft (14.6 m)
U = 50.2 ft/sec (15.3 m/sec)	U = 147 ft/sec (44.8 m/sec)
f_p = 2 Hz	f_p = 15 Hz
PWL_{OA} = 100.1 dB	PWL_{OA} = 121.8 dB

With respect to a rigid body in disturbed flow, Hayden (29)
comments that "there still exists no coherent, experimentally
verified theory which enables one to predict accurately sound
production from an arbitrarily shaped body in an arbitrary
inflow." This absence of a general prediction methodology
is balanced by the ease of application of the spoiler noise
model. Hayden (29) and Beranek (30) summarize work by Yudin (31)
and Gordon (32) on the noise generated by an obstruction in a
duct or pipe. The model relates sound power production to the
pressure drop across the spoiler spanning a pipe. If the
pressure drop is assumed to be equal to the product of the
dynamic pressure and coefficient of drag of the spoiler, the
following engineering equation results:

$$PWL_{OA} = 30 - \log qC_d + 20 \log D_p - 76.1 \qquad (19)$$

where PWL_{OA} = overall sound power dB re 10^{-12} Watt

$\qquad$ q = dynamic pressure, 16/ft^2 (N/m^2)

$\qquad D_p$ = diameter of pipe on test section, ft (m)

$\qquad C_d$ = Coefficient of drag

Subtract 37.4 from the right hand side for SI units.

The width of the spoiler is not a factor in Equation 19 because the formulation assumes the sound power level is dependent on the peak frequency squared, which in turn is inversely dependent on spoiler width.

The one-third octave band spectra peaks at 10 dB below the overall and at a frequency of f_p = 0.2 U/d, where d is the diameter of the spoiler. This frequency must be below the pipe cutoff frequency for Equation 19 to be applicable. The cutoff frequency is defined as f_c = 0.5 c/D_p. The one-third octave band spectra decreases at 3 dB/octave above and below the peak spectral level.

For a 1.5 foot diameter pipe spanning the average test section dimension, and for representative tunnel flow conditions, q = 25 psf in the test section, Equation 19 predicts an overall sound power of 98.5 dB re 10^{-12} Watt. The predicted spectrum peaks at a frequency of 19.6 Hz.

3.2.4 Settling Chamber Cooler Coil Vortex Noise

Upon completion of the return leg of the 8 x 6 foot supersonic wind tunnel circuit in 1957, a serious noise problem was identified and corrected (33). The bank of cooler coils, Figure 1, exhibited discrete frequency vortex shedding which matched one or more "organ pipe resonances" of the heat exchanger boundaries, along with structural resonances. This narrow band phenomenon was eliminated by installation of three vertical baffles in each of seven foot wide sections. In addition, V-shaped plates were installed in place of flat plates between adjacent sections. With completion of the cooler modifications, the noise level was reported to have

been reduced 60 dB in the range from 110 to 170 Hz. No broadband noise measurements are reported for any mid-to-high frequency bands.

Fortunately, a reasonably accurate (± 5 dB) method exists for estimating the overall sound power generated by flow obstructions, such as air conditioning diffusers. Beranek (34) presents an empirical method, attributable to Humbert (35), as follows:

$$PWL_{OA} = 10 \log S + 30 \log \varepsilon + 60 \log U - 31.3 \qquad (20)$$

where S = area, ft^2 (m^2)

ε = pressure drop divided by dynamic pressure, dimensionless

U = velocity, ft/sec (m/sec)

Add 41.3 dB to the right hand side for SI units.

The estimated one-third octave band spectrum is haystack in shape, peaking at 10 dB below the overall level at a frequency $f_p \approx 457 \, U/U_{ref}$, where U_{ref} = 10 ft/sec (3 m/sec). The spectral level decreases approximately 3 dB per octave above and below the peak frequency.

The dimensions of the cooler coils are 32 by 47 feet (14.3 m by 9.7 m). The pressure drop across the cooler coil bank was measured prior to installation of the 9 x 15 foot test section (36). At maximum flow conditions, the pressure drop was 5.7 inches of water. This corresponds to approximately 17 dynamic pressure heads.

The values of the parameters of equation 20, for a test section dynamic pressure of 25 psf (1196 N/m^2) are as follows:

$$S = 1504 \text{ ft}^2 \ (140 \text{ m}^2)$$
$$\epsilon = 17$$
$$U = 13.2 \text{ ft/sec} \ (4 \text{ m/sec})$$
$$PWL_{OA} = 104.4 \text{ dB re } 10^{-12} \text{ Watt}$$
$$f_p = 603 \text{ Hz}$$

Considering that one-half of the acoustic energy propagates upstream, the power transmitted to the settling chamber in the one-third octave band centered at 603 Hz would be 91.4 dB re 10^{-12} Watt.

3.2.5 Tunnel Drive Fan Noise Propagating Through the Dryer Bed

Fan generated noise is attributed by various authors (37,38) to combinations of mechanisms including:

a) Steady blade forces
b) Interference noise (from upstream obstructions)
c) Vortex shedding
d) Inlet turbulence

The first two mechanisms produce sinusoidal tones at the blade passage frequency and multiples thereof. The compressor fan for the facility turns at an average speed of 810 rpm. The drive fan has 52 blades, yielding a blade passage frequency of 702 Hz. The acoustic transmission properties of the dryer bed are not known, making the noise source level estimation impossible. However, identification of contributions from

these noise sources should be relatively easy because of their
sinusoidal nature.

Fan vortex shedding and inlet turbulence exhibit the same U^6
parametric dependence as turbulent boundary layer and vertex
noise. However, the velocity through the 9 x 15 foot low speed
test section is controlled with the flow control doors with
the compressor speed and flow held approximately constant.
Therefore, any broadband noise from the tunnel drive fan would
not be dependent, in either amplitude or frequency, on the low
speed test section flow velocity.

4.0 EXPERIMENTAL RESULTS AND DISCUSSION

The experimental evaluation of the hardwall acoustic measurement
characteristics of the 9 x 15 foot low speed wind tunnel took
place over a period of time from 29 November 1973 to 17 July
1974. The resulting data and discussion of their significance
are organized as follows:

. Chamber Reverberant Decay Measurement
. Sound Power Measurement Calibration
. Directionality Measurement Demonstration
. Tunnel and Microphone Wind-On Noise

4.1 Chamber Reverberant Decay Measurements

The graphic display and measurement of the decay of impulsive
or steady state acoustic signals permits identification of
dominant reflecting surfaces as well as calculation of the
average absorption. Impulsive decays were recorded on
29 November 1973, 24 February 1974, and 27 February 1974.
The relative humidity was not measured in the tunnel, but
Cleveland Weather Bureau data, shown in Table II, indicate
an average of 60% for those days. Based on a limited number
of subsequent measurements, the relative humidity in the
settling chamber is estimated to be significantly lower than
the ambient relative humidity, especially on cold days.

The equipment used for all decay measurement is shown in
Figure 5a. The recordings were played back through an octave
band filter onto a grphic level recorder, and the reverber-
ation times were calculated. With the use of an impulsive
noise source, a graphic level recorder tends to over-react

TABLE II

Relative Humidity, Cleveland, Ohio, Airport
on Static Acoustic Test Days, %

	Date	Type Test	Time of Day		
			10 a.m.	3 p.m.	9 p.m.
Hardwall	29 Nov. 1973	Pistol Decays, ILG	64	54	75
	24 Feb. 1974	Pistol Decays	60	68	78
	27 Feb. 1974	Pistol Decays	45	46	51
	3 April 1974	ILG	43	87	78
	11 July 1974	Shotgun Mic	66	57(38)*	49
	12 July 1974	Shotgun Mic	53	54	40
	15 July 1974	Horn, Reverb. Cal.	64	60	66
	16 July 1974	Horn, Reverb. Cal.	61	46	47
	17 July 1974	Horn, Sword, Direct.	50	35	53

*Measured In Test Section

to the instantaneous increase in signal. This obscures the
initial part of the subsequent decay. To overcome this diff-
culty, the magnetic tape was played in reverse.

Typical settling chamber octave band decays are presented in
Figure 6. The reverberant decays are well behaved with a
single slope. This indicates the predominance of a single
class of room modes, probably floor to ceiling and wall to wall.

Decays for the diffuser section and preparation room are pre-
sented in Figures 7 and 8, respectively. As with the settling
chamber, the curves are well behaved with little or no ambi-
guity about the appropriate reverberation time to use to
characterize the acoustic properties.

The test section decay curves, Figure 9, all have a double
slope characteristic. The initial slope is identified with
the reverberant decay of the test section itself, the energy
is exiting to the other three chambers. The subsequent slope,
which starts 15 to 20 dB from the initial test section level,
is associated with the decay of the settling chamber with some
input from the diffuser and preparation room.

The reverberation times for all the pistol shot recordings
were calculated and averaged. The average reverberation times
were used to calculate the absorption, hall radius, and sound
power-sound pressure difference, for the settling chamber,
preparation room, and diffuser section, Table III.

For the test section, the initial part of the decay was con-
sidered an inaccurate descriptor of the average absorption

TABLE III

Acoustic Properties of Wind Tunnel Chambers
Determined from Decay Measurements and
Calibrated Sound Power Source, Low Relative Humidity (25%)

Chamber	Property	Octave Band Center Frequency, Hz					
		250	500	1K	2K	4K	8K
Settling Chamber 13,000 ft² (1208m²) 100,000 ft³(2832m³)	Reverb. Time Sec.	3.6	3.5	3.0	2.5	1.65	0.95
	$S\alpha_t$, ft²	1360	1400	1630	1960	2970	5160
	α_t	0.10	0.11	0.13	0.15	0.23	0.40
	Hall Radius, ft.	5.2	5.3	5.7	6.2	7.7	10.1
	PWL (−) SPL, dB	15.3	15.5	16.1	16.9	18.7	21.3
Diffuser Section 20,000 ft² (1860m³) 140,000 ft³ (3965m³)	Reverb. Time, Sec.	5.0	4.9	4.1	3.3	1.9	1.0
	$S\alpha_t$, ft²	1370	1400	1670	2100	3600	6900
	α_t	0.07	0.07	0.09	0.11	0.19	0.35
	Hall Radius, ft.	5.2	5.3	5.7	6.4	10.6	11.7
	PWL (−) SPL, dB	15.4	15.5	16.2	17.2	19.6	22.3
Preparation Room 23,000 ft² (2137m²) 100,000 ft³ (2832m³)	Reverb. Time, Sec.	2.6	2.7	2.4	2.0	1.4	0.68
	$S\alpha_t$, ft²	1885	1815	2040	2450	3500	7200
	α_t	0.08	0.08	0.09	0.11	0.15	0.31
	Hall Radius, ft.	6.1	6.0	6.4	7	8.3	12
	PWL (−) SPL, dB	16.8	16.6	17.1	17.9	19.4	22.6
Test Section 1643 ft² (153m²) 3861 ft³ (109m³)	Reverb. Time, Sec.	0.8/4.0	1.1/3.4	0.8/2.8	1.2/2.6	0.8/1.6	0.7
	$S\alpha_t$, ft² (T_{60})	236	172	236	158	236	270
	PWL (−) SPL (ILG)	9.5	9	9	9.2	10.5	10.7
	$S\alpha_t$, ft², (ILG)	355	316	330	445	457	470
	α_t	0.22	0.19	0.2	0.27	0.28	0.29
	Hall Radius, ft	2.7	2.5	2.6	3.0	3.0	3.0

because of the short decays and limited number of reflections.
This inaccuracy was confirmed by observing that the test section
effective absorbing area, Sa_t, calculated from the pistol decays
was consistently less than the area opening to the adjoining
chambers (337 ft^2). To overcome this measurement problem and
resulting inaccuracy, an ILG centrifugal blower, calibrated,
omnidirectional, acoustic source (39) was placed in the test
section and octave band sound pressure levels were measured at
various locations in the test section. A reasonably uniform
acoustic field was observed at radii beyond five feet, and the
test section reverberant properties were calculated from these
data, Table III.

4.2   Sound Power Measurement Calibration

4.2.1   Omni Directional Source

On two occasions, 29 November 1973, and 3 April 1974, settling
chamber sound pressure levels were measured while the ILG source
was in the test section. These data had been used to calibrate
the settling chamber microphones for source sound power in the
previous report (16). With use of decays for the settling
chamber calibration, these data have now been used to determine
π, the fractional portion of the source sound power exiting
to the settling chamber, Table IV. The calculated values of
π differ by 0.2 to 4.8 dB for the two sets of data. These
differences are attributable to one or both of the following:

    1.   source sound power output variability,

    2.   relative humidity uncertainty.

TABLE IV

Estimation of Sound Power Output of ILG Omnidirectional Source In Wind Tunnel Test Section Using Settling Chamber Sound Pressure Level Measurements

Test	Relative Humidity Estimate	Property	Octave Band Center Frequency					
			250	500	1K	2K	4K	8K
29 Nov. 1973 Test 1, 2	25%	SPL_{sc}	60	60	61.7	60.2	53.5	44
		$\Delta, PWL_{sc} - SPL_{sc}$	15.3	15.5	16.1	16.9	18.7	21.3
		$PWL_{sc} = SPL_{sc} + \Delta$	75.3	75.5	77.8	77.1	72.2	65.3
		PWL_{ILG}	80.5	81	81.7	82	79	75.5
		$\Pi, PWL_{ILG} - PWL_{sc}$	-5.2	-5.5	-4.9	-4.9	-6.8	-10.2
3 April 1974 Test II, Test Section Station 0,0	70%	SPL_{sc}	57.5	58	62	61	57.5	52
		$\Delta, PWL_{sc} - SPL_{sc}$	15.3	15.5	15.7	16.0	17.2	18.2*
		$PWL_{sc} = SPL_{sc} + \Delta$	72.8	73.5	78.2	77.0	74.7	70.2
		PWL_{ILG}	80.5	81	81.7	82	79	75.5
		$\Pi, PWL_{ILG} - PWL_{sc}$	-7.7	-7.5	-3.5	-5.0	-4.3	-5.3
Average		$\Pi, ave \; PWL_{ILG} - PWL_{sc}$	-6.5	-6.5	-4.2	-5	-5.5	-7.7
Ratio, connecting area to total test section absorption, Table III		$10 \log(9 \times 15)/S\alpha_t$	-4.2	-3.7	-3.9	-5.2	-5.3	-5.4

*Table III values corrected for relative humidity, equation 4 and Figure 3.

The average value of Π is approximately -6 dB with some
frequency dependence. This says that one-fourth of an omni-
directional source's acoustic energy goes to the settling
chamber.

The bottom line of Table IV lists the ratio of total test
section absorption to the area of the 9 x 15 foot opening
into the settling chamber, expressed in dB. If the test section
were truly reverberant and the settling chamber levels negli-
gible, these values would correspond to Π. These values are
different from the average Π values by -0.2 to 3.9 dB. This is
indicative of the sound power estimation accuracy which can
be achieved with an omnidirectional source in the middle of
the test section using only settling chamber measurements.

In addition to this measurement variability, the acoustic
power distribution also depends on the source location in the
test section. This has been demonstrated by moving the ILG
source within the test section, Figure 10, and by observing
the effect of angle of attack (position) of a 5.5 inch fan
inlet, Figure 11.

In order to overcome the dependence of sound power estimates
on source position, and to an even greater extent the depend-
ence on directionality, the ILG-induced acoustic levels in the
diffuser and preparation room were utilized along with the
settling chamber levels. The sound pressure levels measured
with a hand held sound level meter are listed in Table V.
These octave band levels were converted to sound power
estimates using the PWL-SPL values, Table III, plus a humidity
correction. The humidity was approximately 25% for the

TABLE V

SOUND PRESSURE LEVELS WITH ILG OMNIDIRECTIONAL SOURCES IN WIND
TUNNEL TEST SECTION, HAND HELD SOUND LEVEL METER
3 APRIL 1974, RELATIVE HUMIDITY ESTIMATE 70%

TEST NO.	SOURCE LOCATION	MICROPHONE			OCTAVE BAND CENTER FREQUENCY					
		SC	PR	DS	250	500	1K	2K	4K	8K
II	Test Section, Station 0, 0	X			57.5	58	62	61	57.5	52
			X		62	59.5	58	57.5	54.5	49
				X	57.5	58	58	57	52	46
III	Test Section Station 7, 0	X			58	59.5	61	61.5	59	53
			X		60	58.5	58	56.5	54	48.3
				X	57	57.5	58	56.5	52	45
IV	Test Section, Station 0, -3.5	X			57.5	58.5	61	60.5	59	52.5
			X		60	59	58	57.5	54.5	50
				X	57.5	58	59	57.5	52	43
V	Test Section, Station -15, 0	X			56	56.5	59	59	56.5	49
			X		58.5	56	56.5	56	53.5	47
				X	59.5	61	60.5	59.5	55.5	49
VIII	Test Section, Station -0, 0	X			58	59.5	60	59	57	50.5
			X		61	59.5	59	57.5	54.5	50
				X	57.5	57.5	59	60	55.5	48

chamber calibrations and approximately 70% for the ILG measurements. The $S\alpha_t$ values, Table III, equation 4 and the humidity absorption, Figure 3, were used to calculate humidity corrections, Table VI.

TABLE VI

HUMIDITY CORRECTION, $10 \log \left[\dfrac{S\alpha_t \ (25\%)}{S\alpha_t \ (70\%)} \right]$

Chamber	Frequency Hz			
	1000	2000	4000	8000
Settling Chamber	0.4	0.9	1.5	3.1
Preparation Room	0.4	1.0	2.2	3.2
Diffuser Leg	0.5	1.2	2.1	3.3

The corrected chamber calibrations were applied to the measured sound pressure levels in all three chambers to arrive at sound power estimates, Table VII. The sound power estimates for the individual chambers were summed and compared with the source sound power, Table VII. The summed results are independent of source position. In addition, the difference in source and measured sound power agrees well with the ratio of total test section absorption to open area (expressed in dB), Table VII. This indicates that all of the omni-directional source sound power is accounted for; it is either absorbed in the test section or is divided between the adjoining chambers. Thus, the sound power estimation accuracy for an omni-directional source can be improved to ±1 dB if all three chamber measurements are used.

4.2.2 Sound Power Measurement Calibration Directional Source

As mentioned in the preceding section, early tests by LeRC with a 5.5 inch fan-inlet noise source showed variation in settling

TABLE VII

SOUND POWER OUTPUT OF ILG OMNIDIRECTIONAL SOURCE IN WIND
TUNNEL USING MEASUREMENTS IN THREE CHAMBERS
PWL* = SPL + Δ (TABLE III) + RELATIVE HUMIDITY CORRECTION, TABLE VI

TEST NO.	SOURCE LOCATION	MICROPHONE SC PR DS TOTAL				OCTAVE BAND CENTER FREQUENCY					
		SC	PR	DS	TOTAL	250	500	1K	2K	4K	8K
II	Test Section, Station 0, 0	X				72.8	73.5	77.7	77.0	74.7	70.2
			X			78.8	76.1	74.7	74.4	71.7	68.6
				X		72.9	73.5	73.7	73.0	69.5	64.8
					X	80.5	79.2	80.4	79.8	77.2	72.8
III	Test Section, Station 7, 0	X				73.3	75.0	76.7	77.5	76.2	71.2
			X			76.8	75.1	74.7	73.4	71.2	68.1
				X		72.4	73.0	73.7	72.5	69.5	63.8
					X	79.2	79.3	79.5	79.7	78.0	73.3
IV	Test Section, Station 0, -3.5	X				72.8	74.0	76.7	76.5	76.2	70.7
			X			76.8	75.6	74.7	74.4	71.7	69.6
				X		72.9	73.5	74.7	73.5	69.5	61.8
					X	79.3	78.6	80.5	79.7	78.2	73.7
V	Test Section, Station -15, 0	X				71.3	72.0	74.7	75.0	73.7	67.2
			X			75.3	72.6	73.2	72.9	70.7	66.6
				X		74.9	76.5	76.2	75.5	73.1	67.8
					X	78.8	78.7	79.5	79.2	77.3	71.9
VIII	Test Section, Station -0, 0	X				73.3	73.0	76.1	75.0	74.2	68.7
			X			77.8	76.1	76.1	74.4	71.7	69.6
				X		72.9	73.0	74.7	76.0	72.9	66.8
					X	80.0	79.1	80.1	79.8	77.8	73.1
	PWL Average				X	79.6	79.0	80.0	79.6	77.7	73.0
	ILG SOUND POWER AVERAGE CALIB.				X	80.5	81.0	81.7	82.0	79.0	75.5
	PWL$_{ILG}$ - PWL$_{EST}$				X	0.9	2.0	1.7	2.4	1.3	2.5
	REF, 10 log (Sα_t/337)					1.1	0.7	0.9	2.2	2.3	2.4

*PWL, dB re 10^{-12} Watt; SPL dB re 20 μ N/$_m$2

chamber sound pressure level with angle of attack, Figure 11.
The measurement variation was attributed to source directionality
as well as location in the test section. In order to understand
source acoustic power distribution and improve measurement ac-
curacy, a sound power measurement calibration was performed in
July 1974, with a highly directional source of known character-
istics (40). The source and rotational drive are shown in
Figure 12. In addition to the four settling chamber microphones,
preparation room and diffuser leg microphones were used, Figure
5c. The microphone signals were averaged on line with time
division multiplexers, passed thru log converters, and plotted
as a function of source-to-boom angle ψ of 360° while positioned
at angles of attack, α = 0, 30 and 90°. The horn was driven with
octave band noise centered at 500, 1000 and 2000 Hz, then with
one-third octave band noise centered at 6300, 8000 and 10,000 Hz.
The averaged chamber sound pressures were plotted on-line as a
function of ψ, Figure 13.

The curves for each chamber were replotted and averaged using
the source angle in the tunnel ($\alpha + \psi$) as the common absissa
Figure 14. The average responses so obtained for the individual
chambers were converted to sound power estimates using the
chamber calibrations, Table III, plotted together for each octave
band, and summed. These resulting summation plots had an in-
ordinate contribution from the preparation room microphone. The
summed sound power estimate rose 3 dB when the source was
directed towards the side walls. The preparation room contri-
butions were then reduced by 3 dB. This was justified by con-
sidering that the preparation room microphones were directly
under the test section and were measuring near field as well as
reverberant noise.

The results of the calibration with the directional source so
obtained are presented in Figures 15 through 17. The calcu-
lated summations of sound power vary only ±1 dB with source
angle even though the variation within individual chambers is
as great at ±10 dB. The indicated sound power levels are
compared with the calibrated source levels, Table VIII.

TABLE VIII

ESTIMATION OF SOUND POWER OUTPUT OF HORN DIRECTIONAL SOURCE
IN WIND TUNNEL USING MEASUREMENTS IN THREE CHAMBERS

Data Source	Band Center Frequency, Hz						
	500	1K	2K	4K	6.3K	8K	10K
Indicated Level	112	112	111	107	105	103	100
Calibrated Source Level (40)	(112.5)	112	111	104	100.5	97.5	93.5
Difference, Indicated (−) Cal	−0.5	0	0	3	4.5	5.5	6.5

The differences between indicated and calibration levels are at-
tributed to the direct field radiation of the horn source dom-
inating the settling chamber microphone reverberant field. The
direct field and reverberant field contributions for three dif-
ferent sources are calculated in Table IX. As would be expected,
the more directional the source, the higher the direct field
contribution relative to the reverberant.

The same trends are expected for diffuser and preparation room
measurements, because the distance from source to microphone
are similar. This is confirmed by observing that the sums of
estimated sound power were invariant with angle, Figures 15,
16 and 17.

TABLE IX

ESTIMATION OF REVERBERANT AND DIRECT FIELD CONTRIBUTION TO MEASURED SETTLING CHAMBER SOUND PRESSURE LEVELS FOR THREE DIFFERENT SOURCES

SOURCE	FIELD	QUANTITY	BAND CENTER FREQUENCY, H_z							
			250	500	1000	2000	4000	6300	8000	10,000
ILG	Rev	PWL_{ts}	80.5	81.0	81.7	82.0	79.0	–	75.5	–
		Π (Table IV)	-6.5	-6.5	-4.0	-5.0	-5.5	–	-7.5	–
		$PWL_{sc}=PWL_{ts}+\Pi$	74.0	74.5	77.7	77.0	73.5	–	68.5	–
		Δ^*, $PWL_{sc}-SPL_{sc}$	15.3	15.5	16.0	16.8	18.4	–	21.0	–
		$SPL_{sc}=PWL_{sc}-\Delta$	58.7	59.0	61.7	60.2	55.1	–	47.5	–
	Dir	SPL_{10}	58.2	61.5	63.7	63.3	56.0	–	50.0	–
		$\Delta_r=20 \log 7+A^*$	17.0	17.0	17.0	17.3	18.0	–	19.4	–
		$SPL_{70}=SPL_{10}-\Delta_r$	41.2	44.5	46.7	46.0	38.0	–	30.6	–
		$DI=SPL_{10}-PWL+21$	-1.3	1.5	3	2.3	-2	–	-4.5	–
LE5-2 Speaker, 0.25 Amp	Rev	PWL_{ts}	–	96.2	94.7	96.3	94.7	–	93.7	–
		Π (est)	–	-3.0	-3.0	-3.0	-2.0	–	-2.0	–
		$PWL_{sc}=PWL_{ts}+\Pi$	–	93.2	91.7	93.3	92.7	–	91.7	–
		Δ, $PWL_{sc}-SPL_{sc}$	–	15.5	16.0	16.8	18.4	–	21.0	–
		$SPL_{sc}=PWL_{sc}-\Delta$	–	77.7	75.7	76.5	73.3	–	70.7	–
	Dir	PWL	–	96.2	94.7	95.7	94.7	–	93.7	–
		$10 \log Q = DI$	–	5.5	7.0	7.0	13.0	–	14.0	–
		$SPL_{1.0}=PWL+DI-1$	–	101.7	100.7	101.7	106.7	–	106.7	–
		$\Delta_r=20 \log 70+A$	–	37.0	37.0	37.3	38.0	–	39.4	–
		$SPL_{70}=SPL_1-\Delta_r$	–	64.7	63.7	64.4	68.7	–	67.3	–
Horn 0.25 Amp	Rev	PWL_{ts}	–	112.5	112.0	111.0	104.0	100.5	97.5	93.5
		Π(Fig 15,16,17)	–	-2.0	-1.0	-0.5	-0.5	-0	-0	-0
		$PWL_{sc}=PWL_{ts}+\Pi$	–	110.5	111.0	110.5	104.5	100.5	97.5	93.5
		Δ, $PWL_{sc}-SPL_{sc}$	–	15.5	16.0	16.8	18.4	20.0	21.0	22.1
		$SPL_{sc}=PWL_{sc}-\Delta$	–	95.0	94.0	93.7	96.1	80.5	76.5	71.4
	Dir	PWL	–	112.5	112.0	111.0	104.0	100.5	97.5	93.5
		$10 \log Q = DI$	–	12	19.0	18.5	18.0	22.0	23.5	26.5
		$SPL_{1.0}=PWL+DI-1$	–	123.5	130.0	128.5	121.0	121.5	120.0	119.0
		$\Delta_r=20 \log 70+A$	–	37.0	37.0	37.0	37.3	38.7	39.4	40.2
		$SPL_{70}=SPL_{1.0}-\Delta_r$	–	86.5	93.0	92.0	93.7	82.8	80.6	79.8

*All atmospheric absorption terms calculated for conditions of relative humidity, 30%, temperature 68° F; A = atmospheric absorption,70 ft. from Fig.4

-36-

The implication is that reverberant sound power measurement is dependent on source directivity, even if all three chamber microphones are used. Fortunately, typical inlets are not expected to have directionality indices (DI) in excess of 20 dB like the horn source. The LE5-2 speaker has DI's ranging from 6.5 to 14, which may be more typical. The speaker has a worst case settling chamber sound pressure contribution of reverberant = 70.7 dB versus direct = 67.3 dB. This would raise the measured levels measured by the settling chamber microphones by 1.6 dB, compared with the 6.5 dB worst case error with the horn source.

4.2.3 Hardwall Reverberant Calibration Summary

The measurement of sound power in the hardwall configuration depends on three factors:

a.   The PWL-SPL calibration from the settling chamber, (and preparation room plus diffuser if used)

b.   The fractional part of the source energy exiting to the settling chamber (or absorbed in test section if all three chamber measurements used).

c.   The contribution of the source direct field to the microphone signals in the receiving chambers.

Approximations for these three factors are presented as Figures 18, 19 and 20 respectively. Since the three chambers are reasonably close in response, Figure 18 may be used as the PWL-SPL calibration for all three.

The use of these figures is best explained by example. Suppose the following data were taken in the 4000 Hz octave band when

the measured relative humidity was 50%.

Chamber	SPL
Settling Chamber	84
Preparation Room	81
Diffuser Leg	81

From Figure 18, Δ = 18 dB.

From experience, the source directionality index is assumed to be 10 dB, with the main lobe pointing towards the settling chamber. From Figure 19, Π = -3dB, and from Figure 20 SPL_{rev} - SPL_{dir} = 10 dB.

Using only the settling chamber reading

$$PWL = SPL + \Delta - \Pi$$
$$= 84 + 18 + 3 = 105 \text{ dB}$$

Correcting for the direct field contribution (10 dB below the reverberant field), the final source sound power estimate is 104.6 dB re 10^{-12} watt.

Using all three chamber readings

$$PWL_{sc} = 84 + 18 = 102$$
$$PWL_{pr} = 81 + 18 = 99$$
$$PW_{ds} = 81 + 18 = \underline{99}$$
$$\text{Total} \quad 105 \text{ dB}$$

Again, correcting for the direct field contribution to the
measured sound pressure levels, the source sound power estimate
is 104.6 dB re 10^{-12} watt.

4.3 Direct Field Calibration

As previously reported (16), the direct field measurement
characteristics of omni, and directional sources have been
evaluated by two methods. The decrease in sound pressure level
with distance from a 5.5 inch fan-inlet noise source was
measured by LeRC for both the hard wall (present configuration)
and soft wall cases. The information of interest were the near
field characteristics of the nonideal source and the extent of
the direct acoustic field.

The second method utilized the ILG sound power source to define
the properties of the test section reverberant field (Table III).

Both methods led to an evaluation of the radius at which the
reverberant and direct fields are equal. This radius is nomi-
nally 3.0 feet from all frequencies. Some consistent variations
occur with position in the test section, but precise analysis
is frustrated by the nonstationarity of the fan as a noise
source.

The ability to describe directionality patterns of highly
directional sources has subsequently been evaluated by rotating
the microphone boom around the horn for 180 combinations of horn
orientation, microphone radii, and frequency. The testing was
performed on 17 July 1974. The horn and microphone boom with
omnidirectional microphones are shown in Figure 21. The omni-
directional microphones are mounted on weathervaning "swords"

to keep the microphone pointing into the flow, minimizing
microphone wind noise.

The test conditions and the measured centerline sound pressure
levels are listed in Tables X and XI. These tables show that the
centerline sound pressure level of a highly directional source
can be measured accurately at radii from 2 to 10 feet. More
specifically, the data indicate the following:

1. The reproducability of the results for a given frequency
    band and orientation in the tunnel, expressed as one
    standard deviation, ranges from 0.6 to 1.7 dB.

2. Angling the source towards the wall (Table XI) raised
    the measured source centerline levels from the measurements
    made with the source pointing downstream (Table X) in five
    of six bands.

3. The accuracy in measurement of the one-foot centerline
    sound pressure levels, relative to the calibrated free
    field levels, range from -1.5 dB to 3.4 dB.

4. The decreasing amount of test data for large microphone
    radii (5 and 10 feet) as the source is positioned and
    angled towards the wall (Table XI) emphasizes the
    geometrical constraints in the 9 x 15 foot test section.

5. The data measured at the three foot microphone position
    for $\alpha = 30°$, $\psi = - 90°$, in frequency bands 1000, 2000, and
    4000 Hz, average 10 dB lower than comparable data. It was
    assumed that an attenuator switch position was improperly

Table X.   Hardwall Directionality Test Condition Summary With
Measured Horn Centerline Sound Pressure Levels,
Source Pointing Down Tunnel Centerline

Angle of attack α	Horn angle re inlet ψ	Boom Length ft.	Mic Radius from Horn Face, r, ft.	20 log d, d= r + 4	Input Signal Band Center Frequency Hz											
					1000		2000		4000		6300		8000		10,000	
					Mic SPL+ at radius		Mic SPL at radius		Mic SPL at radius		Mic SPL at radius		Mic SPL at radius		Mic SPL at radius	
					r	1.0'	r	1.0'	r	1.0	r	1.0'	r	1.0'	r	1.0'
0°	0°	4	2	15.5	113	128.5	112	127.5	106.0	121.5	106.5	122	107	122.5	103.2	118.7
		10	2	15.5	114.3	129.8	112.5	128	106	121.5	107	122.5	106	121.5	102	117.5
		6	2.5	16.3	114.5	130.8	113	129.3	106	122.3	107	123.3	106	122.3	102	118.3
		4	3	16.9	111.7	128.6	109.5	126.4	105.0	121.9	105.2	122.1	105.2	122.1	100.7	117.6
		6	3.5	17.5	112.0	129.5	112	129.5	106.0	123.5	105.0	122.5	103.5	121	99.5	117
		4	4	18.1	110.5	128.6	108	126.1	103.3	121.4	104.0	122.1	104	122.1	99.5	117.6
		10	5	19.1	112	131.1	111	130.1	105	124.1	104.5	123.6	102.7	121.8	99	118.1
		6	6	20	109.5	129.5	110	130	104	124	102.5	122.5	102.2	122.2	98.5	118.5
		10	10	22.9	107.5	130.4	107.3	130.2	101	123.9	99	121.9	99.2	122.4	98	120.9
30°	-30°	4	2	15.5	112.2	127.7	112	127.5	105.8	121.3	106.5	122	106.6	122.1	103.3	118.8
		10	2	15.5	114	129.5	112.6	128.1	106	121.5	108	123.5	106.8	122.3	102.2	117.7
		6	2.5	16.3	108	124.3	112	128.3	101	117.3	105.5	121.8	105.5	121.8	100.5	116.8
		4	3	16.9	111	127.9	111	127.9	105.7	122.5	105.8	122.7	106	122.9	102	118.9
		6	3.5	17.5	111.7	129.2	111.6	129.1	105.8	123.3	103	120.5	104	121.5	98.6	116.1
		4	4	18.1	109.7	127.8	109.5	127.6	104.3	122.4	104	122.1	104.9	123	101.8	119.9
		10	5	19.1	111.8	130.9	111.6	130.7	105.1	124.2	103.5	122.6	103.8	122.9	98.3	117.4
		6	6	20	108.6	128.6	109	129	104	124	102	122	102	122	98	118
		10	10	22.9	107.8	130.7	108	130.9	101.5	124.4	98.8	121.7	100.3	123.2	96.5	119.4
Average value (0°/0° and 30°/-30°)					---	129.1	---	128.7	---	122.5	---	122.3	---	122.2	---	118.2
Measurement standard deviation, dB					---	1.6	---	1.4	---	1.7	---	0.7	---	0.6	---	1.2
Free Field, Table IX and Ref. (40)					---	130	---	128.5	---	121	---	121.5	---	120	---	119
Difference, Free Field (−) Average					---	0.9	---	0.2	---	1.5	---	0.8	---	2.2	---	-0.8

+SPL, dB re 20 µ N/m², Horn current 0.25 ampere

Table XI. Hardwall Directionality Test Condition Summary With
Measured Horn Centerline Sound Pressure Levels,
Source Angled Towards Wall

Angle of attack α	Horn angle re inlet ψ	Boom Length ft.	Mic Radius from Horn Face r,ft.	20 log d, d = r + 4	Input Signal Band Center Frequency Hz											
					1000		2000		4000		6300		8000		10,000	
					Mic SPL at Radius		Mic SPL at Radius		Mic SPL at Radius		Mic SPL at Radius		Mic SPL at Radius		Mic SPL at Radius	
					r	1.0'	r	1.0'	r	1.0'	r	1.0'	r	1.0'	r	1.0'
0°	-60°	4	2	15.5	112.7	128.2	113	128.5	107	122.5	107	122.5	108.5	124	105	120.5
		4	3	16.9	112	128.9	112	128.9	107	123.9	106.7	123.6	107.5	124.4	105.3	122.2
		4	44	18.1	111.2	128.3	111	129.1	106	124.1	105.7	123.8	106.5	124.6	103	121.1
30°	-90°	4	2	15.5	113.4	128.9	112.6	128.1	107.1	122.6	107.3	122.8	108.0	123.5	104.0	119.5
		4	3	16.9	102.2	119*1	102.0	118*9	97.9	114*8	105.5	122.4	106.3	123.2	104.9	121.8
		6	3.5	17.5	110	127.5	112.0	129.5	107.0	124.5	104.2	121.7	105.4	122.9	103.6	121.1
		4	4	18.1	100.8	118*9	100.9	119*	97.9	116*	104.8	122.9	105.9	124	102.4	120.5
		6	6	20	107.9	127.9	111.2	131.2	106.4	126.4	103.5	123.5	104.5	124.5	101.5	121.5
Average value (0°/-60°,30°/-90°)					---	128.5	---	129.1	---	124.4	---	122.9	---	123.9	---	121
Measurement standard deviation, dB						0.6		0.9		1.4		0.7		+0.6		+0.9
Free Field, Table IX and Ref. 40					---	130	---	128.5	---	121	---	121.5	---	120	---	119
Difference, Free Field (−) Average					---	-1.5	---	0.6	---	3.4	---	1.4	---	3.9	---	2.0

*Levels increased by 10 dB for averaging

documented. The levels were arbitrarily increased by
10 dB for averaging.

Typical directionality plots obtained on-line are presented
in Figure 22. Typical horn directivity curves were replotted
relative to the source centerline levels and compared with
anechoic conditions in Figures 23 through 26. These figures
show the characteristic result that the main lobe of the
directionality pattern is well defined to the 3 dB point where
it begins to broaden out. This characteristic does not change
significantly with radius from the source. However, the skirt
of the directionality pattern is raised by acoustic reflections
for the six foot radius measurements (Figures 25 and 26)
relative to the three foot radius measurements (Figures 23 and
24). Therefore, the hall radius which is 3.0 feet for hardwall
test section appears to be a limitation on the direct field
measurement of highly directional sources as well as omni-
directional sources.

4.4 Tunnel and Microphone Wind-On Noise

With the tunnel running, both the settling chamber and test
section microphones evidence levels in excess of the electrical
noise floor. Typical settling chamber measurements are presented
as Figure 27 for test section dynamic pressures (q) ranging from
9.5 to 45 psf (455 to 2153 N/m^2). Normalizing these data by the
third power of the dynamic pressure yields a good fit, Figure 28.
In addition to the normalized sound pressure levels, Figure 28
also shows the prediction of grille noise attributed to the
cooler coil bank. This prediction was derived from the sound
power generation model, Section 3.2.4 of this report, and the

settling chamber calibration, Table III. The low frequency
cooler coil predicted levels are significantly lower than the
measured levels. Above 2000 Hz, the predicted levels approach
the measured levels, suggesting a significant contribution.

Figure 29 shows normalized sound pressure levels for the pre-
paration room. These levels are similar to those measured in
the settling chamber. This is the same result as observed with
an omnidirectional source in the test section, Table V.

Test section microphone, wind-on, noise measurements for
dynamic pressures of 20 to 60 psf (957 to 2871 N/m^2) are shown
in Figure 30. These data were normalized by 30 log q/q_{ref},
and are presented in Figure 31. Also presented in Figure 31 are
predictions of microphone wind noise, turbulent boundary layer
noise, and vortex noise from inlet support and trailing edges.
The sound pressure level predictions are derived from the sound
power level predictions, Sections 3.2.1, 3.2.2, and 3.3.3,
respectively, along with the test section calibration, Table III.
Only the noise predicted for the transition of the test section
to the diffuser, which is admittedly inappropriate, agrees with
the measured data over all frequency bands. In spite of
inappropriate application of the noise generation model, the
favorable comparison of model and measured results indicates
that significant noise generation may be associated with flow
entering into the diffuser. The microphone turbulence generated
predicted levels intersect the measured levels in the high
frequency bands, indicating a contribution to the test section
microphone measured levels, at least for $q \leq 25$ psf.

With respect to microphone wind noise, the shape of the predicted
spectra is different from the measured spectra, Figure 31. In

addition, the measured spectrum is different, in shape, from
other microphone, turbulence generated, noise measurements.
Figure 32. Finally, the measurements made in the test section
vary as U^6, not U^4. All these factors suggest that the test
section microphone is sensing acoustic noise, not pseudo-noise
from turbulence.

Figure 33 compares the normalized settling chamber measurements
with levels which could be attributed to test section sources.
The agreement again suggests that the measured test section
levels are indeed acoustic.

5.0   CONCLUSIONS AND RECOMMENDATIONS

The results of this study indicate that accurate source sound
power estimations can be made in the hardwall configuration
using settling chamber sound pressure level measurements along
with relative humidity levels and approximations of source
directivity. The measurement standard deviation ranges from
0.2 to 3.9 dB.

The accuracy of source sound power estimations can be improved
if preparation room and diffuser leg sound pressure level
measurements are used along with settling chamber sound pressure
level measurements. In addition, approximation of source
directivity would be required only to avoid errors due to
direct field levels exceeding reverberant field levels, not
for sound power distribution. With these steps the measurement
standard deviation may be reduced to $\pm$ 1.0 dB.

Accurate direct field measurements in the test section are
limited to a radius of 3 feet by the reverberant field, with
the one exception of a highly directional source pointing
directly upstream. The measurement reproducibility ranges
from 0.6 to 1.7 dB (one standard deviation). The source measure-
ment accuracy ranges from - 1.5 to 3.4 dB. This may be due in
part to source strength variation.

The dominant source of wind-on microphone noise cannot be
precisely identified from analytic models and available data.
However, the results suggest the following conclusions:

1.   Sound pressure levels measured by test section microphones
     are due to true acoustic levels, not turbulence induced
     pseudo-noise.

2. The most likely area of significant noise generation is
    the transition from the test section to the diffuser.

If reduction of wind-on noise is required, measurements should
be made to support or contradict these conclusions. Removing
the nose cone from a test section microphone and measuring wind-
on noise would be the most instructive. Surveys down the
diffuser would also be of benefit.

The conduct of these tests has served to emphasize various
procedural errors, equipment problems, and pitfalls. The
following recommendations are intended to help avoid subsequent
problems.

1. Measure relative humidity in the settling chamber and
    relate to weather bureau readings. Utilize for sound
    power estimation from existing settling chamber sound
    pressure data.

2. Utilize a calibration, electro dynamic omni-directional
    source for subsequent evaluation and calibrations.

3. On-line presentation of levels is feasible and should be
    encouraged.

4. Maintaining end-to-end calibration traceability is
    essential.

5. The driven shield connection between cathode follower and
    sword should be checked routinely (the sensitivity should
    not be changed by moving the microphone from cathode
    follower to sword).

6. The test section should be lined with acoustical absorptive
    material in order to measure directivity (already done).

7. When using a microphone in the preparation room for source
    sound power estimation, place the microphone in the center
    of the work area, not near the test section slots.

6.0 SYMBOL DEFINITION

The symbols used throughout this report are principally
defined with English units because the wind tunnel dimensions
and dynamic pressure are described in English units. However,
nondimensional and engineering relations are expressed in
both English and SI units for reference as follows:

Symbol	Definition	Units
A	Atmospheric absorption at 70 feet, dB	-
c	Speed of sound	ft/sec (m/sec)
C_d	Coefficient of drag	-
d	Spoiler diameter	ft(m)
DI	Directivity index, 10 log Q	-
D_p	Pipe diameter	ft (m)
f	Frequency	Hz
f_c	Cutoff frequency	Hz
f_p	Peak frequency	Hz
k	Constant of proportionality, expressed in dB	-
m	Atmospheric absorption	1/ft (1/m)
p(t)	Fluctuating dynamic pressure	lb/ft^2 (N/m^2)
p(t)	Time average rms pressure	lb/ft^2 (N/m^2)
P_i	Fraction of source sound power to that exiting to the ith chamber	-
PWL	Sound power level, dB re 10^{-12} Watt	-

Symbol	Definition	Units
PWL_{OA}	Overall sound power level, dB re 10^{-12} Watt	–
$PWL(\omega)$	One-third octave band sound power level, dB re 10^{-12} Watt	–
q	Dynamic pressure	lb/ft^2 (N/m^2)
Q	Directivity	–
r	Radius	ft (m)
r_H	Hall radius	ft (m)
S	Area	ft^2 (m^2)
SPL	Sound pressure level, dB re 20 $\mu N/m^2$	–
T_R	Reverberation time (60 dB)	seconds
u	Fluctuating velocity	ft/sec (m/sec)
U	Mean velocity	ft/sec (m/sec)
V	Volume	ft^3 (m^3)
W	Edge length	ft (m)

Symbol	Definition	Units
α	Angle of attack	degrees
α	Acoustic absorption coefficient	–
α_t	Average total absorption	–
α_{SAB}	Sabine absorption (in the absence of atmospheric absorption)	–
β	Angle of microphone boom relative to inlet centerline	degrees
γ	Angle between source centerline and representative transition point	degrees
δ	Boundary layer thickness	ft (m)
δ^*	Boundary layer displacement thickness	ft (m)
Δ	$PWL_i - SPL_i$ dB	–
Δ_r	Attenuation due to spherical spreading, 20 log r	–
ϵ	Normalized pressure drop	–
Π	Power index, 10 log P	–
ρ	Density	$slugs/ft^3 (kg/m^3)$
τ	Turbulence index, u/U	–
ψ	Angle of source relative to inlet centerline	degrees
ω	Radial frequency, $2\pi f$	radians/sec

REFERENCES

1. Yuska, J.A., Diedrich, J.H., Clough, N., "Lewis 9 x 15
    Foot V/STOL Wind Tunnel," NASA TM X-2305, July 1971.

2. Beranek, Leo L., Labate, Samuel, and Ingard, Uno:
    Acoustical Treatment for the NACA 8-by 6-Foot Supersonic
    Propulsion Wind Tunnel. NACA TN 3378, 1955.

3. Rentz, P.E., Scharton, T.D., Wilby, J., "Shotgun and
    Cannon Directional Microphone Calibrations and Wind Tunnel
    Acoustic Measurements," BBN Technical Memorandum 19410-4,
    18 July 1975.

4. Bies, D.A., "Investigation of the Feasibility of Making
    Model Acoustic Measurements in the NASA Ames 40 x 80 Foot
    Wind Tunnel," BBN Report 1870 (Contract NAS2-5742),
    April 1970

5. Bies, D.A., "Investigation of the Feasibility of Making
    Model Acoustic Measurements in the NASA Ames 40 x 80 Foot
    Wind Tunnel," BBN Report 2088 (Contract NAS2-6206), 1971.

6. Arndt, R.E.A., Boxwell, D.A., "A Preliminary Analysis of
    the Feasibility of Rotor Noise Measurements in the AMRDL-
    Ames 7 x 10 foot Wind Tunnel," NASA Working Paper,
    October 1971.

7. Arndt, R.E.A., Boxwell, D.A., "A State-of-the-Art Report
    on Aeroacoustical Testing in Conventional Wind Tunnels,"
    Paper at 84th Meeting Acous. Soc. Amer., Miami Beach,
    Florida, November 1971.

8. Vér, I.L., Malme, C.I., Meyer, E.B., "Acoustical
    Evaluation of the NASA Langley Full-Scale Wind Tunnel,"
    BBN Report 2100, (NAS1-9559), January 1971.

9. Vér, I.L., "Acoustical Modeling of the Test Section of the
    NASA Langley Research Center's Full-Scale Wind Tunnel,
    Bolt Beranek and Newman Report 2280, Contract NAS1-9559,
    November 1971.

10. Vér, I.L., "Acoustical Evaluation of the NASA Langley
    V/STOL Wind Tunnel," BBN Report 2288 (Contract NAS1-9559),
    December 1971.

11. Holbeche, T.A., Williams, J., "Acoustic Considerations for
    Noise Experiments at Model Scale in Subsonic Wind Tunnels,"
    Royal Aircraft Establishment Rech. Rep. 72155, September 1972.

12. Oetting, R.B., "Preliminary Noise Measurements in the Open-
    Jet of the VKI Low Speed Wind Tunnel, L-1," Von Karman
    Institute for Fluid Dynamics Tech., Note 89, May 1973.

13. Vér, I.L., Franken, Peter A., "Conceptual Design Study of the
    Noise Control Treatment for the NASA Full-Scale Subsonic
    Wind Tunnel," BBN Report 2368, 15 June 1972.

14. Wilby, J.F., Scharton, T.D., "Evaluation of the NASA Ames #1
    7 x 10 Foot Wind Tunnel as an Acoustic Test Facility," BBN
    Report 2936, 30 June 1975.

15. Hayden, R.E., Murray, B.S., Galaitsis, A.G., "Preliminary
    Investigation of Acoustic Requirements for NLR 8 x 6 m Low
    Speed Wind Tunnel," BBN Report 3087, June 1975.

16. Piersol, A.G., Rentz, P.E., "Utilization and Enhancement of the NASA Lewis 9 x 15 Foot V/STOL Wind Tunnel for Inlet Noise Research," BBN Report 2743, 19 May 1974.

17. Morse, P.M., Vibration and Sound, McGraw Hill Book Company, Inc., New York, 1948, page 387.

18. Beranek, L.L., Noise and Vibration Control, McGraw Hill Book Company, New York, 1971, page 228.

19. IBID, page 242.

20. Aerospace Recommended Practice, ARP 866, "Standard Values of Atmospheric Absorption as a Function of Temperature and Humidity," Revised October 1973, Society of Automotive Engineers, 485 Lexington Ave., New York, N. Y.

21. Beranek, L.L., Noise and Vibration Control, McGraw Hill Book Company, New York, 1971, page 170.

22. Beranek, L.L., Acoustics, McGraw Hill Book Company, New York, 1954, page 114.

23. Fuchs, H.V., "Note on Aero-acoustic Measurements in Open-Jet Wind Tunnels," Institut Fuer Turbulenzforschung, Berlin, Report IB357-74/4 (1974).

24. Bruel and Kjaer Production Data Brochure 13-003, "Condenser Microphone Cartridges."

25. Rasmussen, G., "Windscreening of Microphones," Bruel and Kjaer, unpublished technical report, 9 pages.

26. Noiseux, D.U., Noiseux, N.B., Kadman, Y., "Development,
     Fabrication and Calibration of a Porous Surface Microphone
     in an Aerofoil," BBN Report 3022 (NASA CR 137652),
     March 1975.

27. Noiseux, D.U., "Study of Porous Surface Microphones for
     Acoustic Measurements in Wind Tunnels," BBN Report 2539,
     April 1973.

28. NASA Lewis letter, Reference Contract NAS 3-19410, from
     J. H. Dietrich to P. E. Rentz, dated December 10, 1974.

29. Hayden, R.E., "Noise from Interaction of Flow with Rigid
     Surfaces: A Review of Current Status of Prediction
     Techniques," NASA CR-2126, April 1973.

30. Beranek, L.L., <u>Noise and Vibration Control</u>, McGraw Hill
     Book Company, New York, 1971, page 518.

31. Yudin, E. Y., "The Acoustic Power of the Noise Created by
     Airduct Elements," *Sov. Phys.-Acoust.*, vol. 1, pp 383-398,
     1955.

32. Gordon, C., "Spoiler-generated flow noise," Part I,
     "The Experiment," and Part II, "Results," *J. Acoust. Soc.
     Am.*, vol. 43, pp. 1041-1048, 1968, and vol. 45, pp. 214-
     223, 1969.

33. Godman, R.R., and Stein, S., "Elimination of Noise in the
     Heat Exchanger of a Supersonic Wind Tunnel," NASA Lewis
     Flight Propulsion Laboratory internal memorandum, 1957.

34. Beranek, L.L., Noise and Vibration Control, McGraw Hill
     Book Company, New York, 1971, page 522.

35. Hubert, M., "Untersuchungen uber Geräusche durchstromter
     Gitter," doctoral dissertation, Berlin Tech. Univ., 1960.

36. Unpublished NASA Lewis report, transmitted via communication
     from D. Deitrick, 5/28/76.

37. Daly, B.B., "Noise Level in Fans," *Journal of the Institute
     of Heating and Ventilating Engineers*, pp. 39-51, May, 1958.

38. Sharland, I.J., "Sources of Noise in Axial Flow Fans,"
     J. Sound and Vibration, Vol. 1, No. 3, pp. 302-322, 1964.

39. Beranek, L.L., Noise and Vibration Control, McGraw Hill
     Book Company, New York, 1971, page 144.

40. BBN Technical Memorandum No. 19410-3, "Directional Acoustical
     Source Characteristics," Peter E. Rentz and John F. Wilby,
     July 1975.

41. Noiseux, D. U., "Study of Porous Surface Microphones for
     Acoustic Measurements in Wind Tunnels," BBN Report 2539,
     Submitted to: NASA Ames Research Center, April 1973.
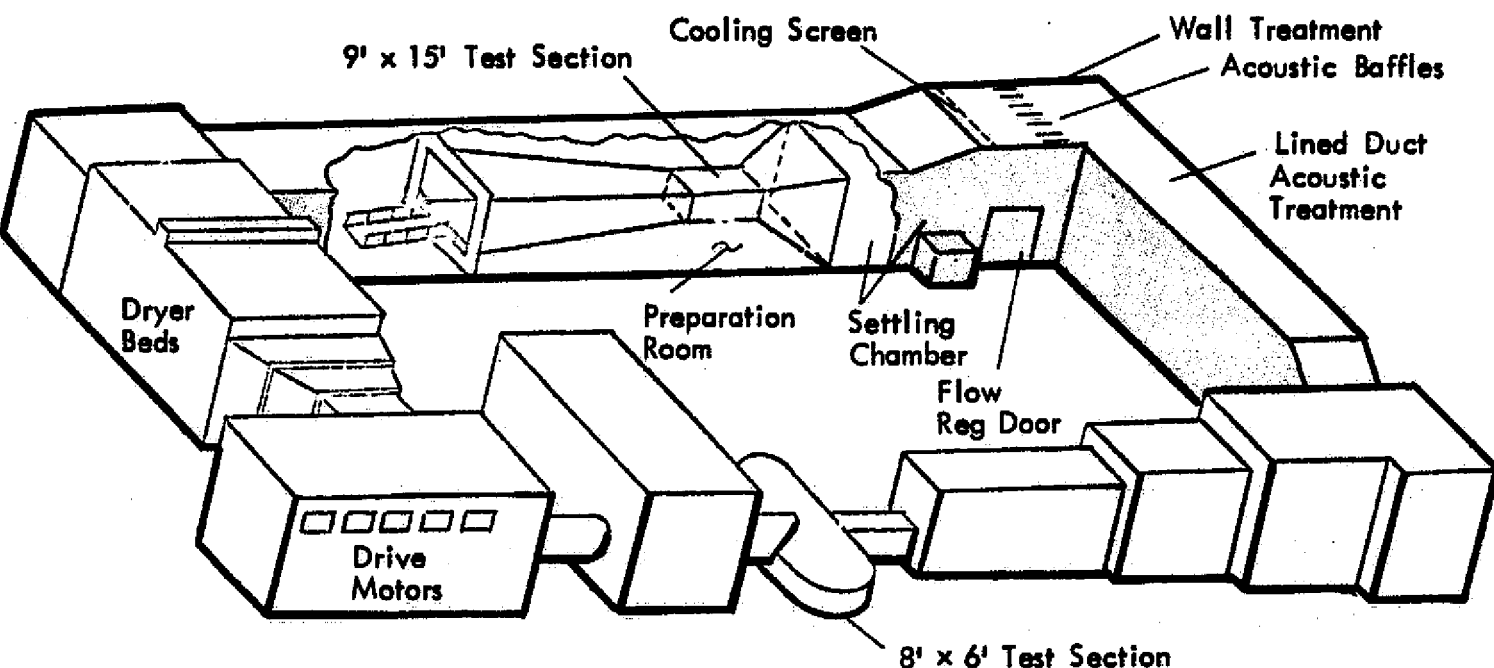
FIGURE 1. NASA LEWIS 9 x 15 FOOT LOW SPEED TEST SECTION IN RETURN LEG OF 8 x 6 FOOT SUPERSONIC WIND TUNNEL
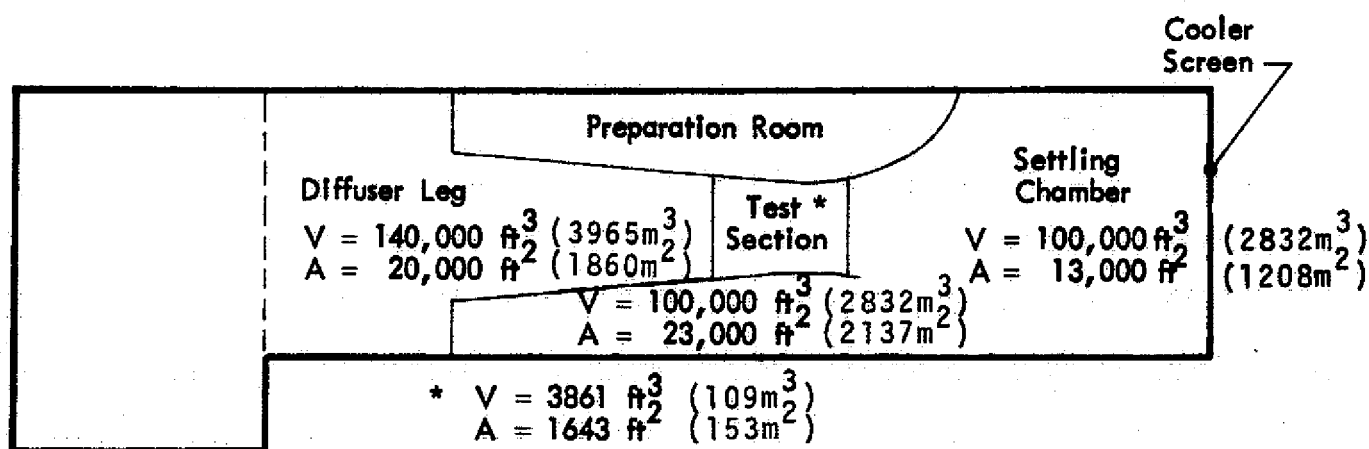
FIGURE 2. FOUR CHAMBER ACOUSTIC MODEL OF LeRC 9 x 15 FOOT LOW SPEED WIND TUNNEL
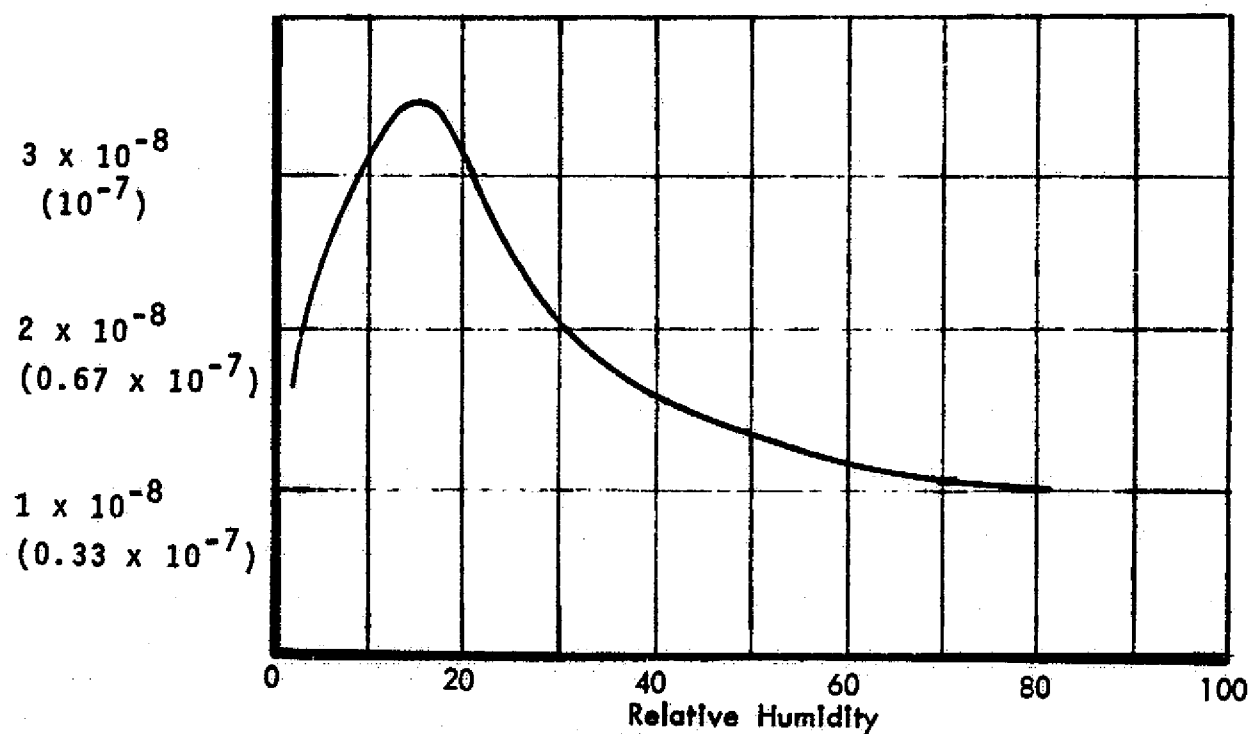
FIGURE 3. ENERGY ATTENUATION CONSTANT FOR AIR IN A REVERBERANT CHAMBER, DERIVED FROM REFERENCE 19
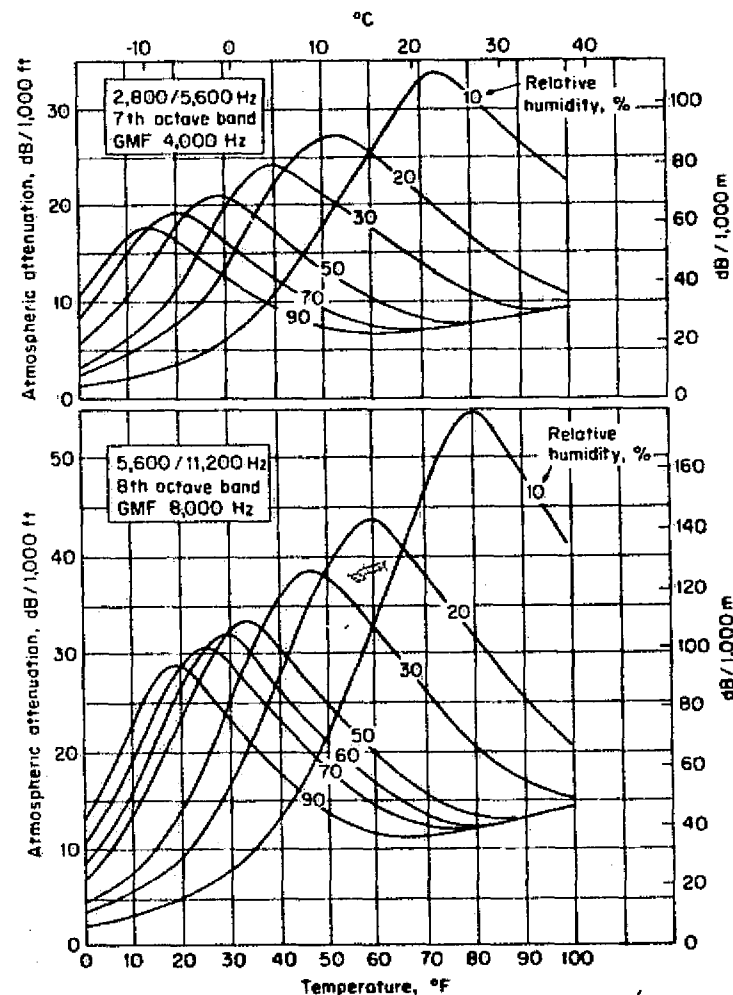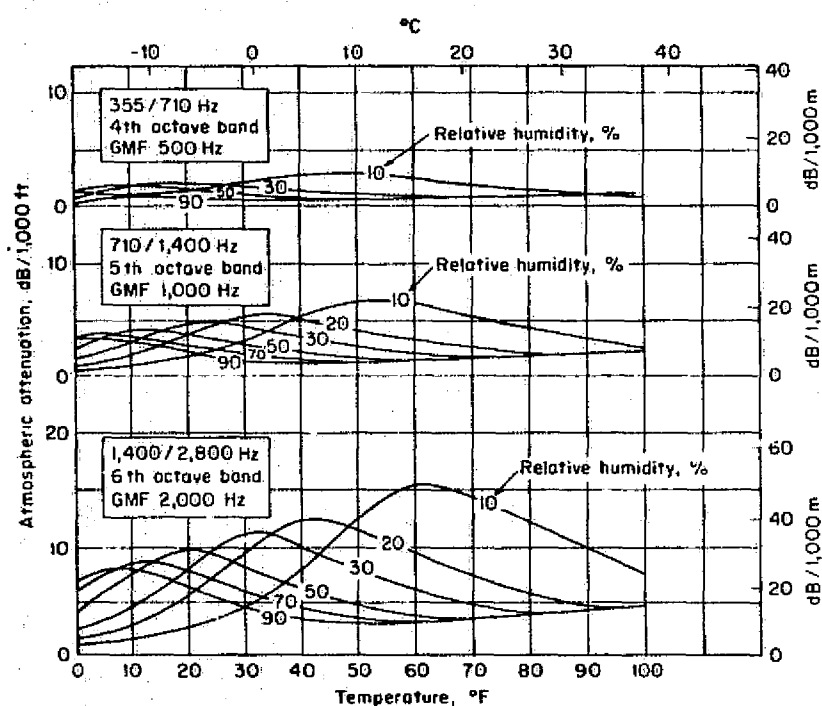
FIGURE 4. ATMOSPHERIC ATTENUATION FOR AIRCRAFT-TO-GROUND
PROPAGATION IN dB/1000 FT (OR dB/1000 m) FOR
OCTAVE BANDS CENTERED AT 500, 1000, 2000, 4000
AND 8000 Hz (21)
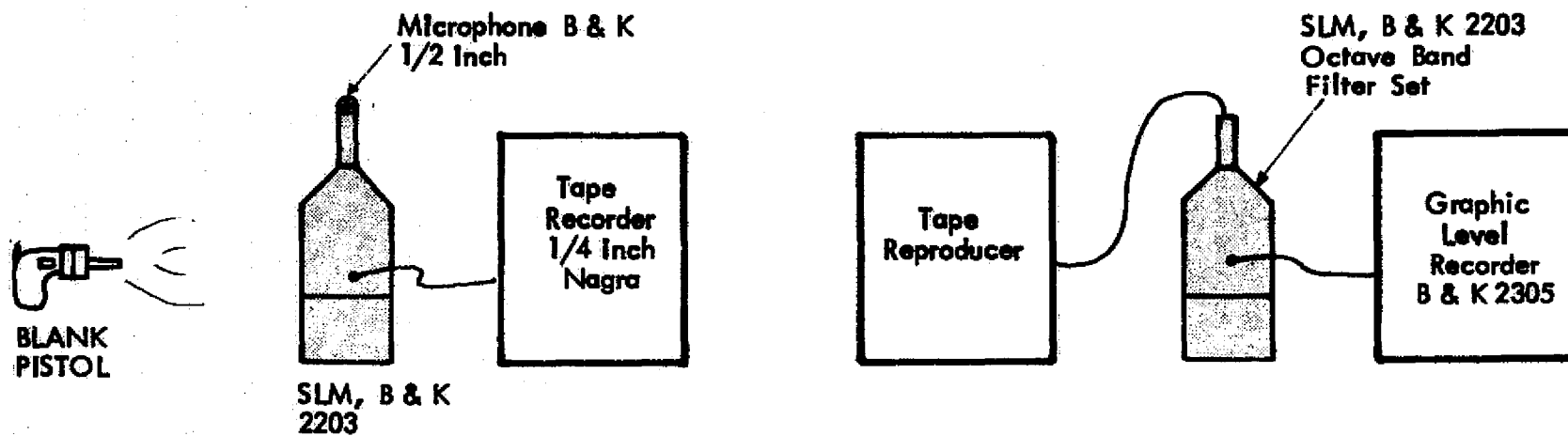
(a) IMPULSE DECAY RATE MEASUREMENT
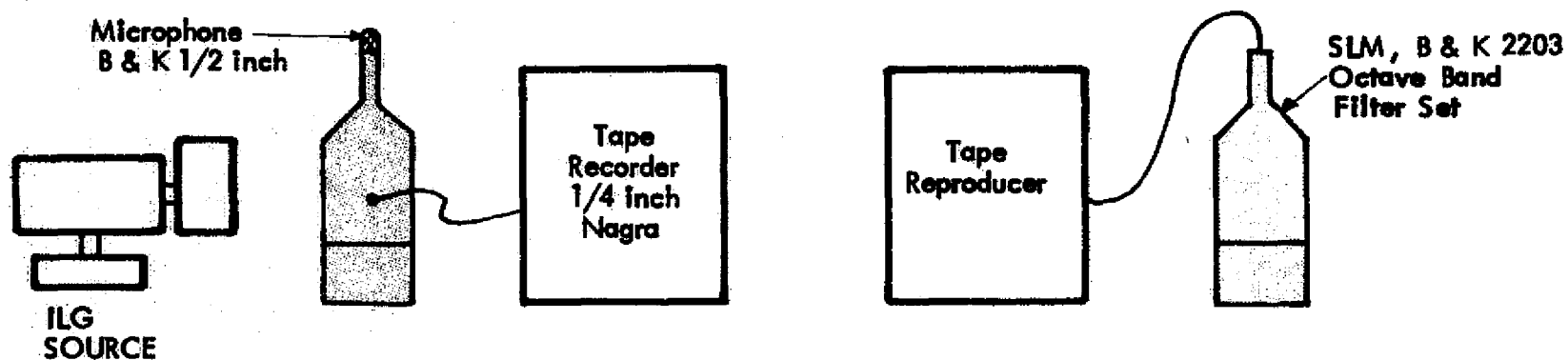
(b) SOUND PRESSURE MEASUREMENT, CALIBRATED SOUND POWER SOURCE

FIGURE 5. TEST APPARATUS AND INSTRUMENTATION BLOCK DIAGRAM

SETTLING CHAMBER

TEST SECTION

PREPARATION ROOM

(c) HARDWALL REVERBERANT CALIBRATION, DIRECTIONAL SOURCE

B & K 2607 AMPS

INSTRUMENT ROOM

CONTROL ROOM

Mike Boom Control, β

Angle of Attack Cont., $\propto$

FIGURE 5. (Cont)

TEST SECTION

SETTLING CHAMBER

PREPARATION ROOM

(d) HARDWALL DIRECTIONAL CALIBRATION, DIRECTIONAL SOURCE

INSTRUMENT ROOM

CONTROL ROOM
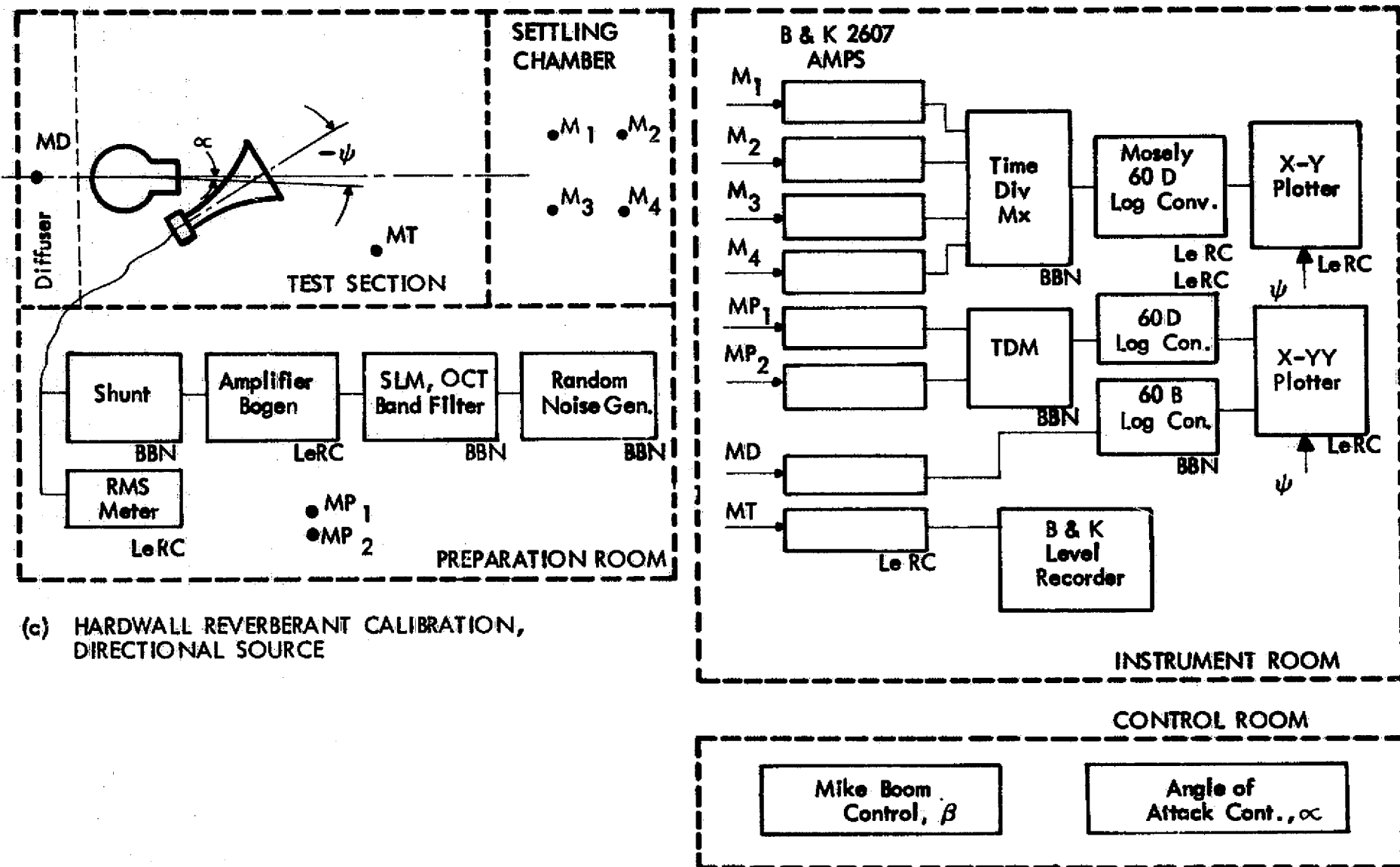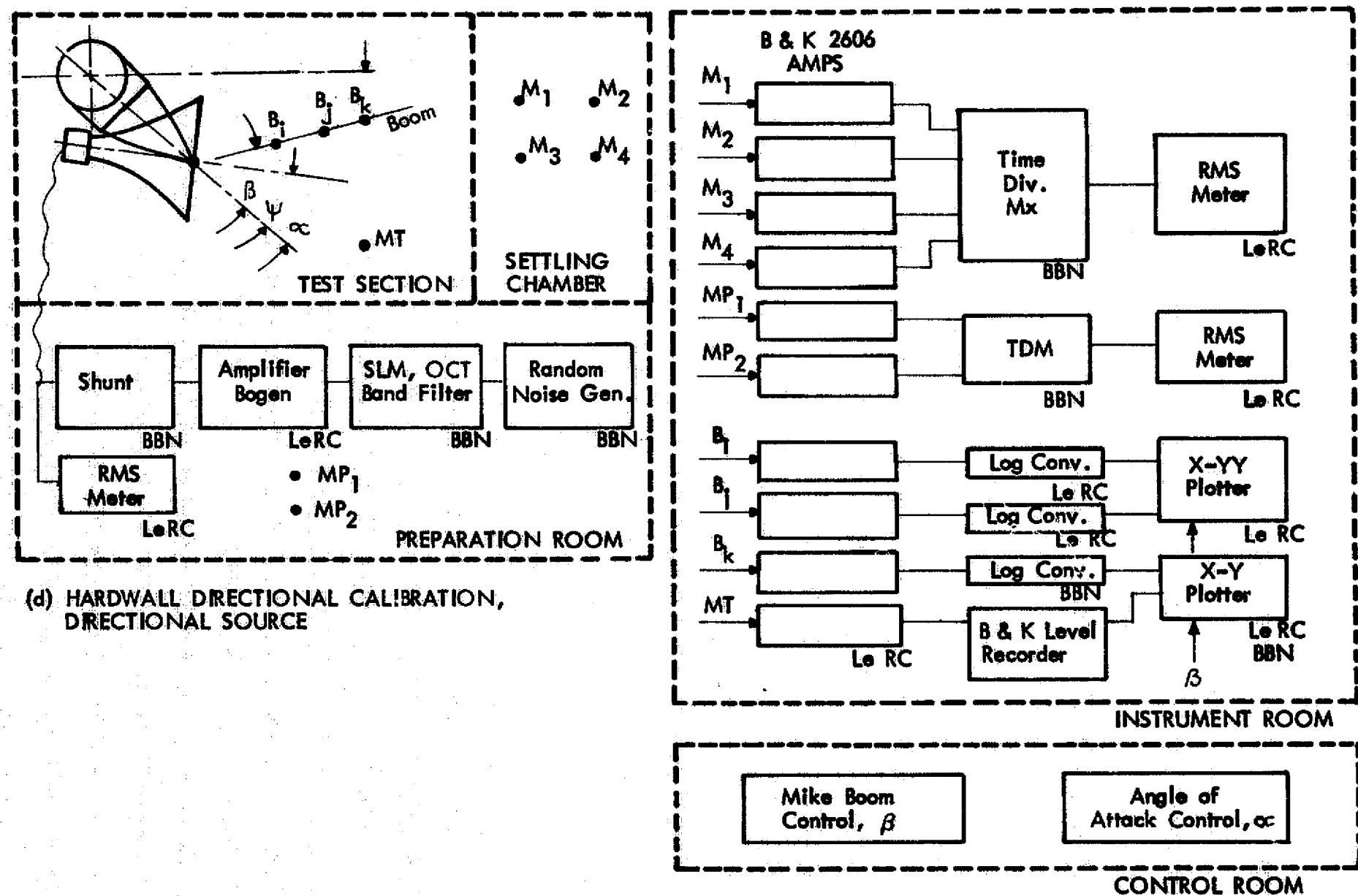
FIGURE 5. (Cont)
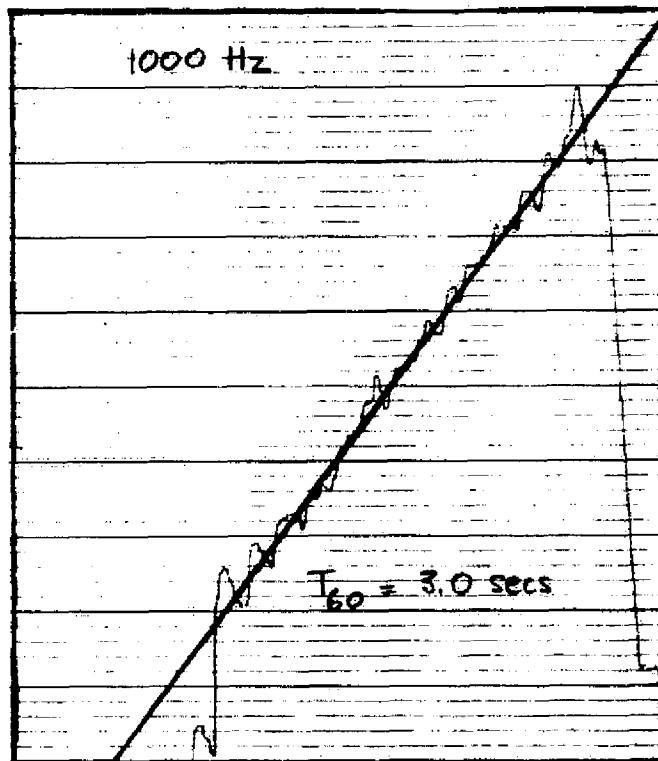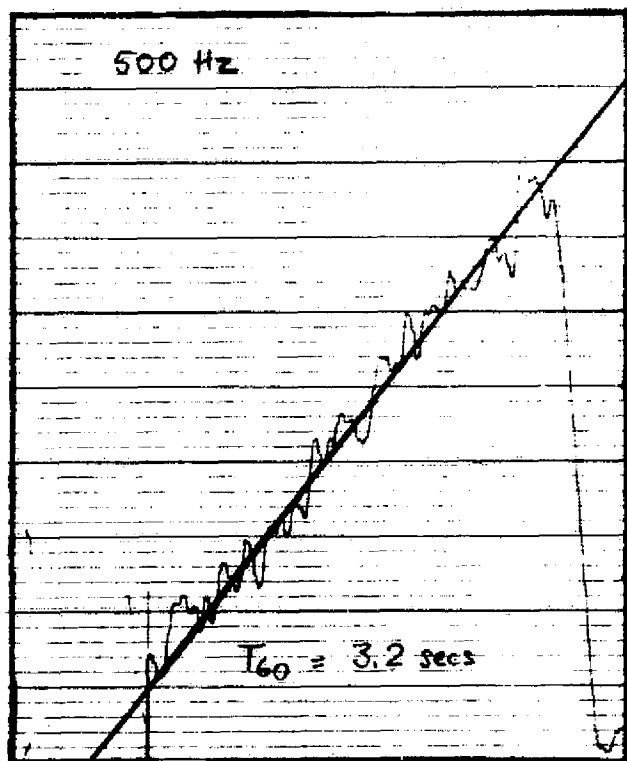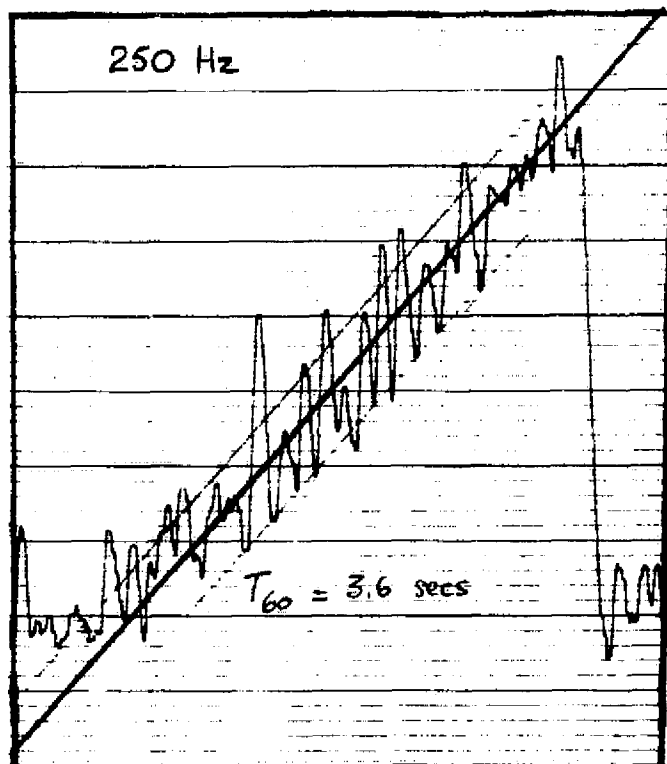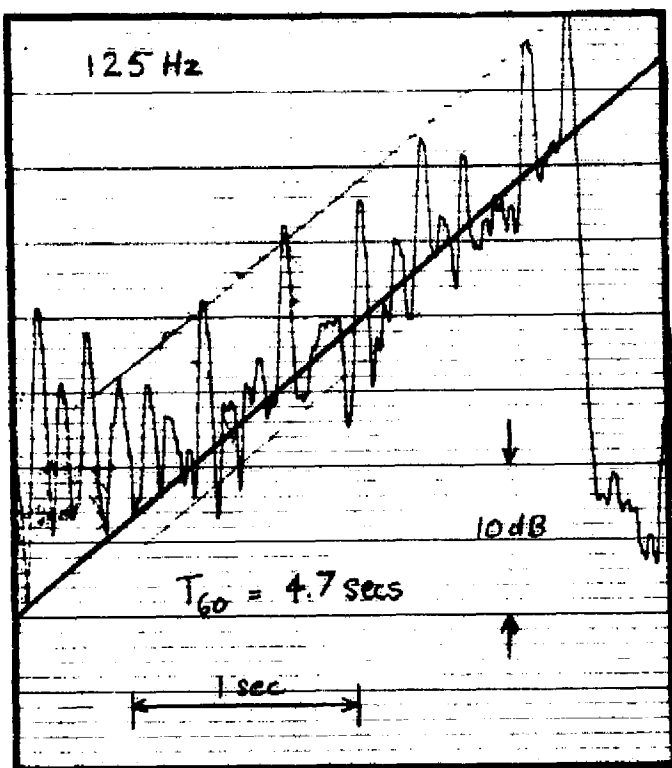
FIGURE 6. SETTLING CHAMBER OCTAVE BAND REVERBERANT DECAYS, 24 FEB 1974, TEST 2 (Tape Played Backwards)

FIGURE 6. (Cont)

125 Hz

$T_{60} = 5.8$ secs

250 Hz

$T_{60} = 5.8$ secs

500 Hz

10 dB

$T_{60} = 4.9$ secs

1 sec

1000 Hz

$T_{60} = 4.1$ secs
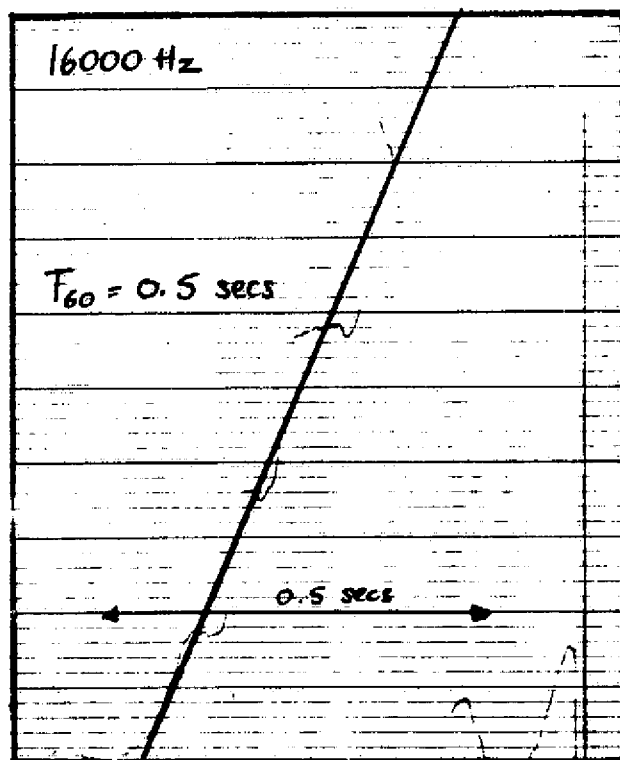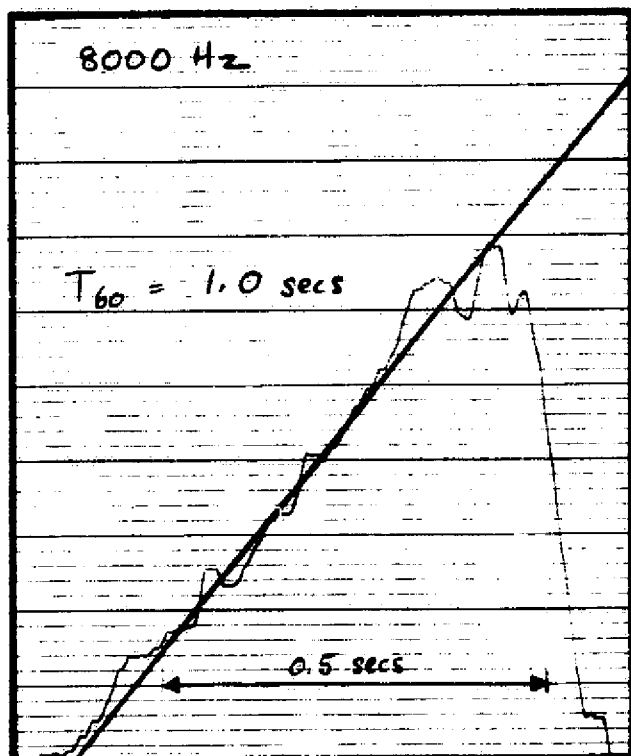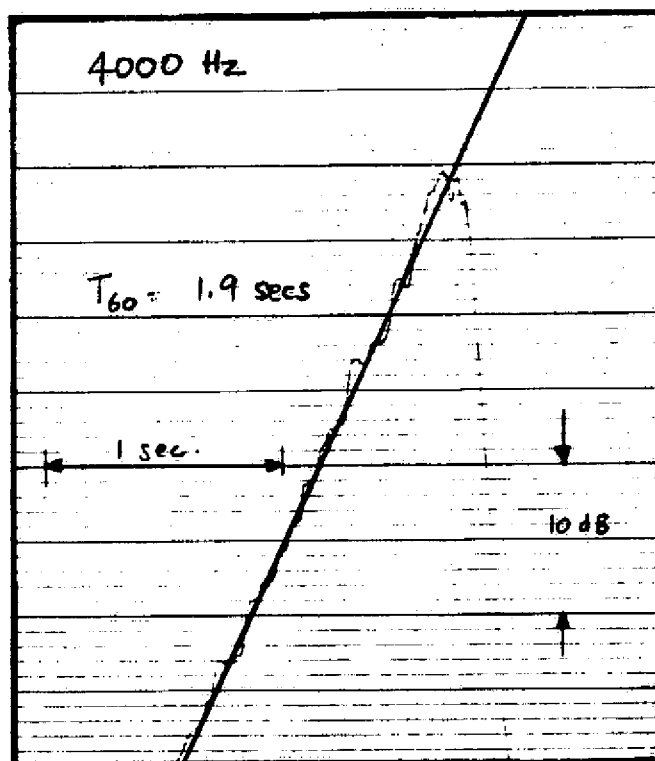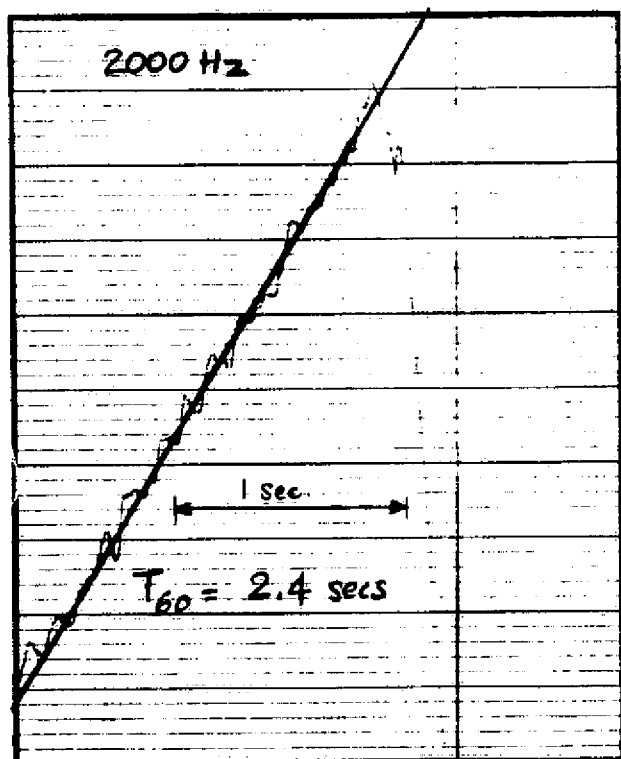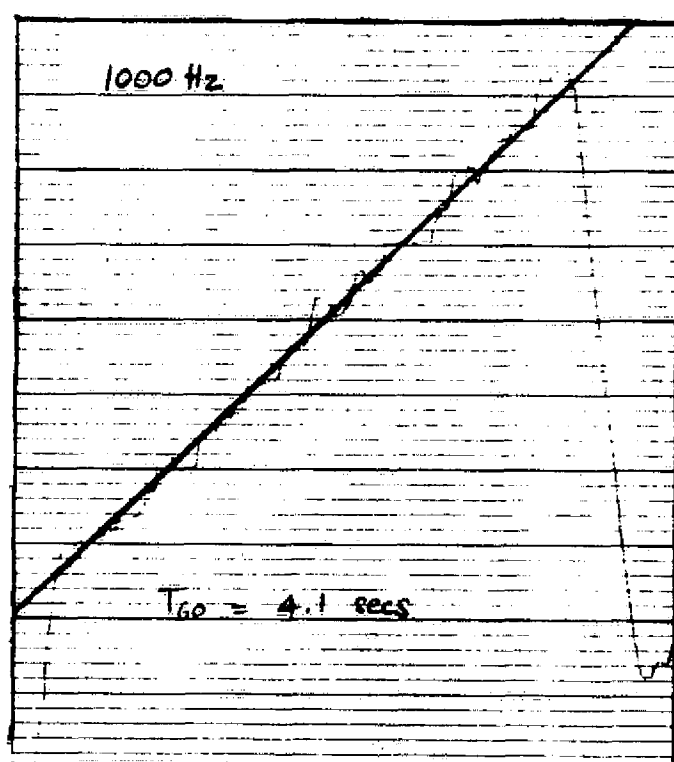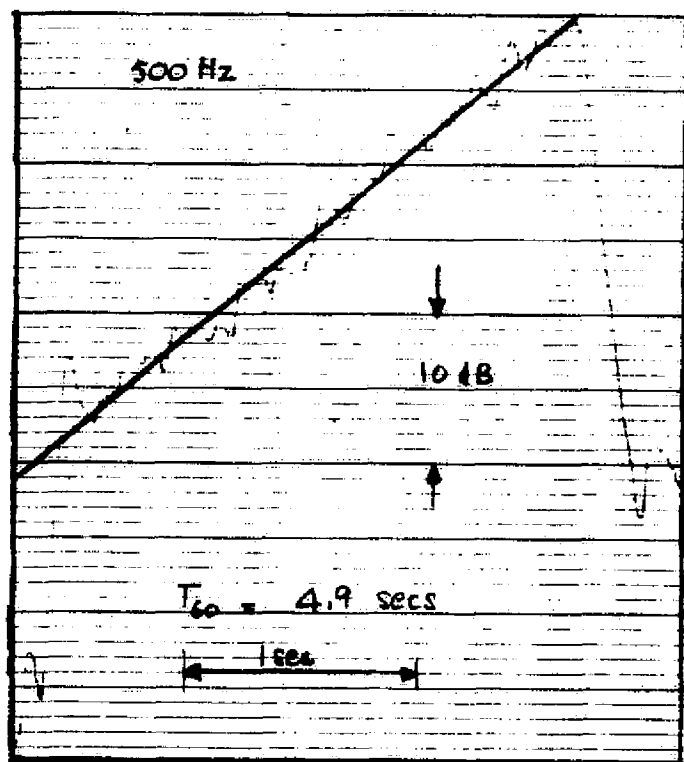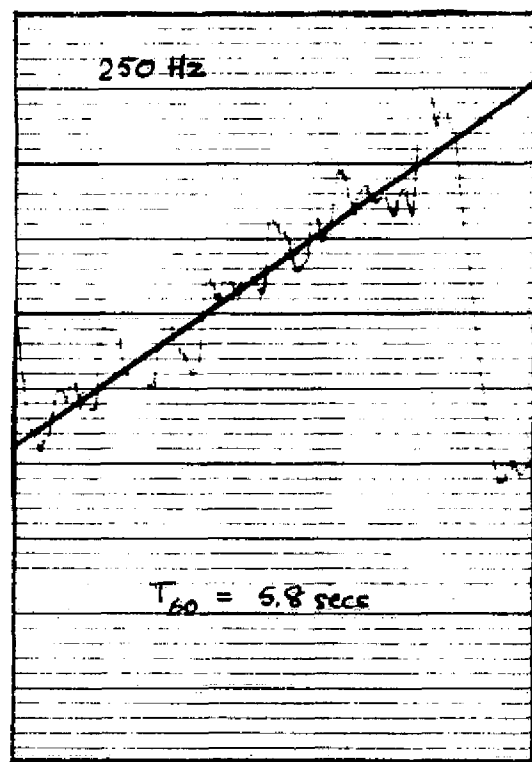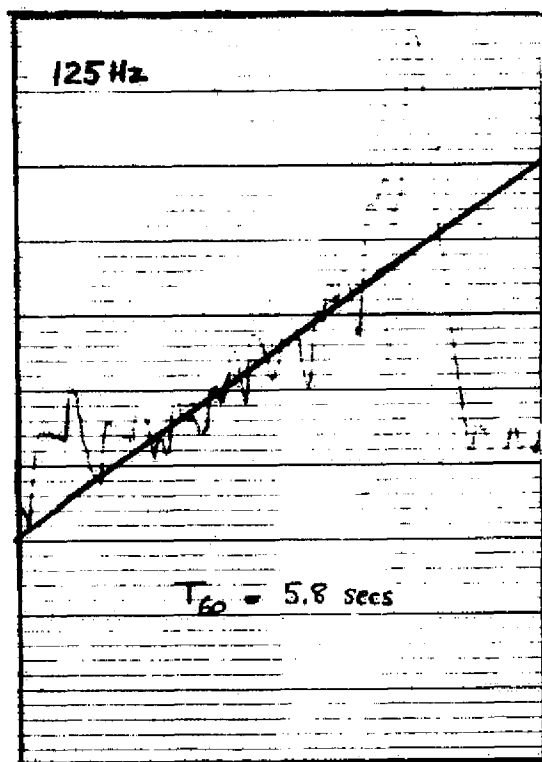
FIGURE 7. DIFFUSER LEG OCTAVE BAND REVERBERANT DECAYS,
29 NOV 1973, TEST 2 (Tape Played Backwards)

2000 Hz

1 sec

$T_{60} = 3.4$ secs

4000 Hz

1 sec

$T_{60} = 1.7$ secs

8000 Hz

$T_{60} = 0.8$ secs

0.5 secs

16000 Hz

10 dB

$T_{60} = 0.52$ secs

0.5 secs
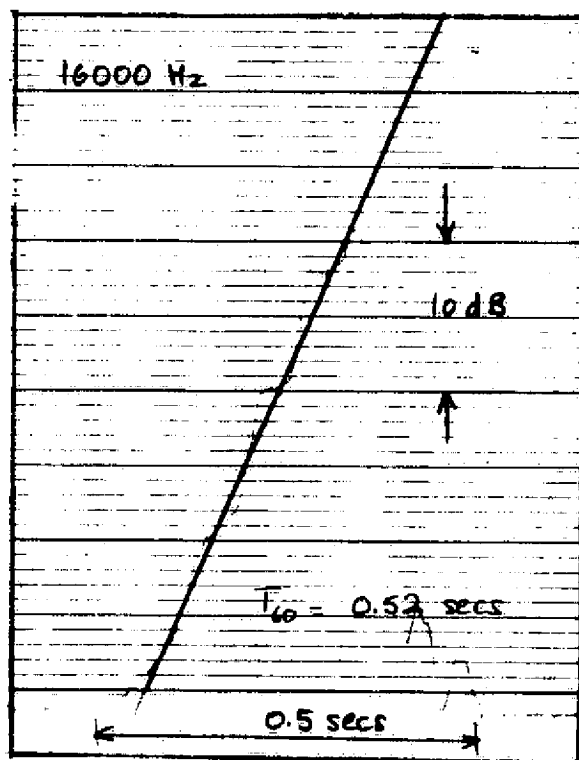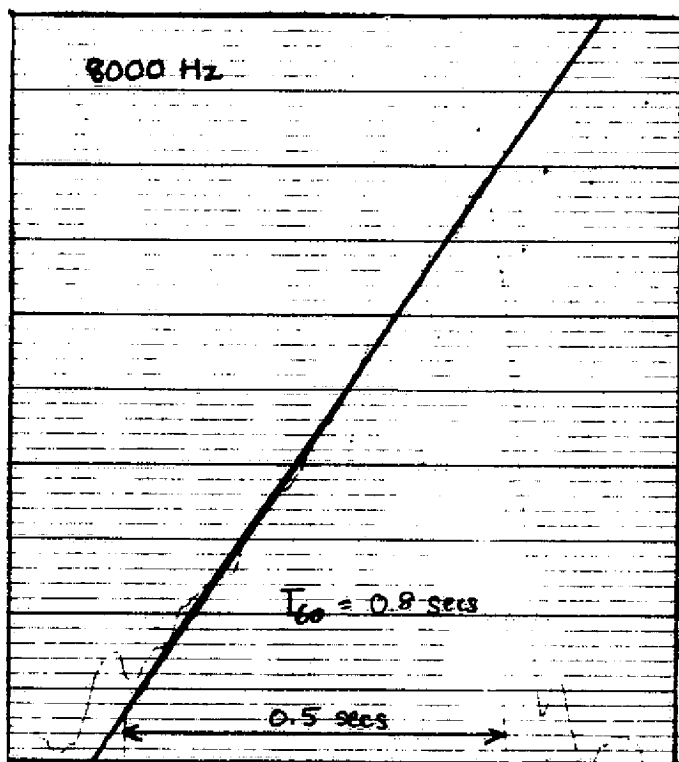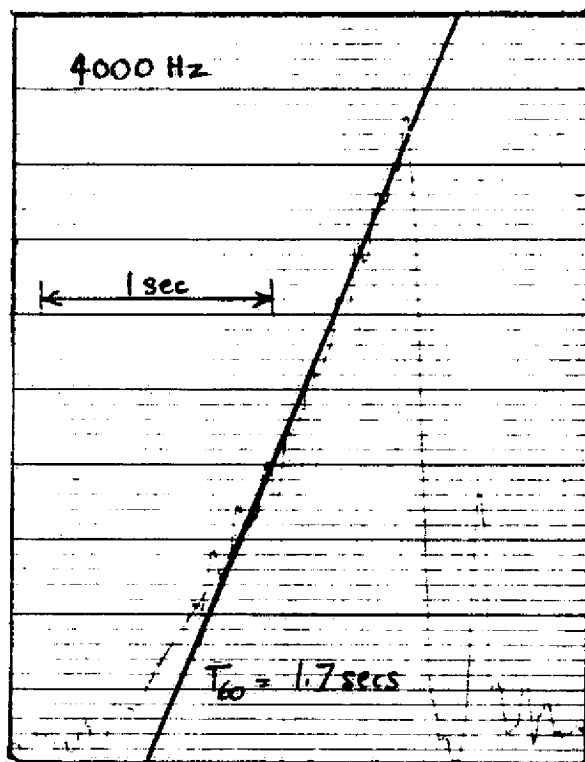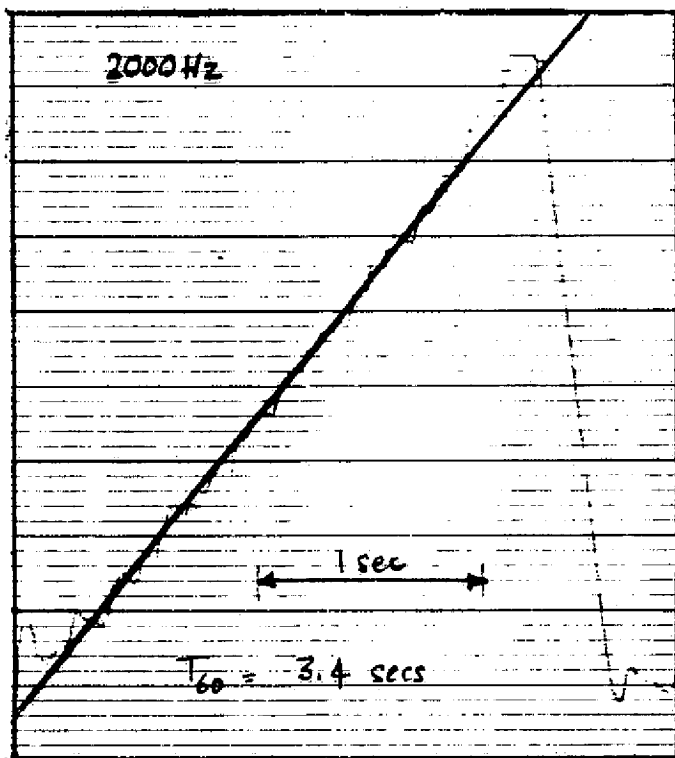
FIGURE 7.   (Cont)
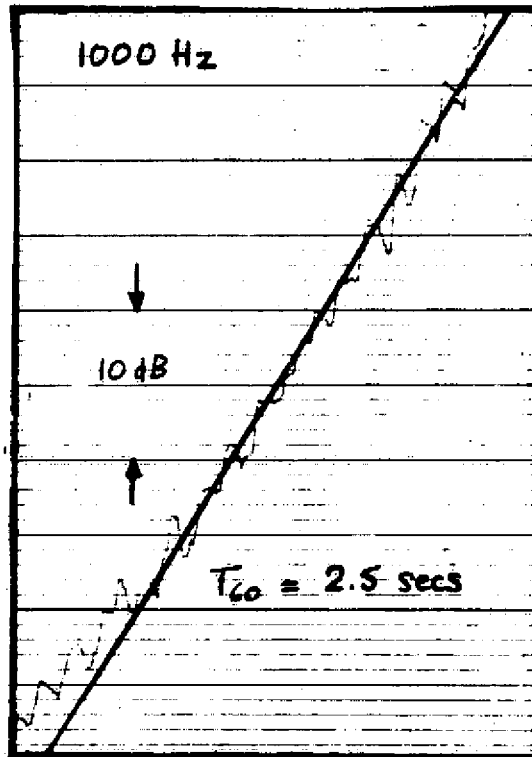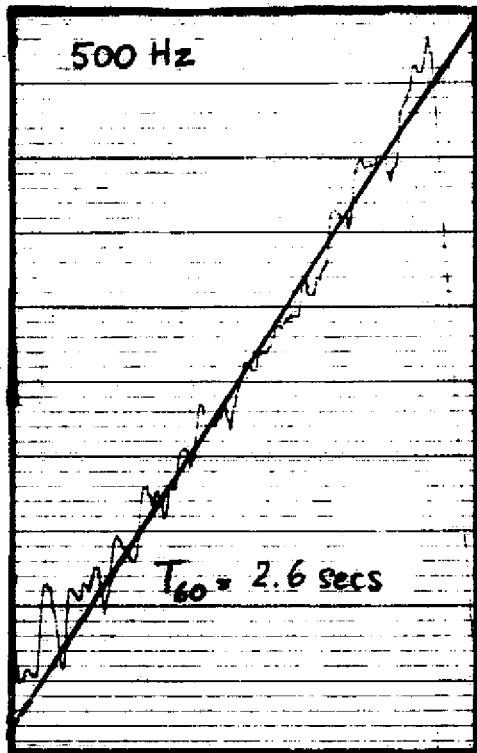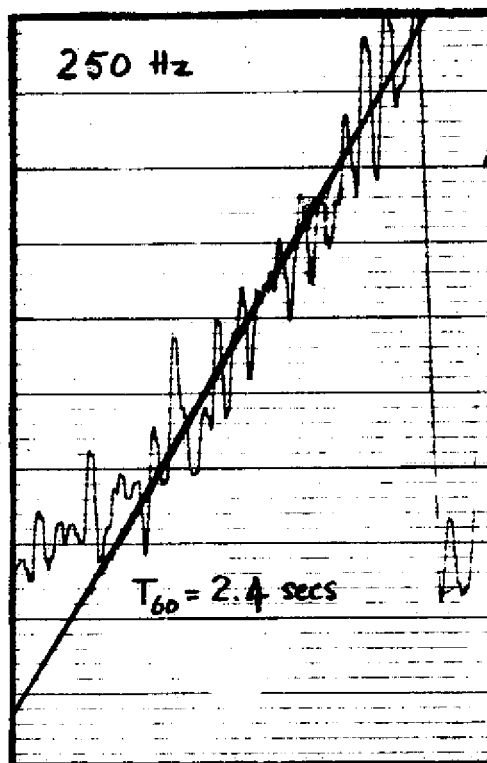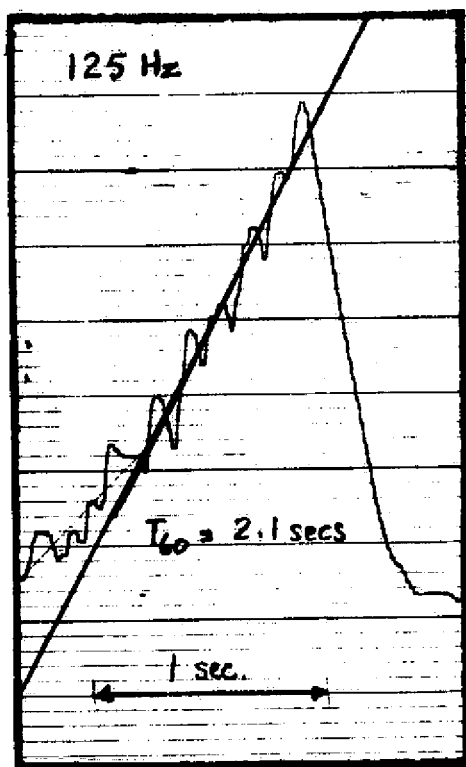
FIGURE 8. PREPARATION ROOM OCTAVE BAND REVERBERANT DECAYS,
24 FEB 1974, TEST 1 (Tape Played Backwards)

FIGURE 8. (Cont)

125 Hz

10 dB

T_{60} = 3.8 secs

250 Hz

T_{60} = 0.8 secs
(Test Section)

T_{60} = 4.0 secs

(Settling Chamber)

500 Hz

T_{60} = 1.1 secs

T_{60} = 3.4 secs

1000 Hz

T_{60} = 0.8 secs

T_{60} = 2.8 secs

10 dB

1 sec
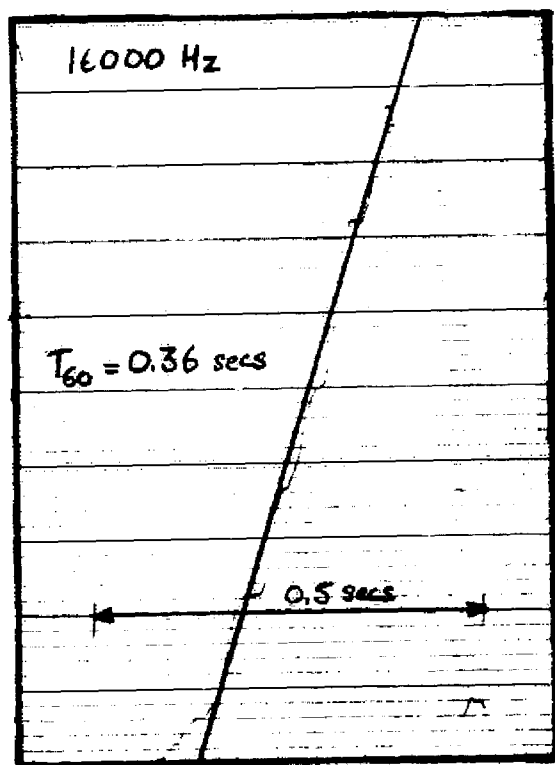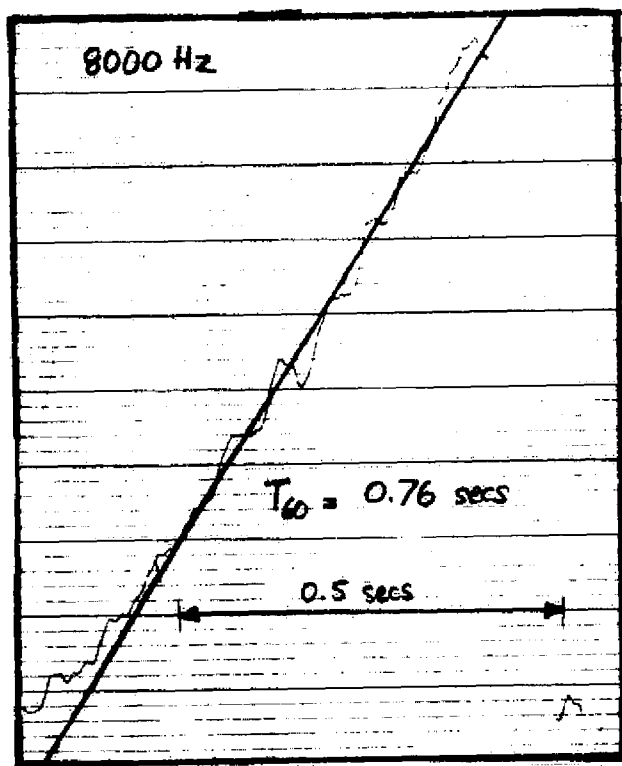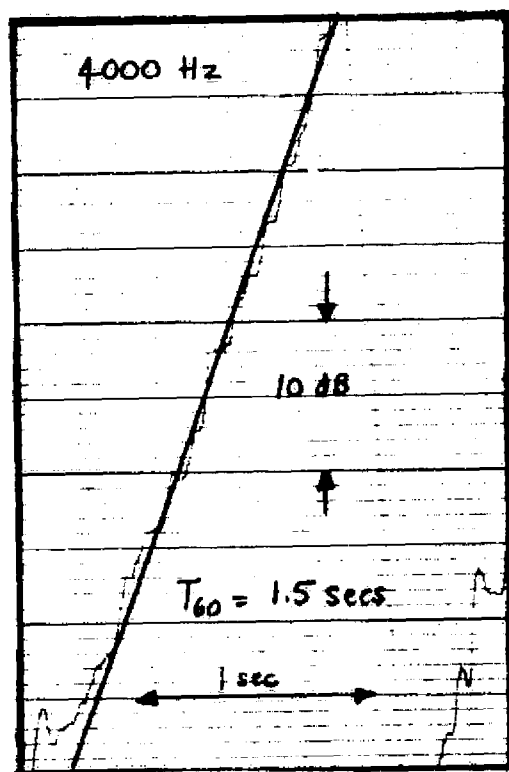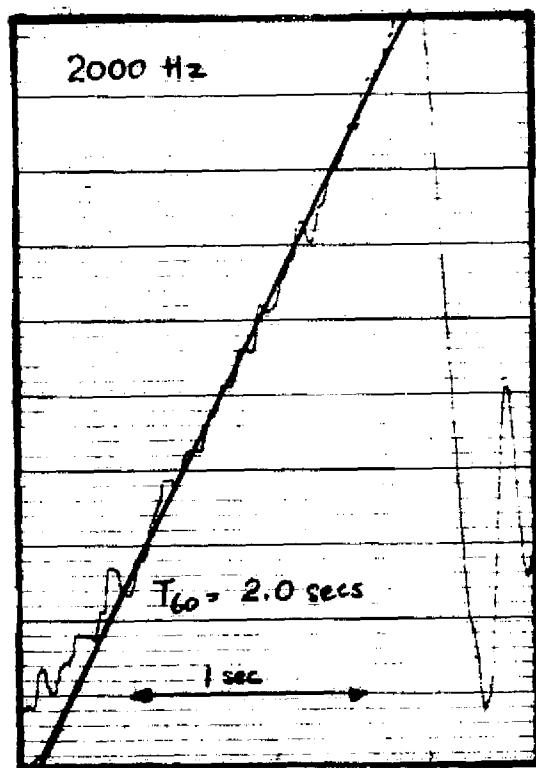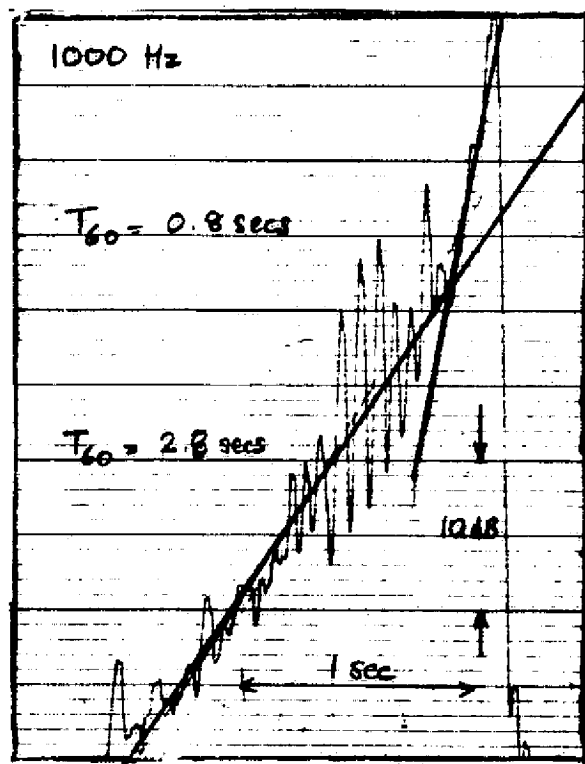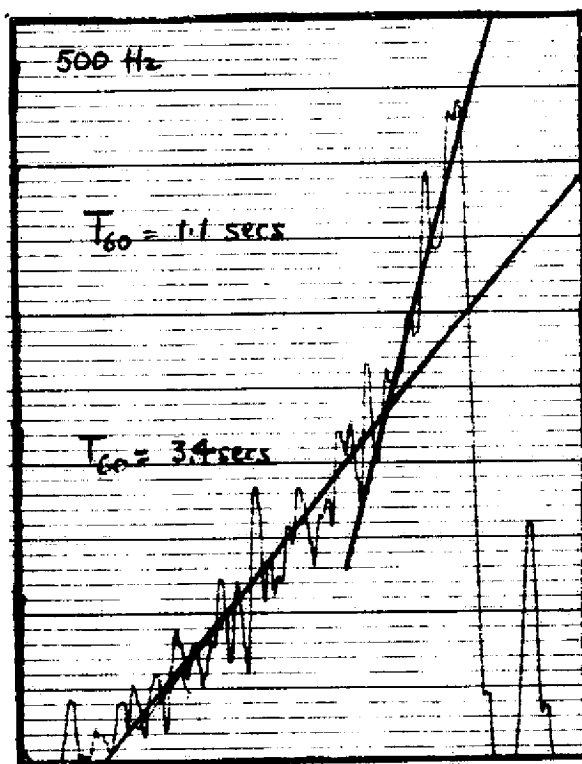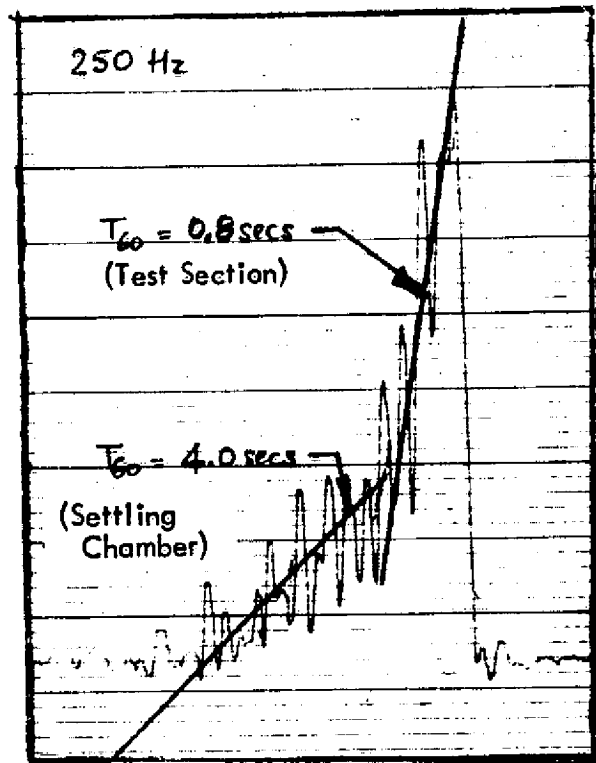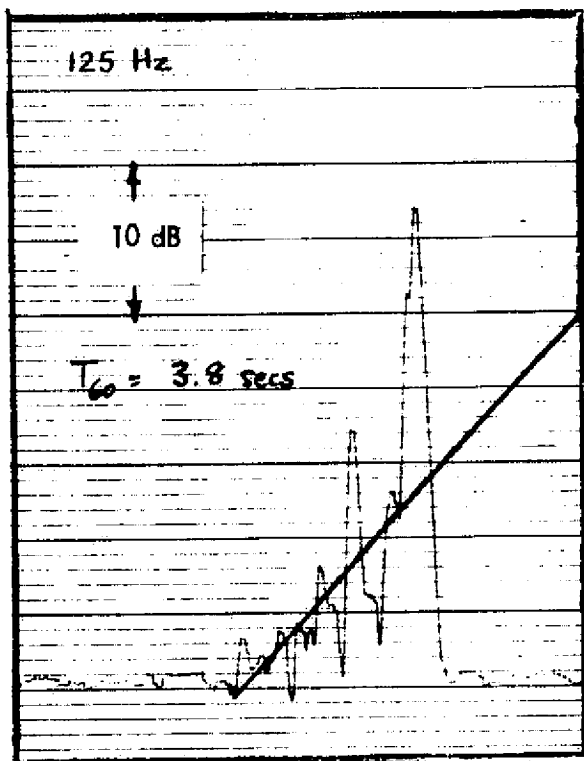
FIGURE 9. TEST SECTION OCTAVE BAND REVERBERANT DECAYS,
27 FEB 1974, TEST 2 (Tape Played Backwards)
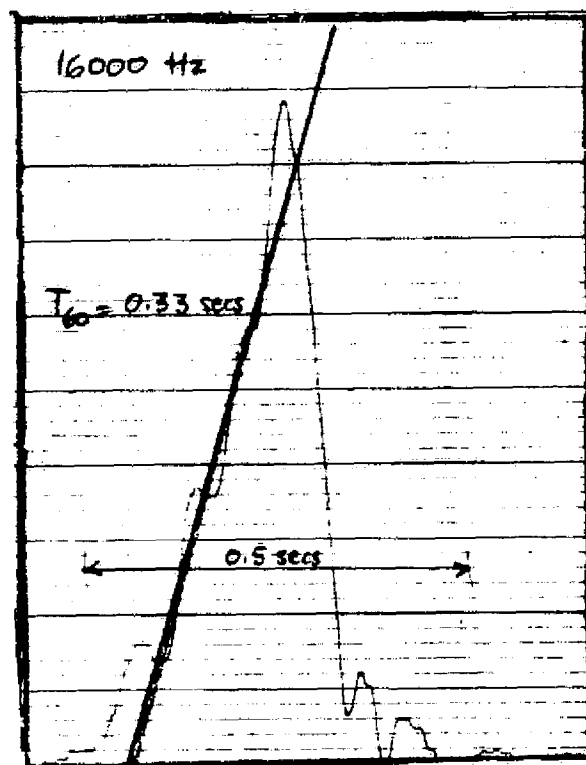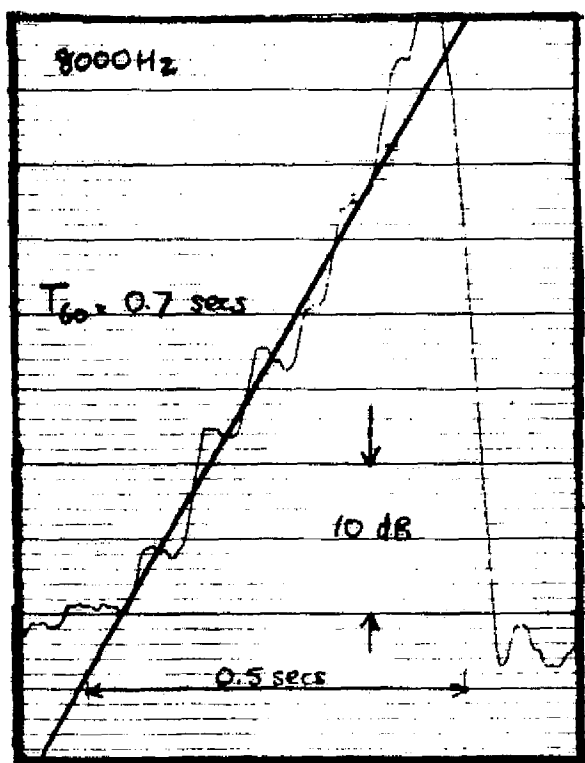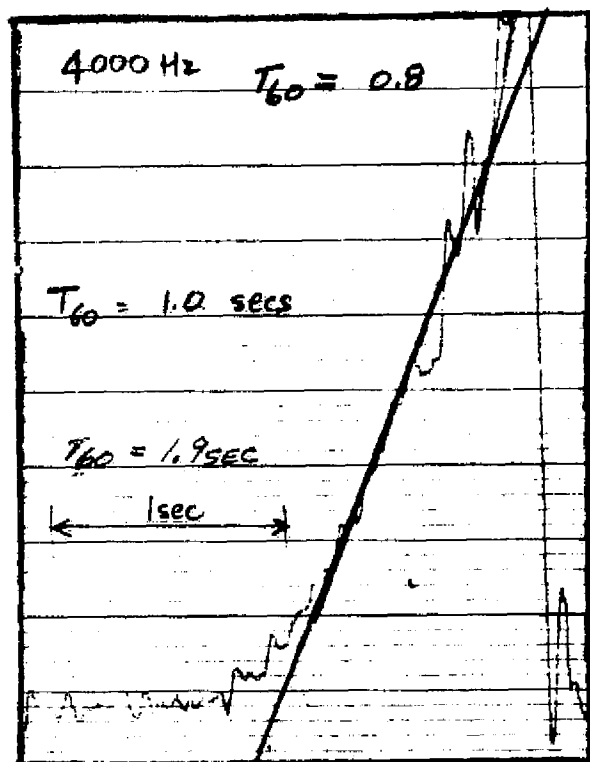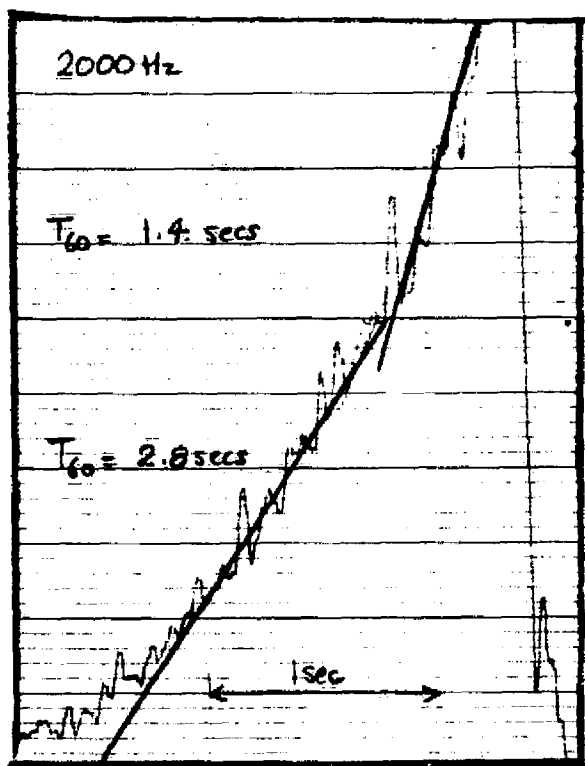
FIGURE 9. (Cont)
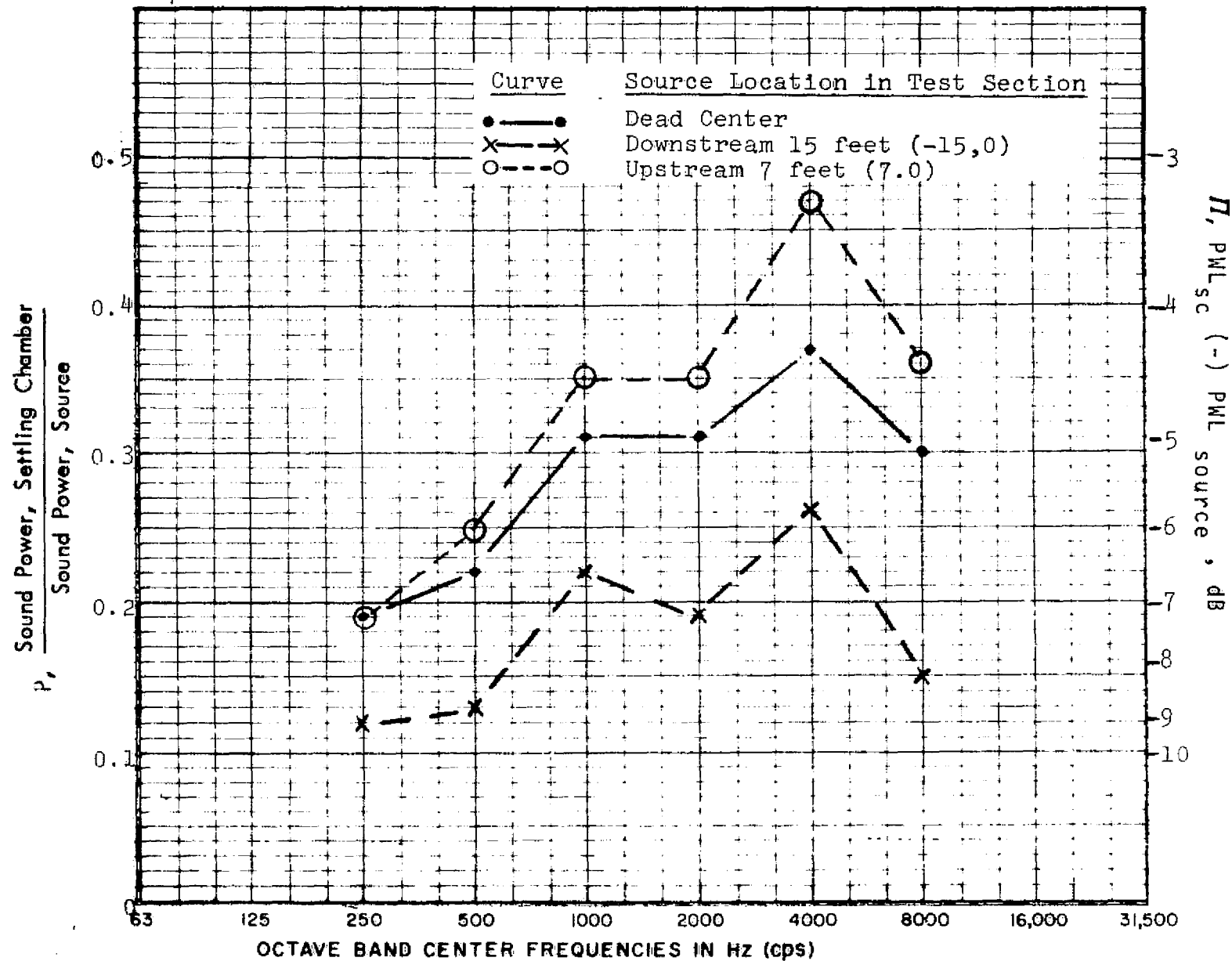
FIGURE 10.   SOURCE SOUND POWER TRANSMITTED TO SETTLING CHAMBER FOR
DIFFERENT ILG OMNI-DIRECTIONAL SOURCE LOCATIONS
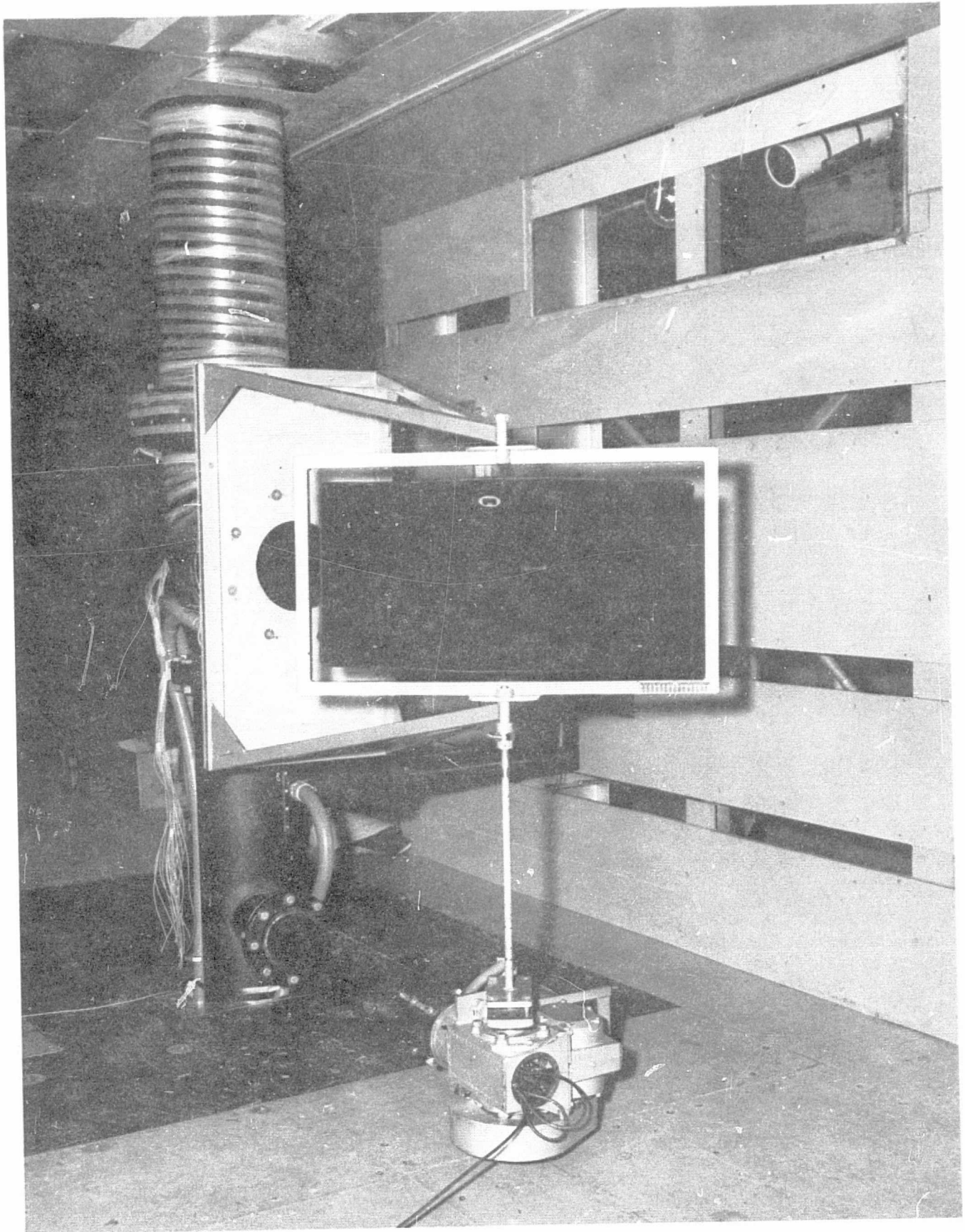
FIGURE 12. ROTATING DIRECTIONAL SOURCE, REVERBERANT
HARDWALL SOUND POWER CALIBRATION
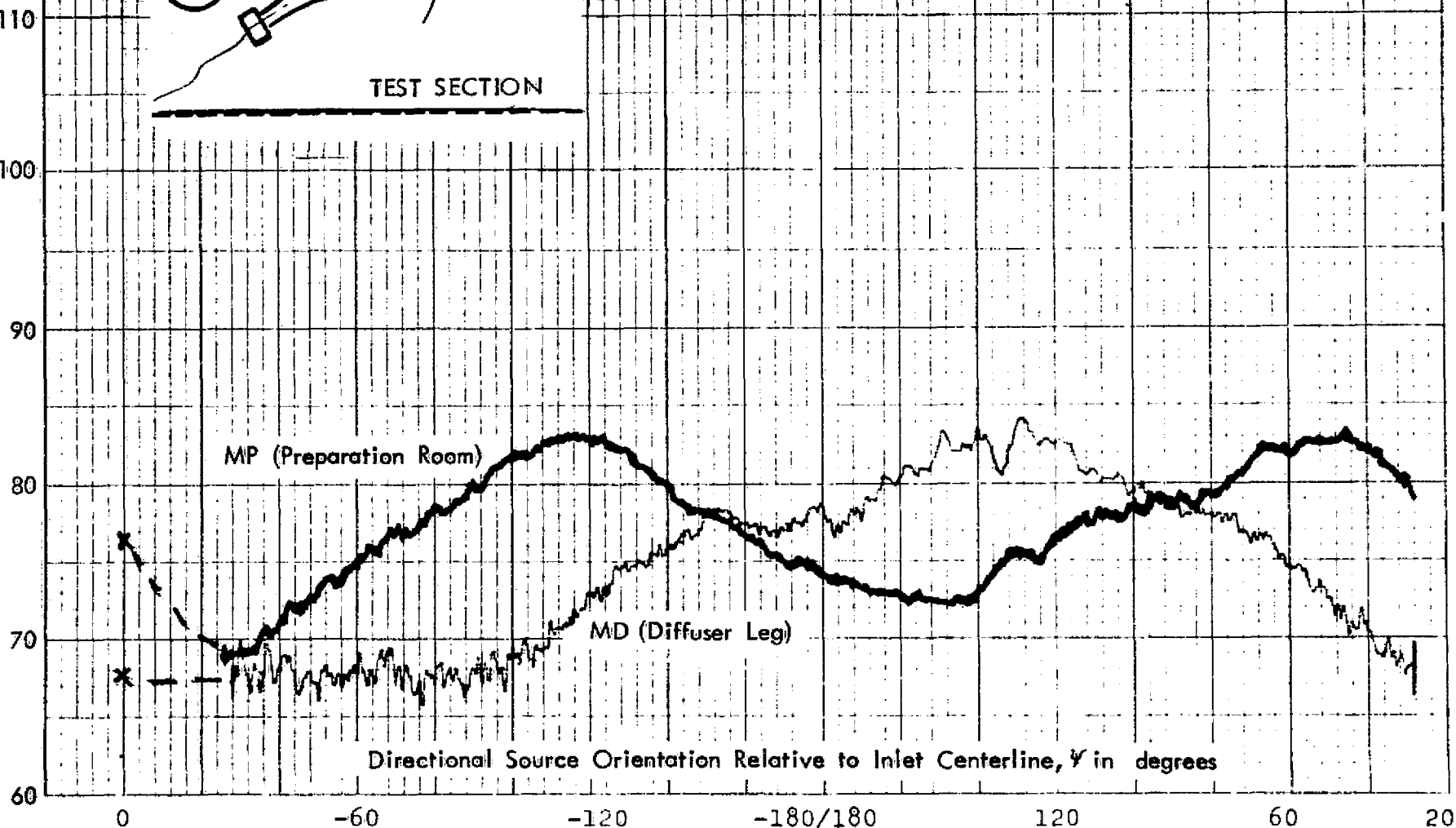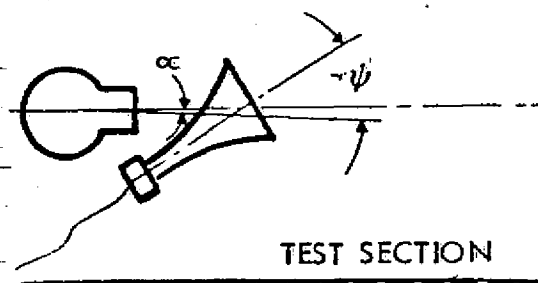
FIGURE 13. TYPICAL ON-LINE PLOT HARDWALL REVERBERATION TEST, DIRECTIONAL SOURCE, PREPARATION ROOM AND DIFFUSER LEG MICROPHONES
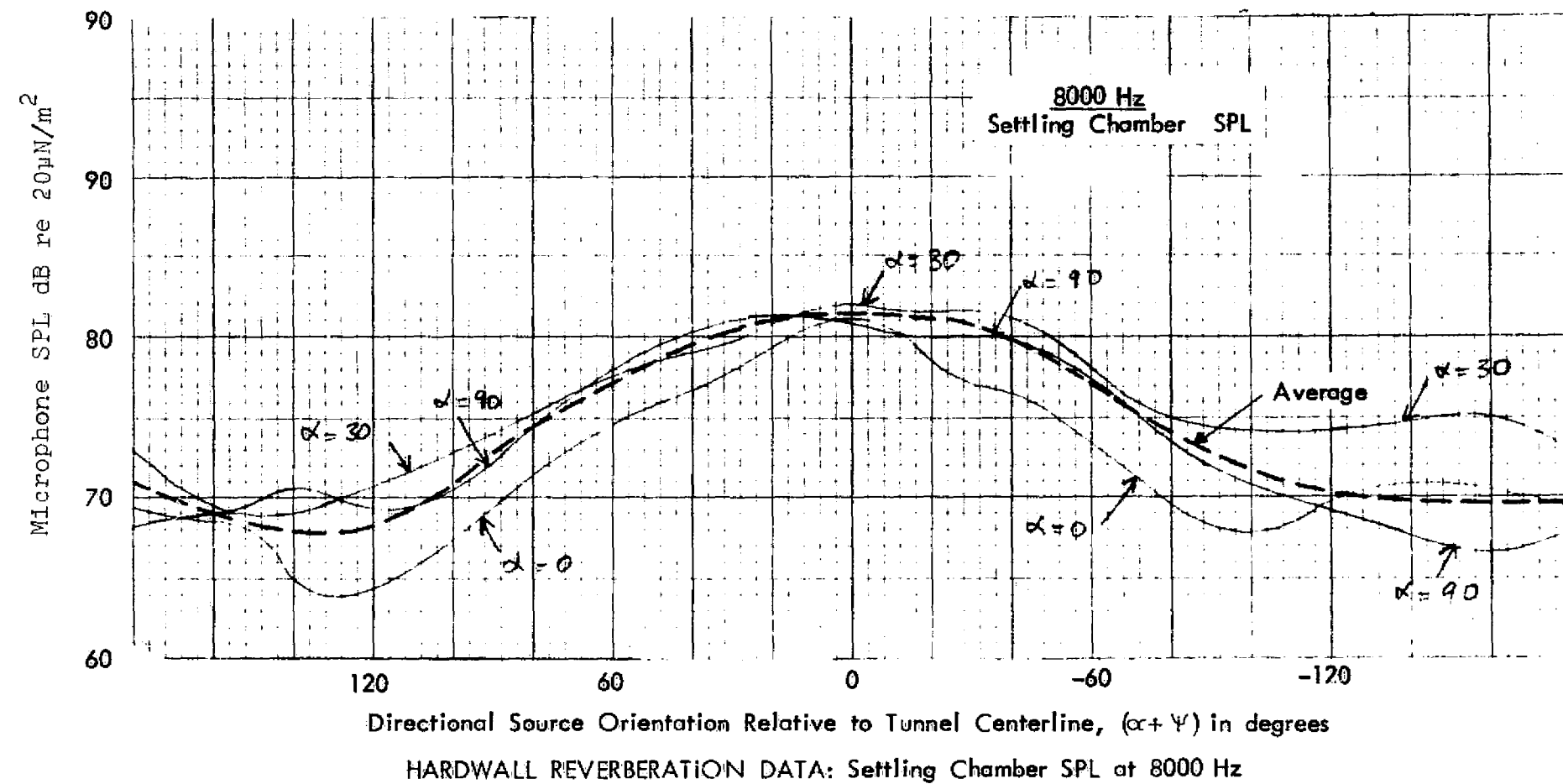
FIGURE 14. TYPICAL REPLOT OF ON-LINE DATA, HARDWALL REVERBERATION WITH DIRECTIONAL SOURCE
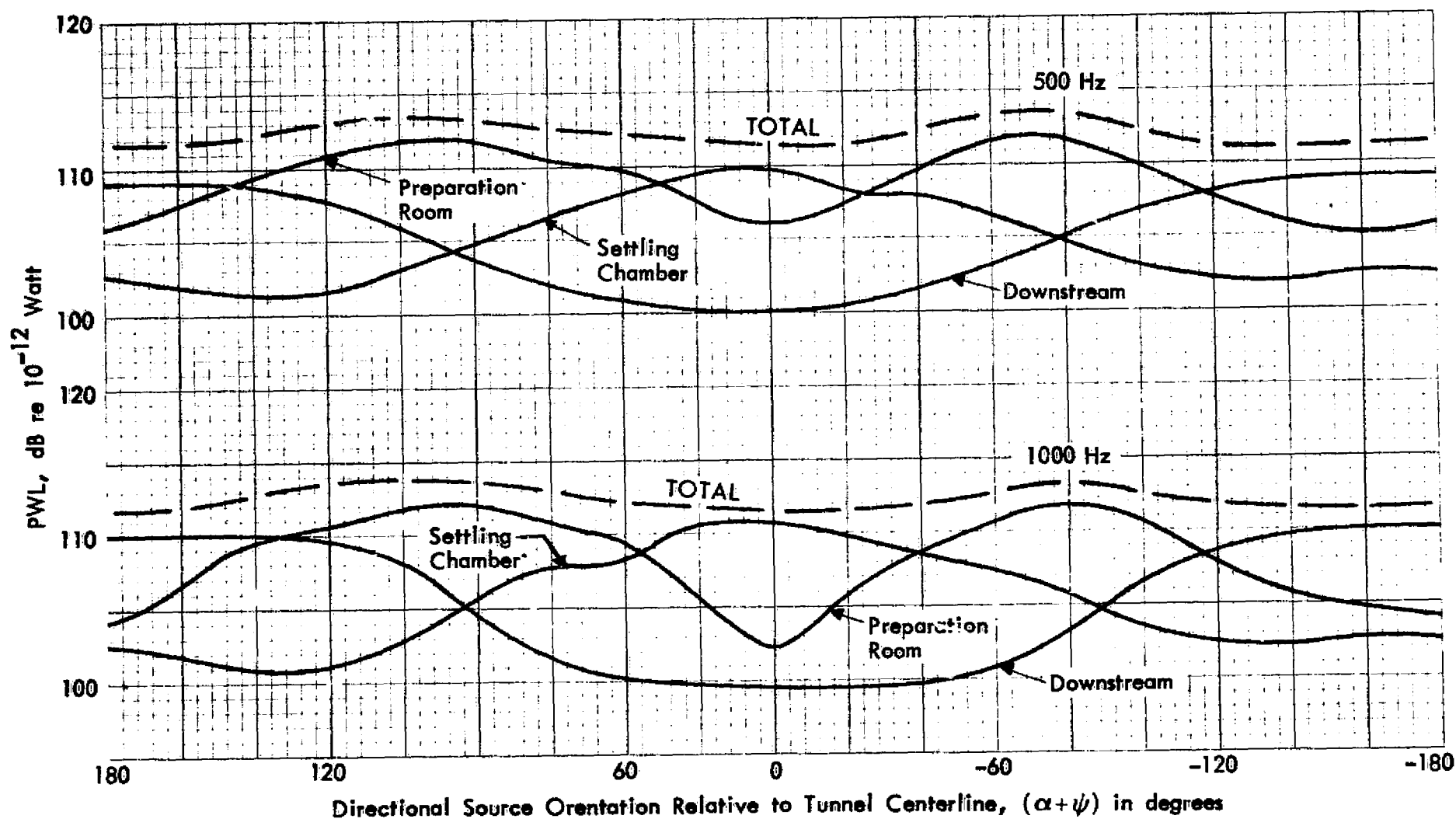
FIGURE 15. INDIVIDUAL CHAMBER AND TOTAL MEASURED SOUND POWER AS A FUNCTION OF DIRECTIONAL SOURCE ANGLE, 500 AND 1000 Hz
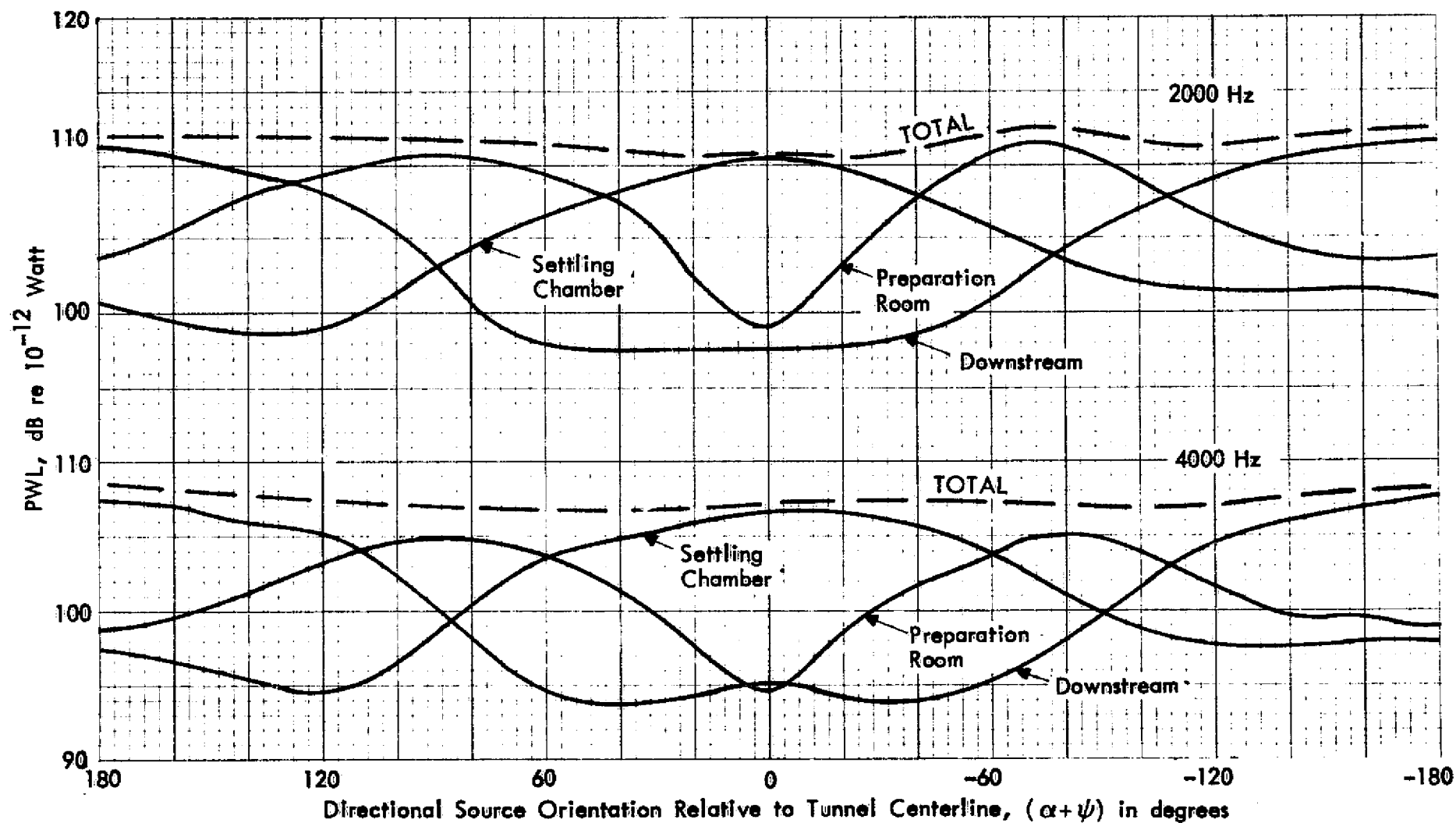
FIGURE 16. INDIVIDUAL CHAMBER AND TOTAL MEASURED SOUND POWER AS A FUNCTION OF DIRECTIONAL SOURCE ANGLE, 2000 and 4000 Hz
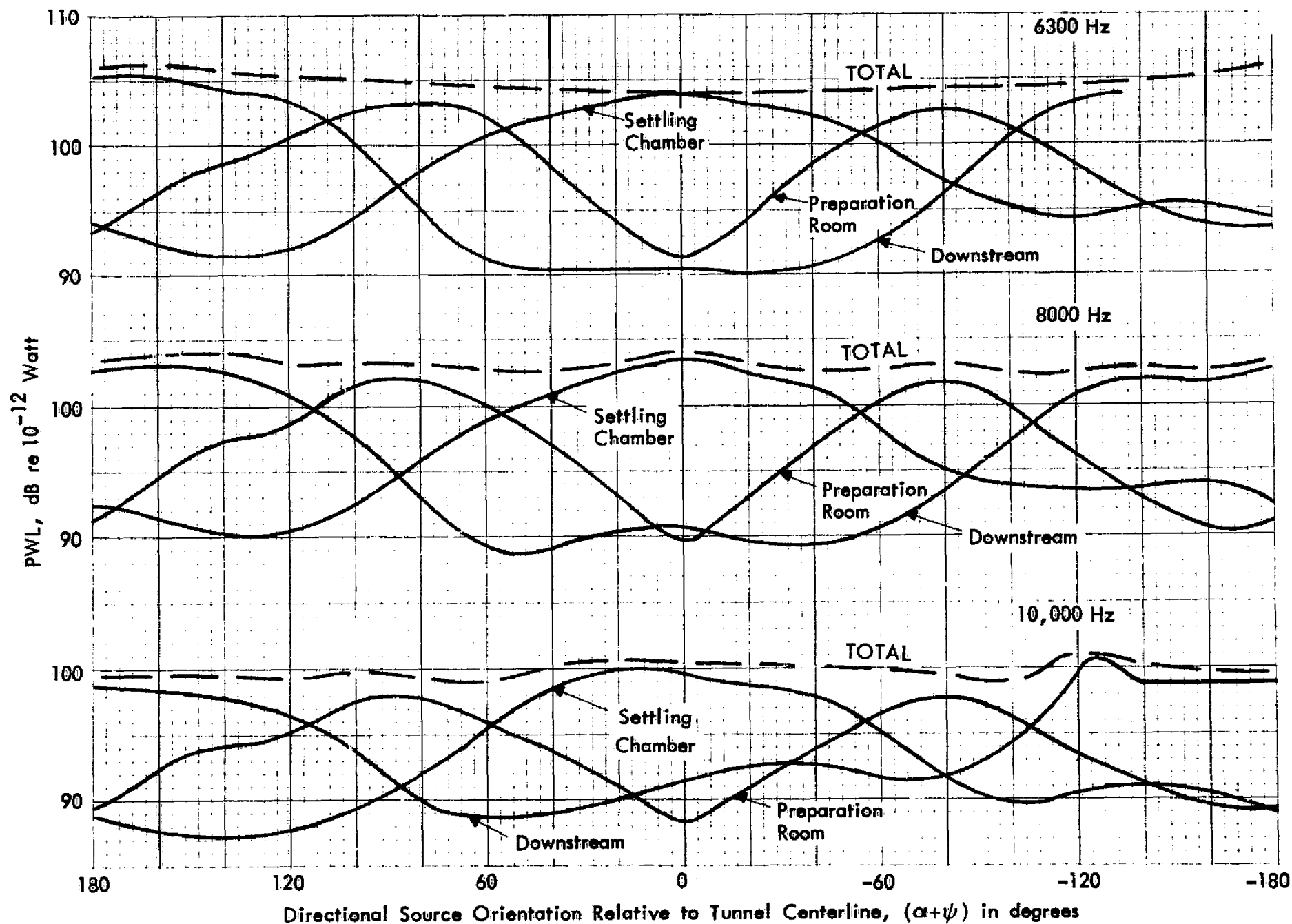
FIGURE 17.   INDIVIDUAL CHAMBER AND TOTAL MEASURED SOUND POWER AS A FUNCTION OF DIRECTIONAL SOURCE ANGLE, 6300, 8000 and 10,000 Hz
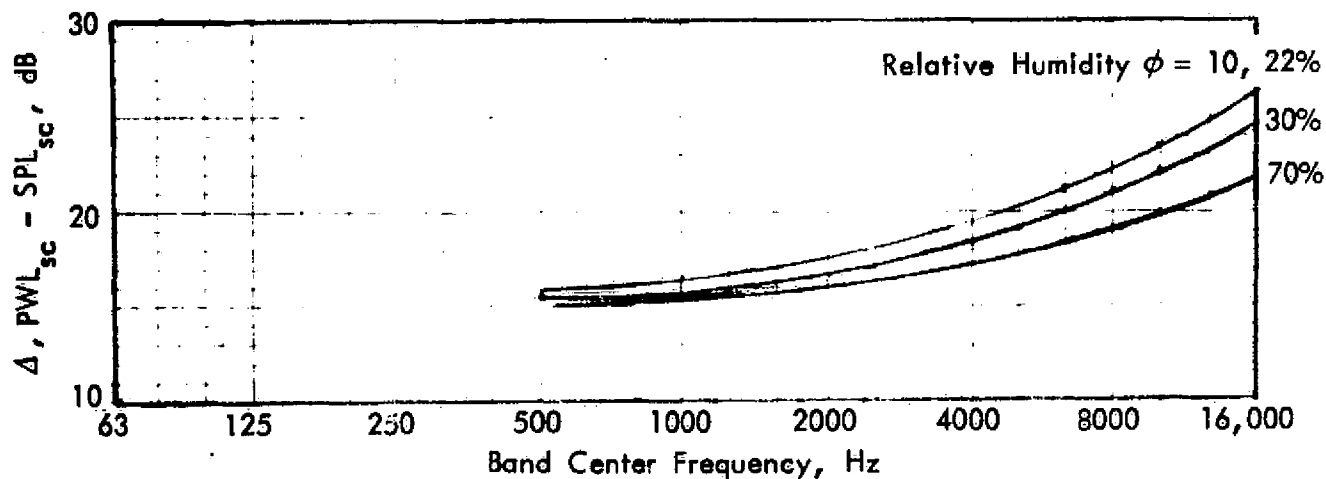
FIGURE 18. SETTLING CHAMBER SOUND POWER CALIBRATION, ALSO USABLE FOR PREPARATION ROOM AND DIFFUSER SECTION
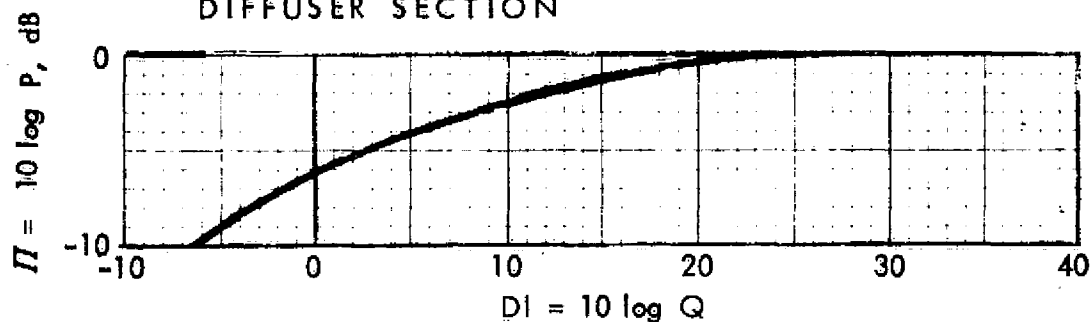
FIGURE 19. APPROXIMATION FOR SOURCE SOUND POWER EXITING TO SETTLING CHAMBER AS A FUNCTION OF SOURCE DIRECTIVITY INDEX, APPLICABLE FOR $(\alpha + \psi) = \pm 60°$
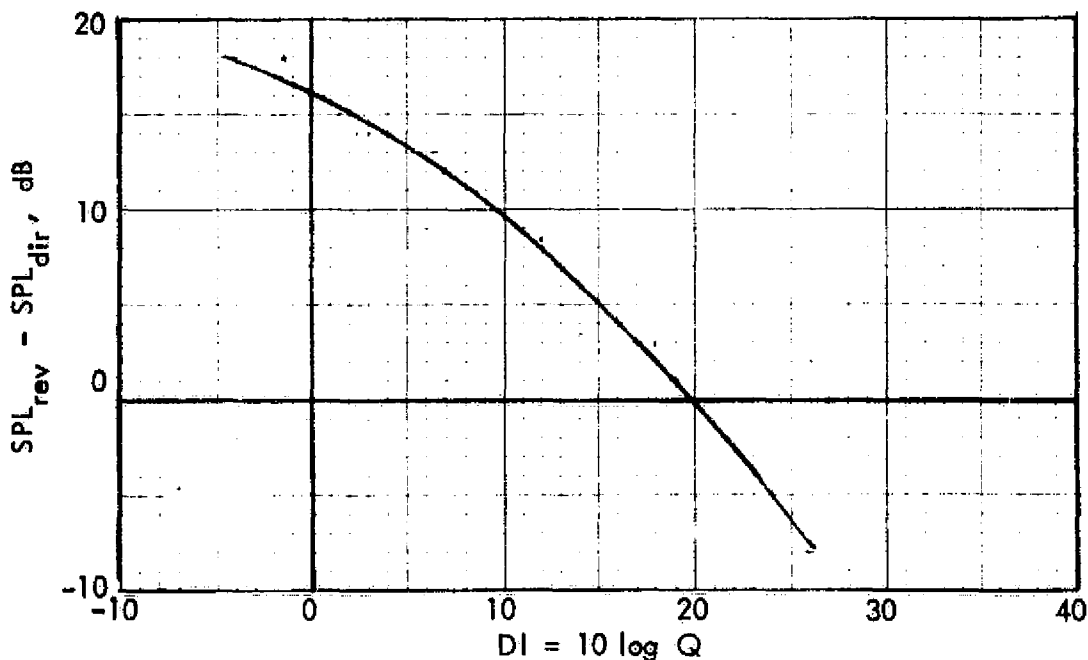
FIGURE 20. APPROXIMATION FOR DIFFERENCE IN SETTLING CHAMBER REVERBERANT AND DIRECT FIELD AS A FUNCTION OF SOURCE DIRECTIVITY INDEX
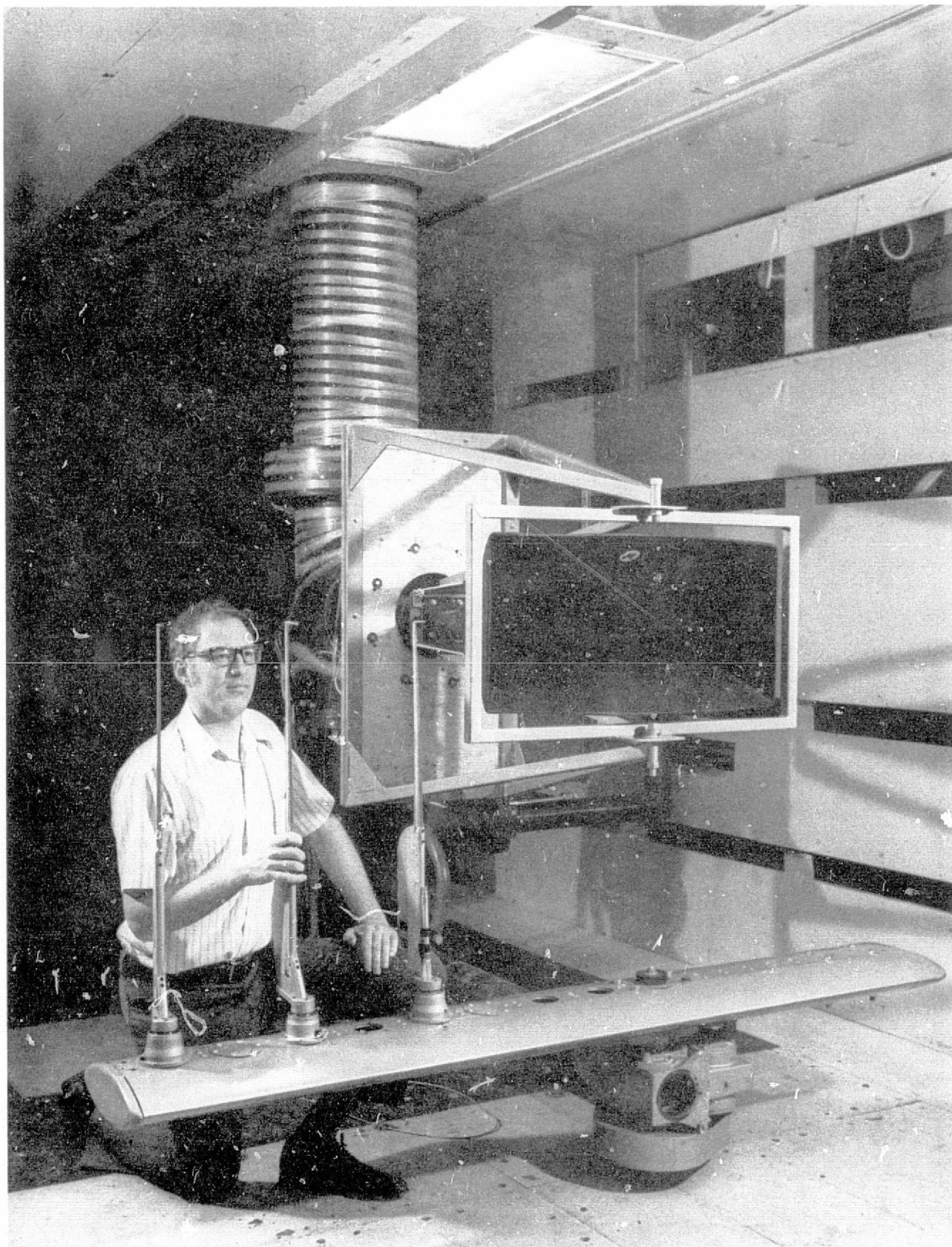
FIGURE 21.   DIRECTIONAL SOURCE AND MICROPHONE BOOM WITH
MICROPHONES AT 2, 3, AND 4 FOOT POSITIONS

FIGURE 22. TYPICAL ON-LINE PLOT, HARDWALL DIRECTIONALITY TEST
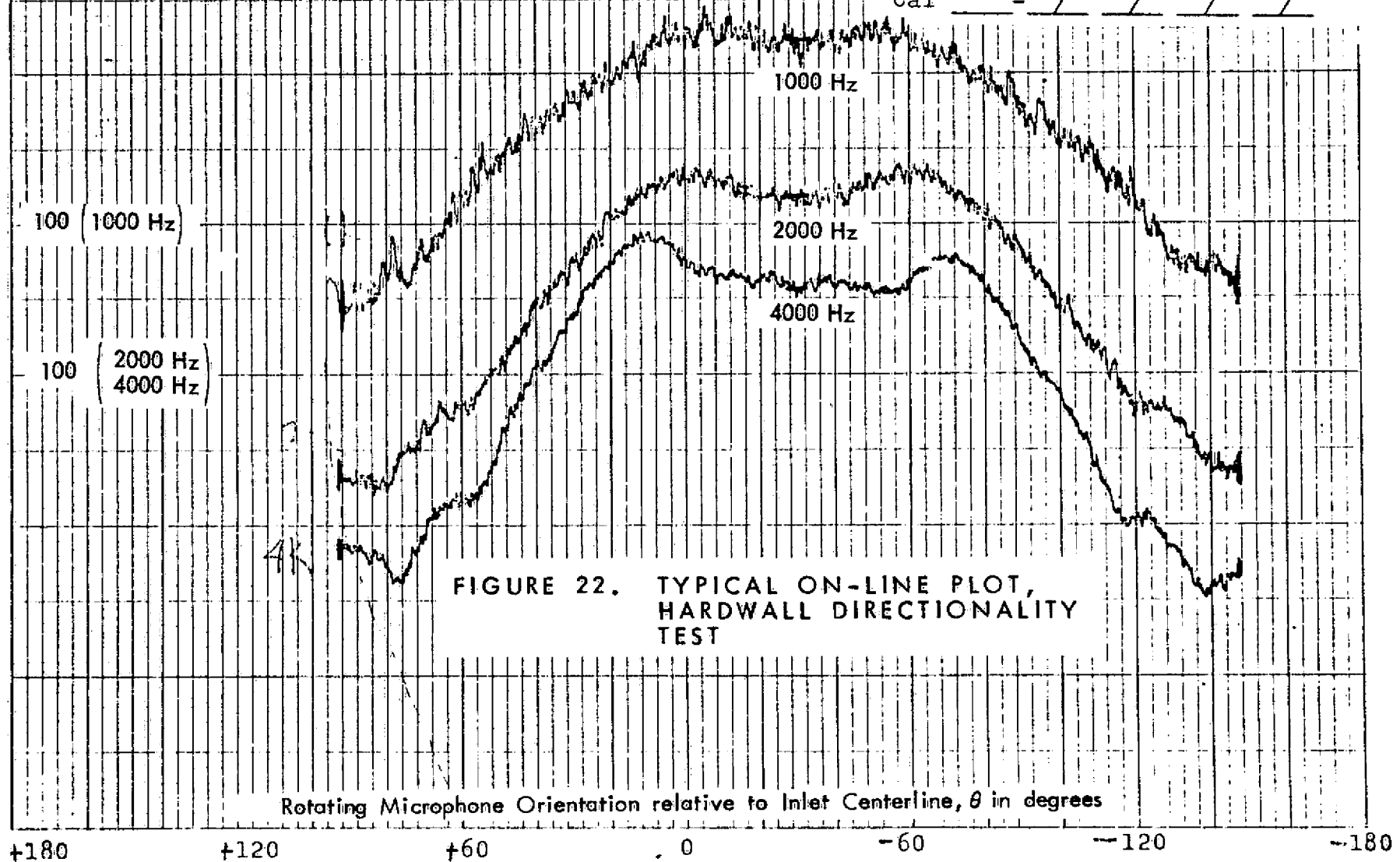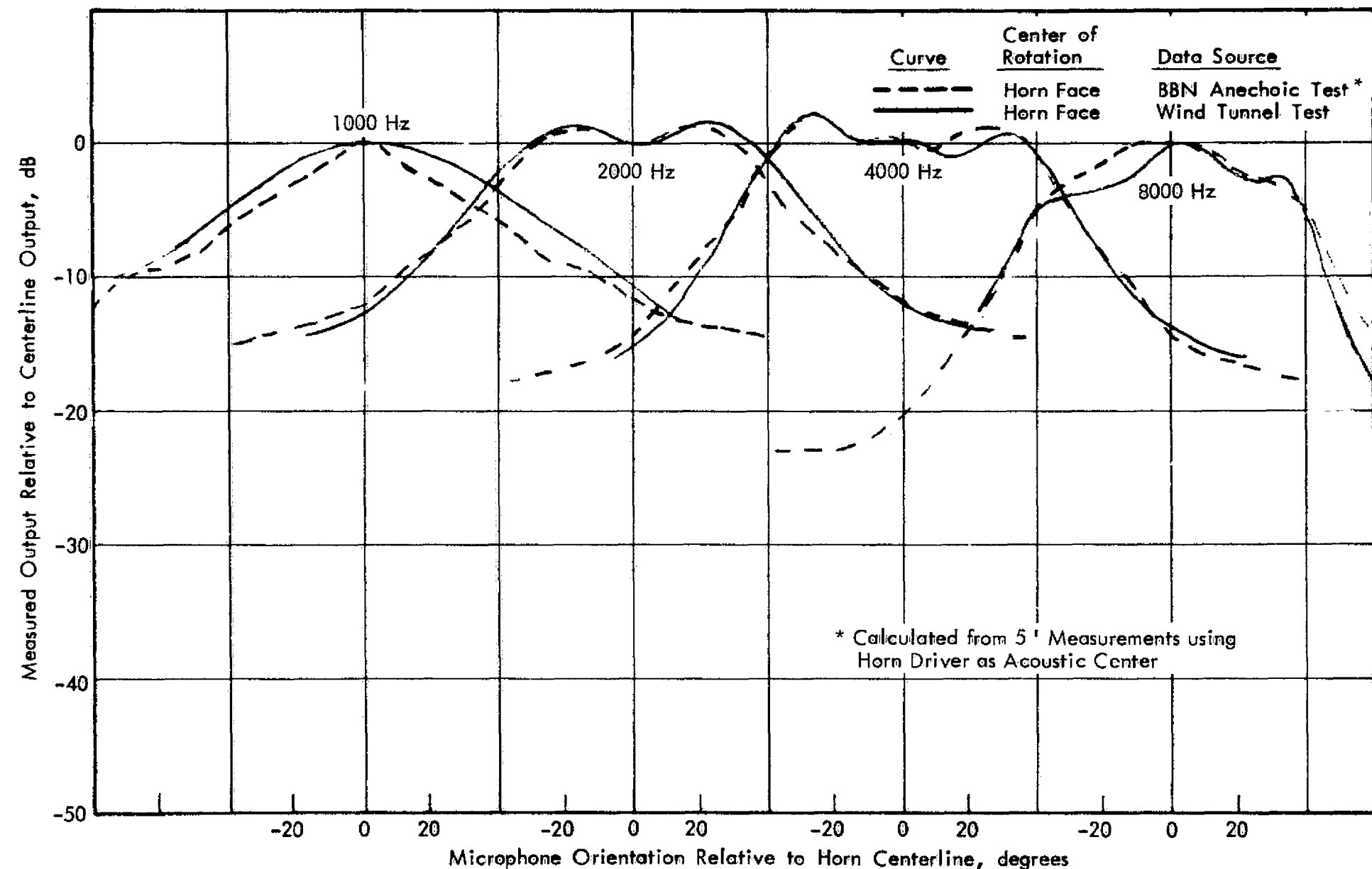
FIGURE 23. COMPARISON OF HORN DIRECTIONALITY MEASUREMENTS AT THREE FOOT RADIUS IN HARDWALL TEST SECTION, ALONG TUNNEL CENTERLINE ($\alpha = \psi = 0$), AND IN ANECHOIC CHAMBER.
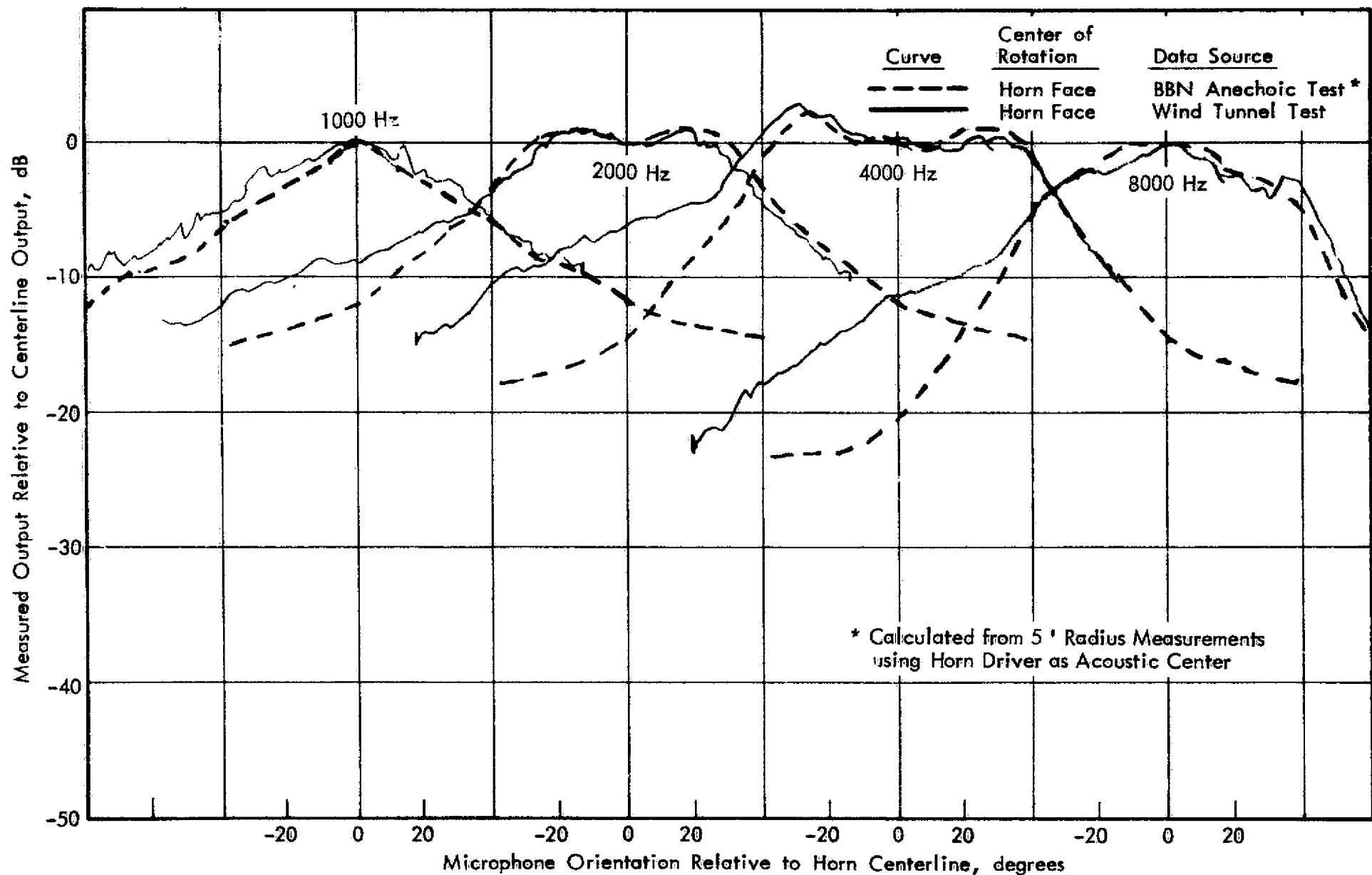
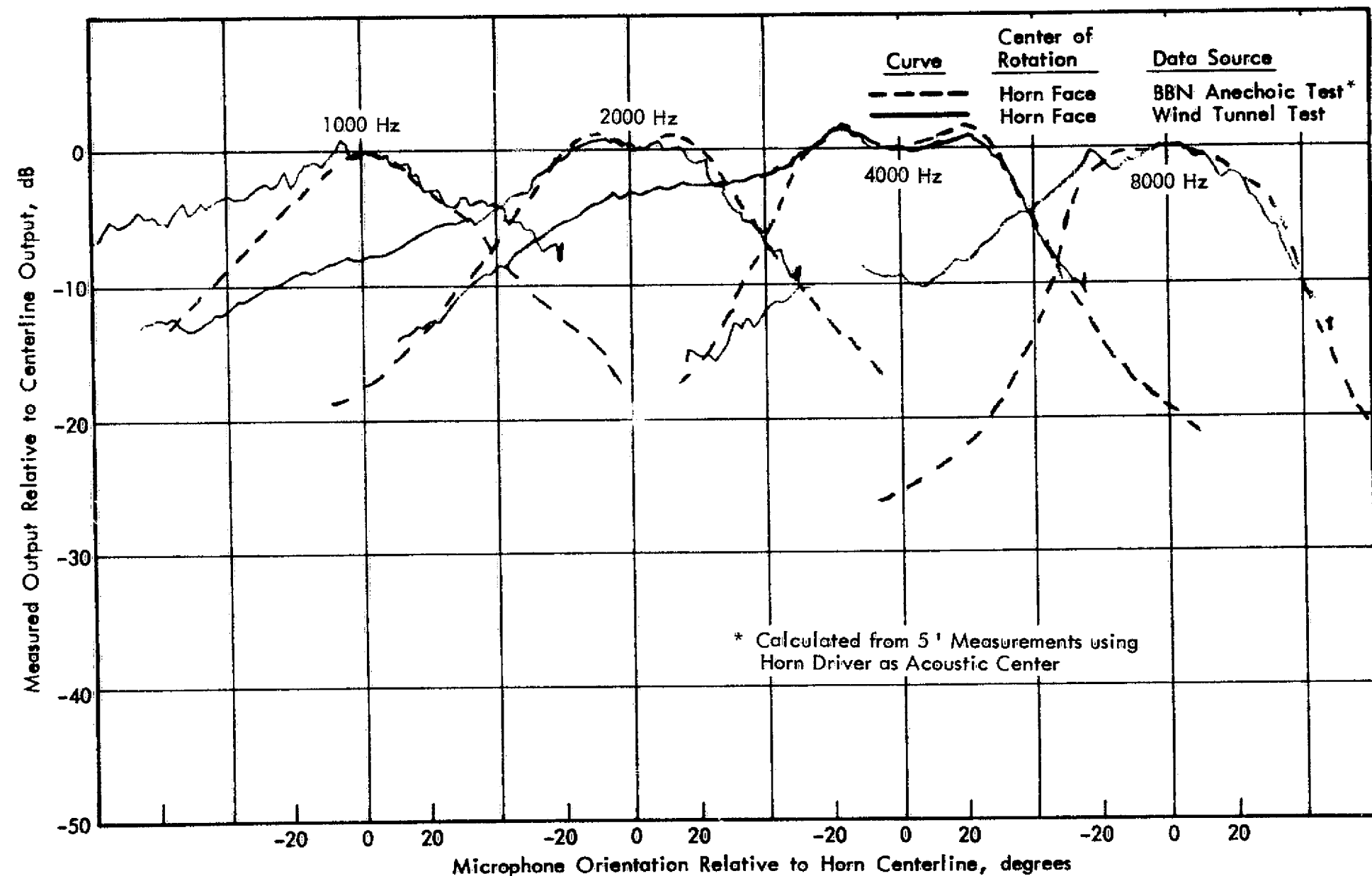FIGURE 24. COMPARISON OF HORN DIRECTIONALITY MEASUREMENTS AT THREE FOOT RADIUS IN HARDWALL TEST SECTION, ANGLED TOWARDS WALL ($\alpha = 30^\circ$, $\psi = -90^\circ$), AND IN ANECHOIC CHAMBER.
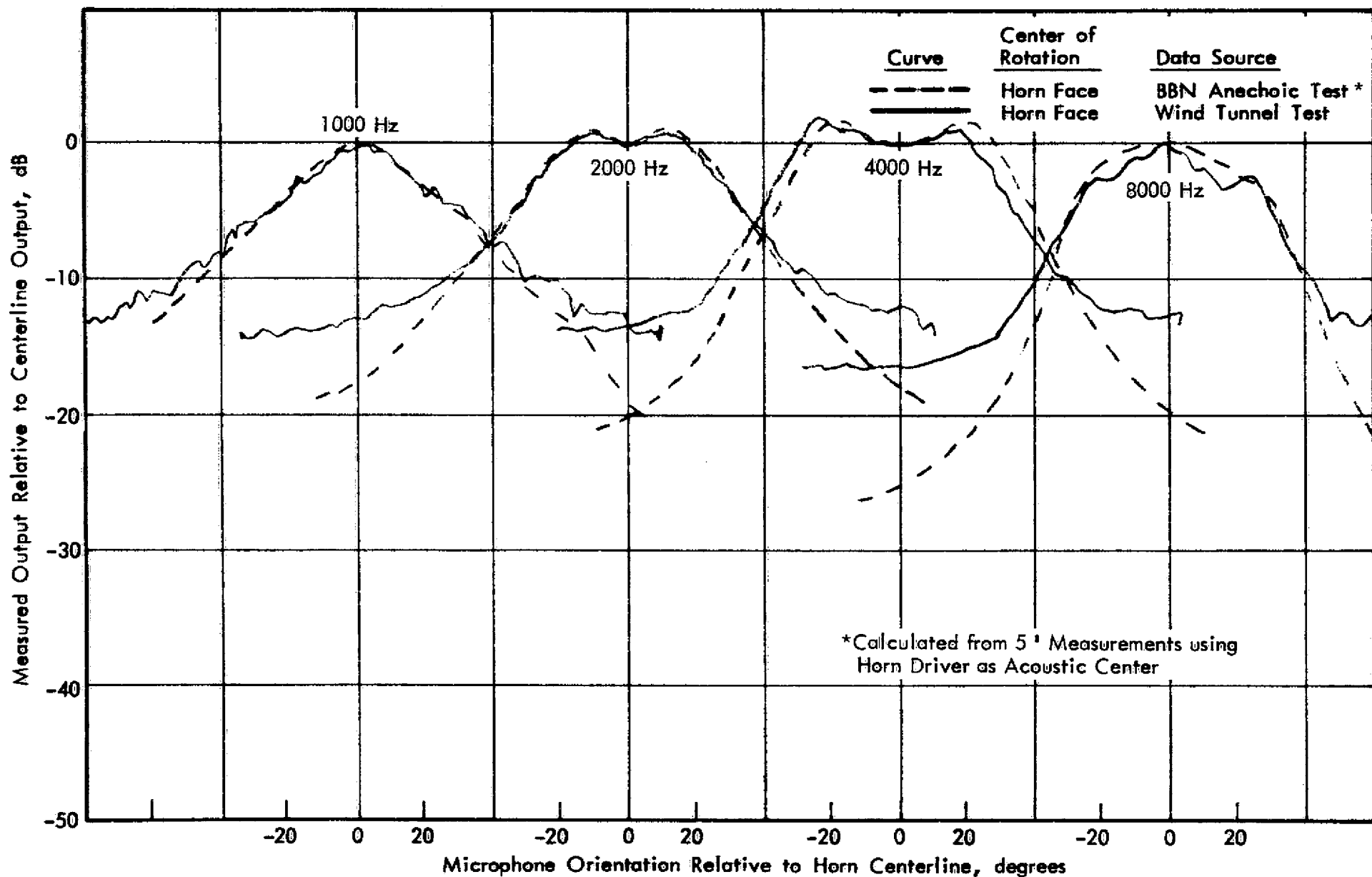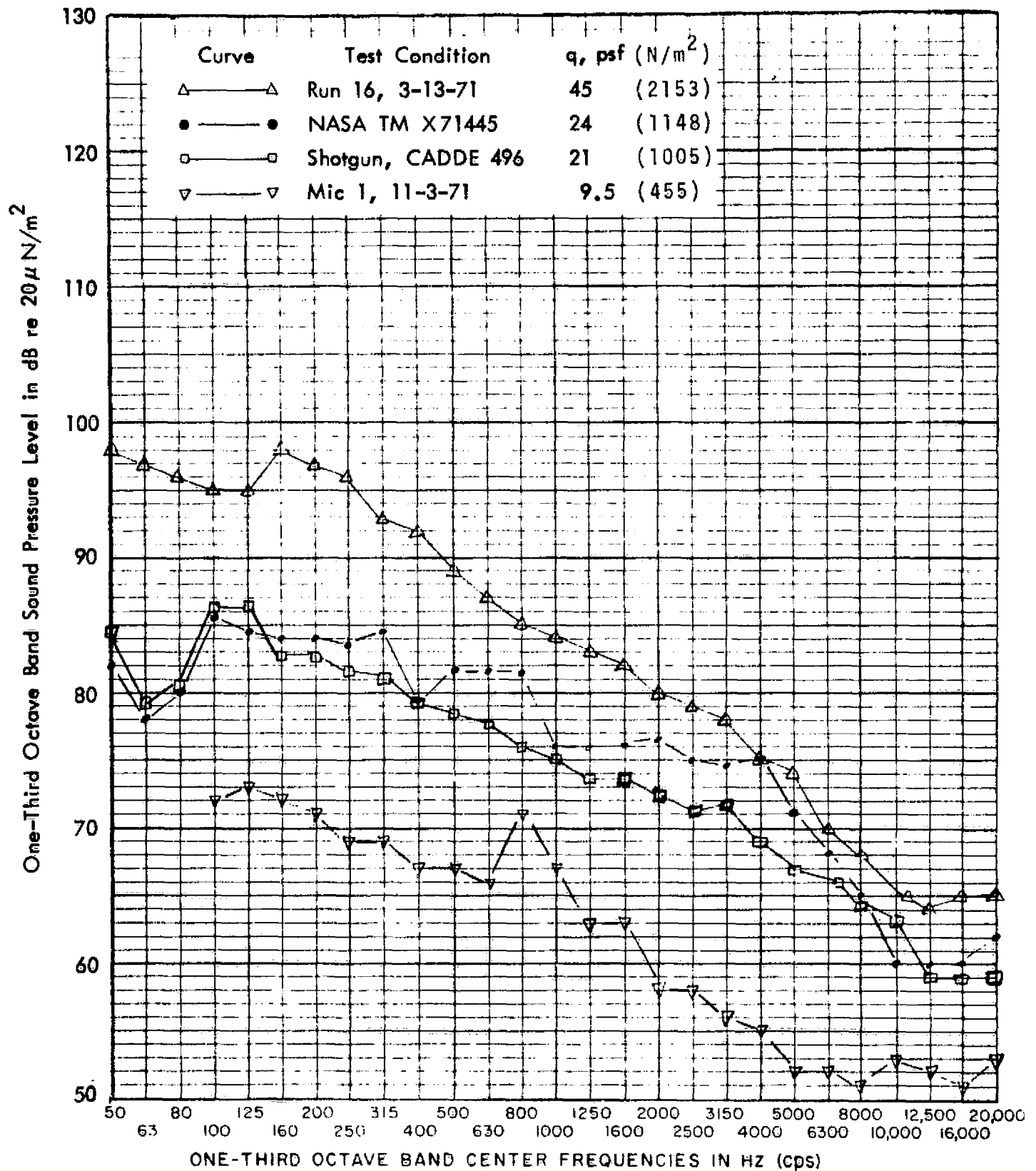
FIGURE 25. COMPARISON OF HORN DIRECTIONALITY MEASUREMENTS AT SIX FOOT RADIUS IN HARDWALL TEST SECTION , ALONG TUNNEL CENTERLINE ($\alpha = 30°$, $\psi = -30°$), AND IN ANECHOIC CHAMBER .

FIGURE 26. COMPARISON OF HORN DIRECTIONALITY MEASUREMENTS AT SIX FOOT RADIUS IN HARDWALL TEST SECTION, ANGLED TOWARDS WALL ($\alpha = 30°$, $\psi = -90°$), AND IN ANECHOIC CHAMBER.

FIGURE 27. SETTLING CHAMBER, WIND-ON, MEASURED ONE-THIRD
OCTAVE BAND SOUND PRESSURE LEVELS
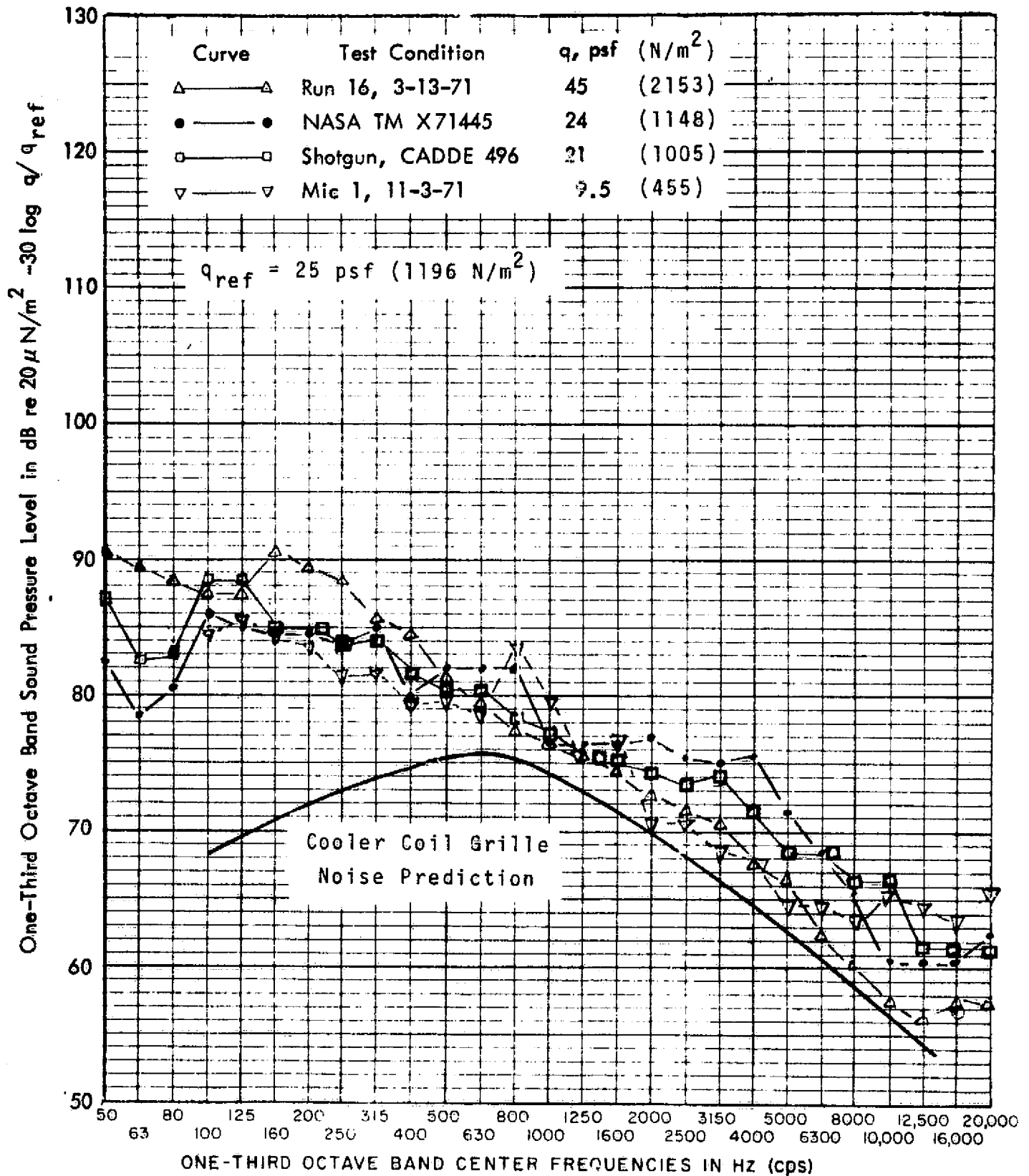
FIGURE 28. NORMALIZED SETTLING CHAMBER, WIND-ON, MEASURED ONE-THIRD OCTAVE BAND SOUND PRESSURE LEVELS
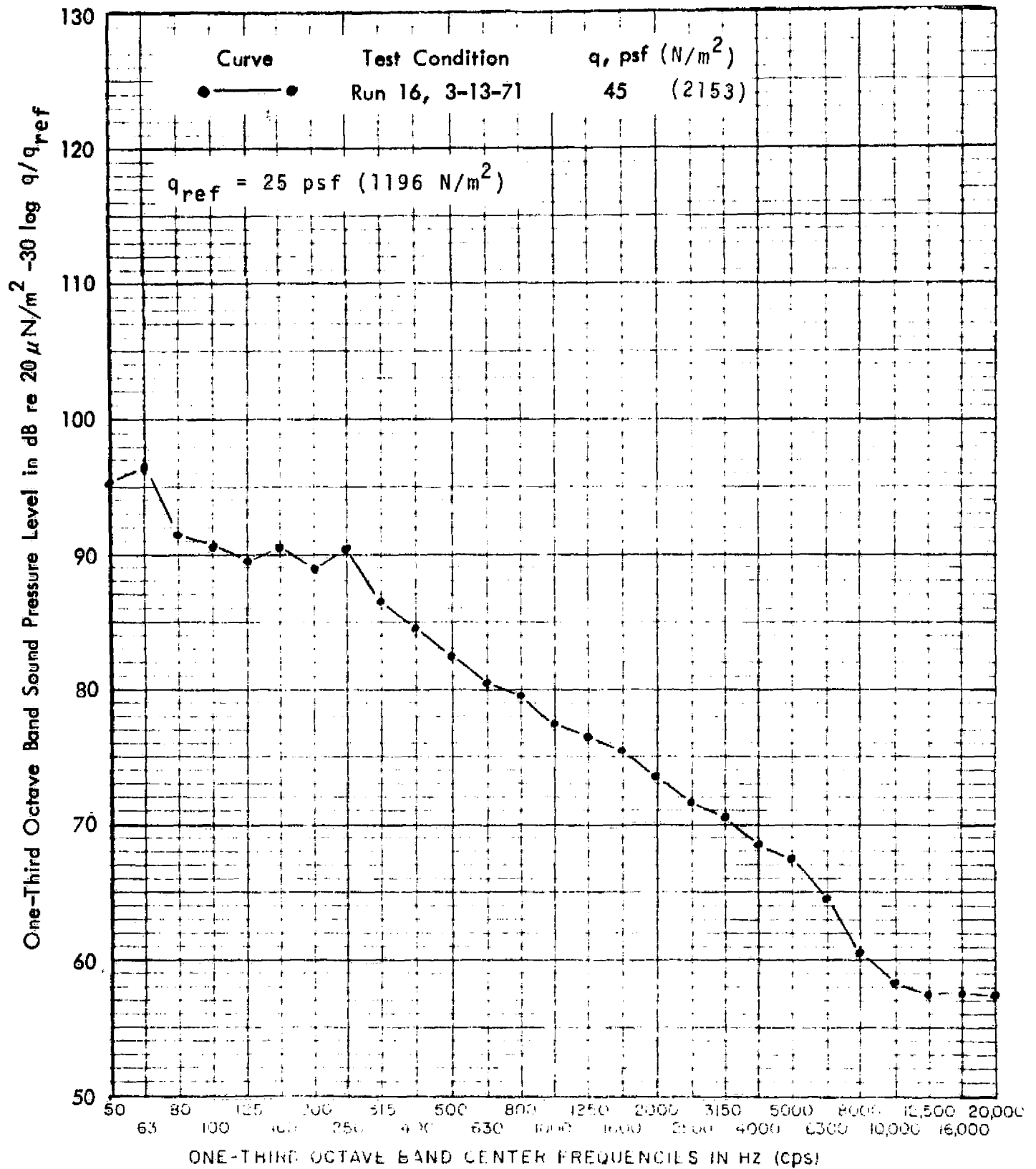
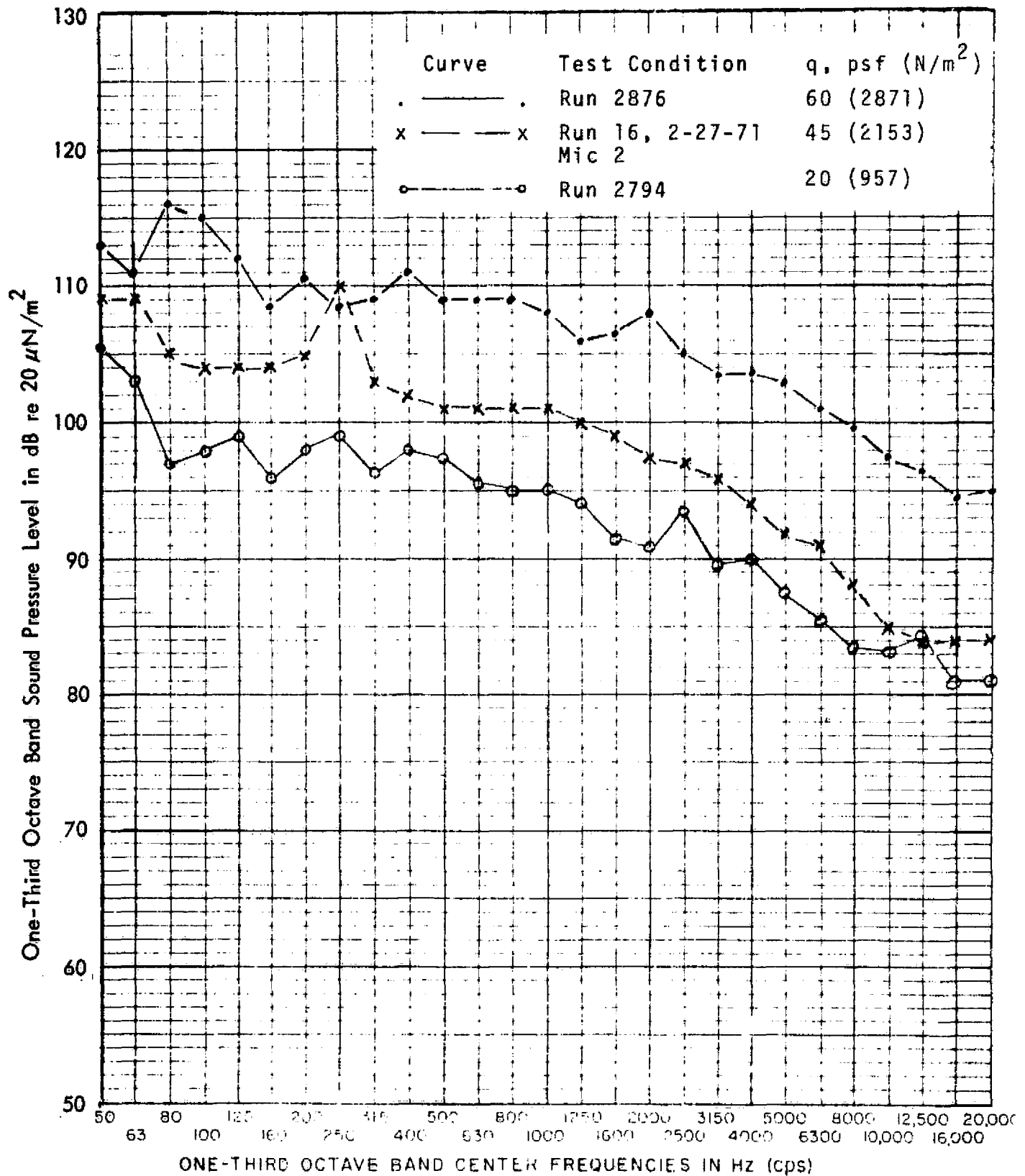FIGURE 29. NORMALIZED PREPARATION ROOM, WIND-ON, MEASURED ONE-THIRD OCTAVE BAND SOUND PRESSURE LEVELS

FIGURE 30. TEST SECTION MICROPHONE INDICATED SOUND
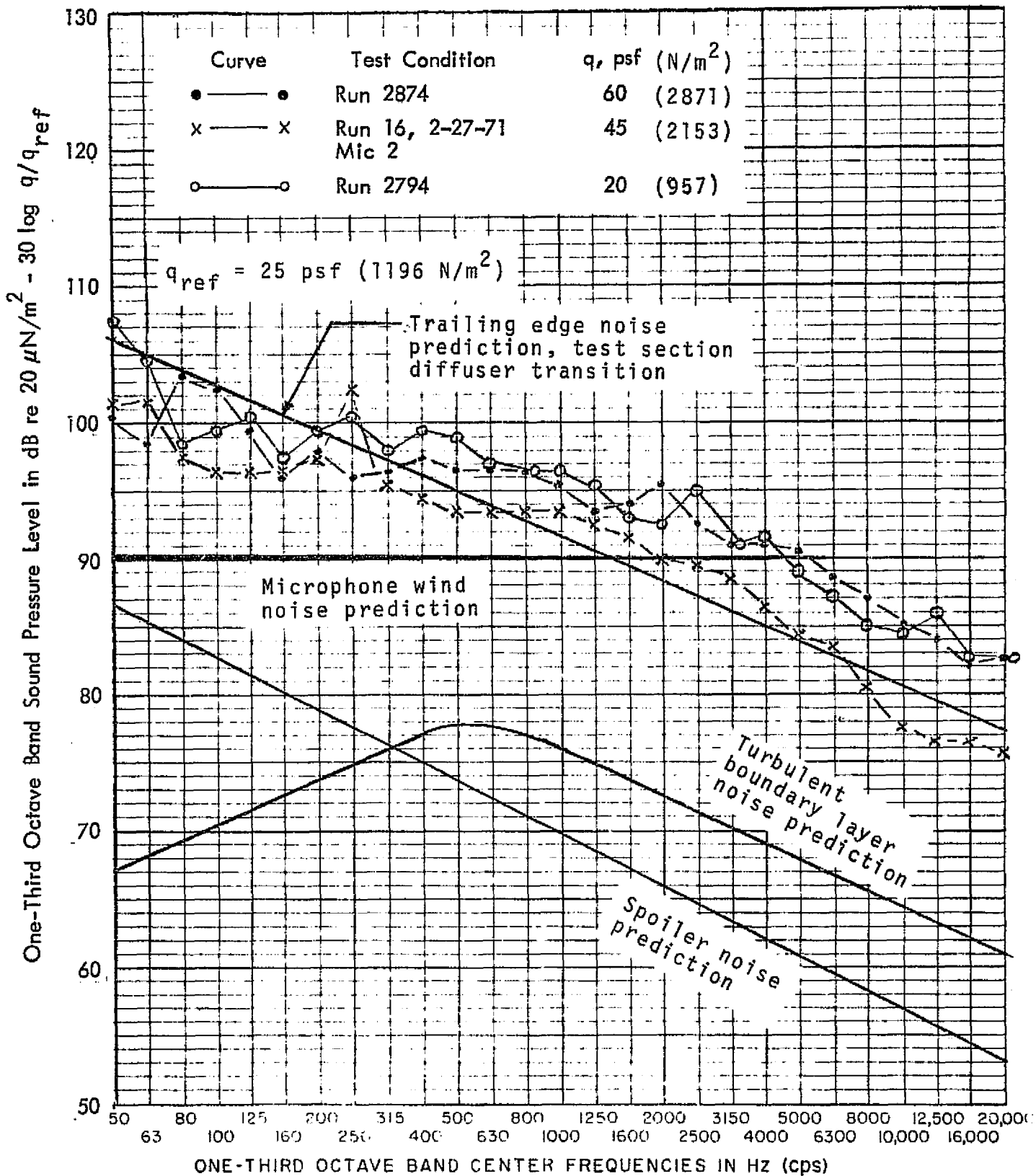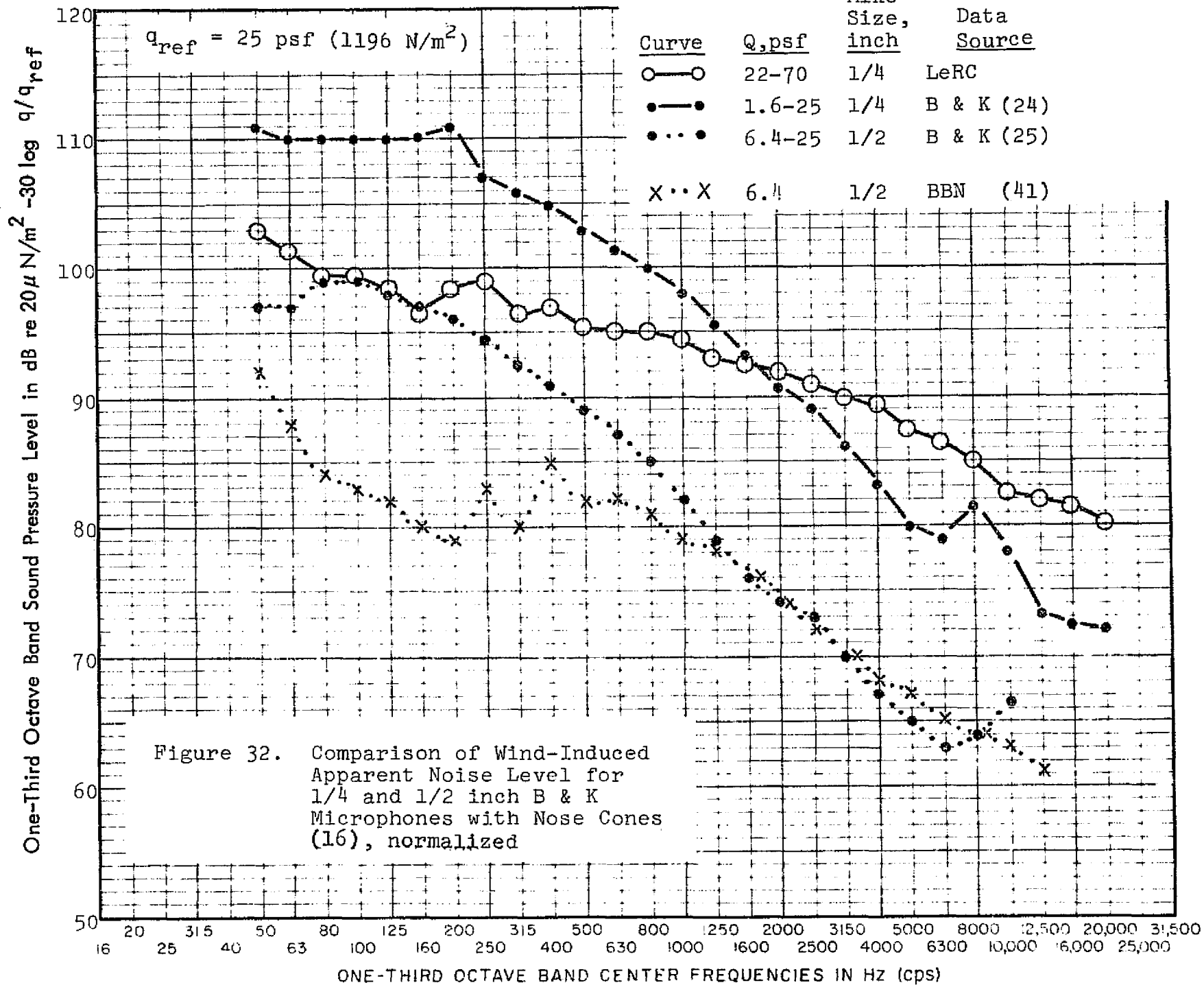PRESSURE LEVEL, ONE-QUARTER INCH MICROPHONE
WITH NOSE CONE

FIGURE 31. NORMALIZED TEST SECTION INDICATED SOUND PRESSURE LEVELS, ONE-QUARTER INCH MICROPHONE WITH NOSE CONE

Figure 32. Comparison of Wind-Induced Apparent Noise Level for 1/4 and 1/2 inch B & K Microphones with Nose Cones (16), normalized
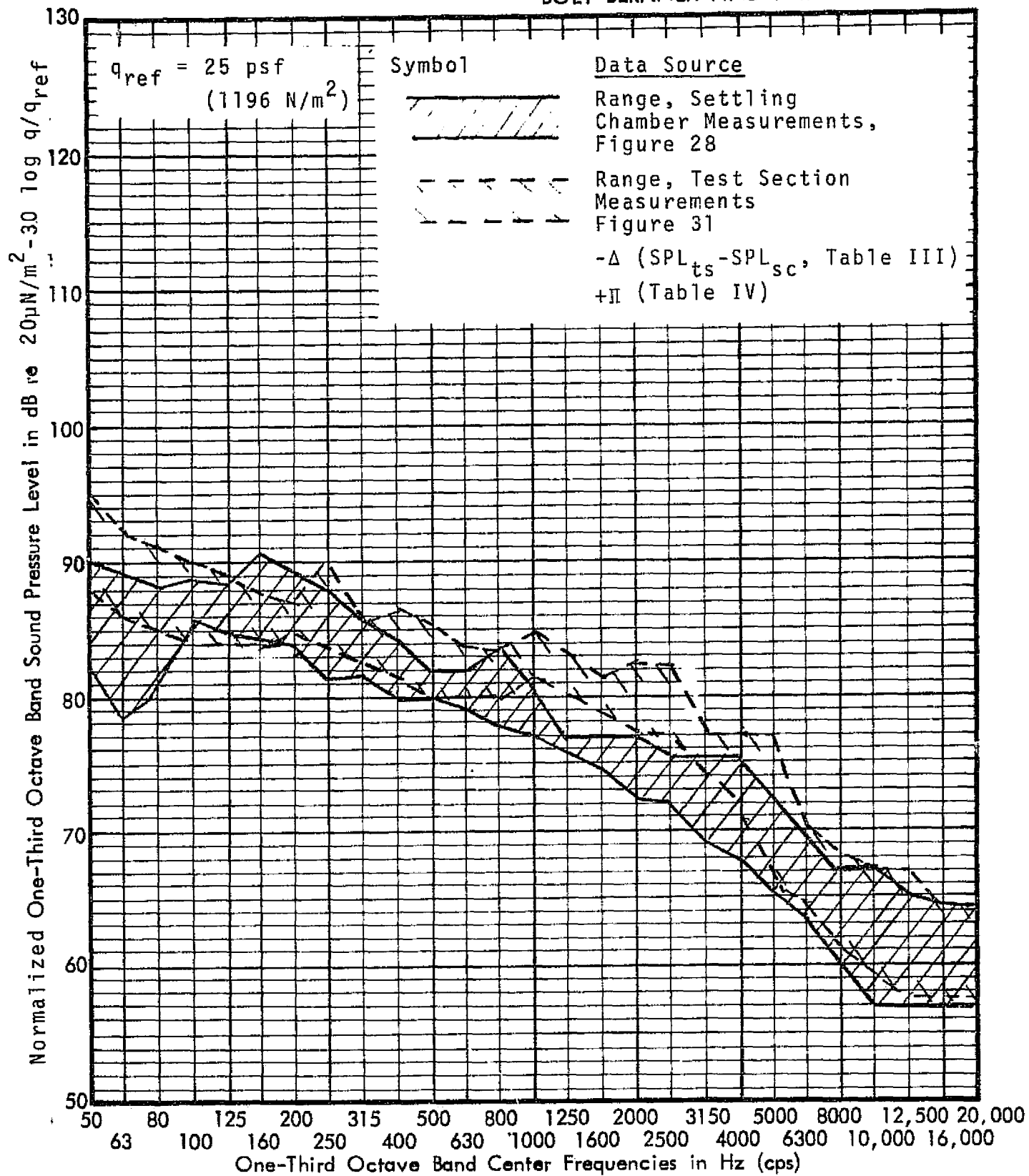
Figure 33. COMPARISON OF NORMALIZED SETTLING CHAMBER WIND-ON
MEASURED SOUND PRESSURE LEVELS AND ESTIMATED LEVELS
BASED TEST SECTION MICROPHONE MEASUREMENTS.